

Characterization Well R-31 Completion Report



*Produced by the Environmental Restoration Project
Groundwater Investigations Focus Area*

Cover photo shows a modified Foremost DR-24 dual-rotary drill rig. The DR-24 is one of several drill-rig types being used for drilling, well installation, and well development in support of the Los Alamos National Laboratory Hydrogeologic Workplan. The Hydrogeologic Workplan is jointly funded by the Environmental Restoration Project and Defense Programs to characterize groundwater flow beneath the 43-square-mile area of the Laboratory and to assess the impact of Laboratory activities on groundwater quality. The centerpiece of the Hydrogeologic Workplan is the installation of up to 32 deep wells in the regional aquifer.

An Affirmative Action/Equal Opportunity Employer

This report was prepared as an account of work sponsored by an agency of the United States Government. Neither the Regents of the University of California, the United States Government nor any agency thereof, nor any of their employees make any warranty, express or implied, or assume any legal liability or responsibility for the accuracy, completeness, or usefulness of any information, apparatus, product, or process disclosed, or represent that its use would not infringe privately owned rights. Reference herein to any specific commercial product, process, or service by trade name, trademark, manufacturer, or otherwise does not necessarily constitute or imply its endorsement, recommendation, or favoring by the Regents of the University of California, the United States Government, or any agency thereof. The views and opinions of authors expressed herein do not necessarily state or reflect those of the Regents of the University of California, the United States Government, or any agency thereof. Los Alamos National Laboratory strongly supports academic freedom and a researcher's right to publish; as an institution, however, the Laboratory does not endorse the viewpoint of a publication or guarantee its technical correctness.

*Characterization Well R-31
Completion Report*

*David Vaniman
Jon Marin
William Stone
Brent Newman
Patrick Longmire
Ned Clayton
Rick Lewis
Richard Koch
Stephen McLin
Giday WoldeGabriel
Dale Counce
David Rogers
Rick Warren
Emily Kluk
Steve Chipera
David Larssen
William Kopp*



Characterization Well R-31 Completion Report

Produced by the Groundwater Investigations Focus Area

This report was prepared as an account of work sponsored by an agency of the United States Government. Neither the Regents of the University of California, the United States Government nor any agency thereof, nor any of their employees make any warranty, express or implied, or assume any legal liability or responsibility for the accuracy, completeness, or usefulness of any information, apparatus, product, or process disclosed, or represent that its use would not infringe privately owned rights. Reference herein to any specific commercial product, process, or service by trade name, trademark, manufacturer, or otherwise does not necessarily constitute or imply its endorsement, recommendation, or favoring by the Regents of the University of California, the United States Government, or any agency thereof.

Los Alamos National Laboratory strongly supports academic freedom and a researcher's right to publish; as an institution, however, the Laboratory does not endorse the viewpoint of a publication or guarantee its technical correctness. By acceptance of this article, the publisher recognizes that the U.S. Government retains a nonexclusive, royalty-free license to publish or reproduce the published form of this contribution, or to allow others to do so, for U.S. Government purposes. Los Alamos National Laboratory requests that the publisher identify this article as work performed under the auspices of the U.S. Department of Energy.

TABLE OF CONTENTS

| | | |
|--|--|-----------|
| 1.0 | INTRODUCTION..... | 1 |
| PART I: SITE ACTIVITIES..... | | 1 |
| 2.0 | PREPARATORY ACTIVITIES..... | 1 |
| 3.0 | DRILLING | 3 |
| 3.1 | Phase I Drilling | 3 |
| 3.1.1 | Phase I Drilling Chronology | 4 |
| 3.1.2 | Phase I Drilling Summary | 4 |
| 3.2 | Site Preparation for Phase II Drilling | 4 |
| 3.3 | Phase II Drilling | 7 |
| 3.3.1 | Phase II Drilling Chronology | 8 |
| 3.3.2 | Phase II Drilling Summary | 11 |
| 3.4 | Overall Summary of Drilling Performance..... | 12 |
| 4.0 | WELL CONSTRUCTION..... | 13 |
| 4.1 | Production Casing | 13 |
| 4.2 | Annular Fill..... | 13 |
| 4.3 | Well Development | 16 |
| 4.3.1 | Surging..... | 16 |
| 4.3.2 | Airlifting | 16 |
| 4.3.3 | Pumping..... | 16 |
| 4.3.4 | Well Development Issues | 18 |
| 4.4 | Wellhead Completion | 18 |
| 5.0 | HYDROLOGIC TESTING | 19 |
| 6.0 | WESTBAY™ INSTRUMENTATION..... | 20 |
| 7.0 | GEODETC SURVEY OF COMPLETED WELL..... | 23 |
| PART II: ANALYSES AND INTERPRETATIONS | | 24 |
| 8.0 | GEOLOGY | 24 |
| 8.1 | Alluvium (0- to 24-ft depth) | 30 |
| 8.2 | Bandelier Tuff (Ash Flows of the Otowi Member, 24- to 264-ft depth; Guaje Pumice Bed of the Otowi Member, 264- to 280-ft depth)..... | 30 |
| 8.3 | Sediment Beneath the Bandelier Tuff (280- to 285-ft depth) | 30 |
| 8.4 | Cerros del Rio Lavas, Interflow Units, and Subflow Deposits of the Cerros del Rio Volcanic Field (285- to 710-ft depth) | 31 |
| 8.4.1 | Cerros del Rio Alkalic to Tholeiitic Lavas (285- to 534-ft depth), Including a Sedimentary Horizon (444- to 450-ft depth) | 32 |
| 8.4.2 | Cerros del Rio Basaltic Andesite Lavas (534- to 596-ft depth)..... | 35 |
| 8.4.3 | Alluvial Scoria Within the Cerros del Rio Lavas (596- to 625-ft depth)..... | 36 |
| 8.4.4 | Cerros del Rio Low-Ni,Cr Alkalic Basalt Lavas (625- to 703-ft depth) and Flow-Base Sediments (703- to 710-ft depth)..... | 36 |
| 8.5 | Puye Formation Sediments: Fanglomerates and River Gravels (710-ft depth to TD of 1103 ft) | 36 |
| 8.5.1 | Puye Formation Fanglomerates (710- to 780-ft depth) | 37 |
| 8.5.2 | Puye Formation River Gravels (“Totavi”) and Intercalated Fanglomerates (780-ft depth to TD of 1103 ft)..... | 40 |

| | | |
|-------------|--|-----------|
| 9.0 | BOREHOLE GEOPHYSICS..... | 41 |
| 9.1 | Borehole Geophysical Survey Methods | 42 |
| 9.1.1 | Gross Gamma Radiation (Laboratory Tool)..... | 42 |
| 9.1.2 | Caliper (Laboratory Tool) | 42 |
| 9.1.3 | Multi-Finger Caliper (MFC) Tool (Schlumberger) | 42 |
| 9.1.4 | Accelerator Porosity Sonde (APS; Schlumberger) | 42 |
| 9.1.5 | Hostile Natural Gamma Spectroscopy (HNCS) Tool (Schlumberger)..... | 43 |
| 9.1.6 | Electromagnetic Thickness Tool (ETT; Schlumberger) | 43 |
| 9.2 | Results..... | 44 |
| 9.2.1 | Stratigraphic Analysis Based on GR Logging Data (Laboratory Tool) | 44 |
| 10.0 | HYDROLOGY | 45 |
| 10.1 | Hydrology of Unsaturated Zones | 46 |
| 10.1.1 | Moisture Content..... | 46 |
| 10.1.2 | Matric Potential | 46 |
| 10.2 | Hydrology of Saturated Zones..... | 48 |
| 10.2.1 | Groundwater Occurrence..... | 48 |
| 10.2.2 | Groundwater Movement | 48 |
| 11.0 | GEOCHEMISTRY OF SAMPLED WATERS..... | 50 |
| 11.1 | Geochemistry of Vadose-Zone Pore Waters | 50 |
| 11.1.1 | Anion Results | 51 |
| 11.1.2 | Stable Isotope Results | 51 |
| 11.2 | Geochemistry of Regional Aquifer Waters..... | 51 |
| 11.2.1 | Methods | 56 |
| 11.2.2 | Results of Geochemical Analysis of Regional Aquifer Samples from the Cerros del Rio Lavas in R-31 | 58 |
| 11.2.3 | Results of Geochemical Analysis of Regional Aquifer Samples from Puye Formation River Gravels in R-31 | 59 |
| 12.0 | SUMMARY OF HYDROGEOLOGIC FEATURES AT SCREENED INTERVALS..... | 60 |
| 13.0 | IMPLICATIONS OF R-31 FOR CONCEPTUAL MODELS OF GEOLOGY, HYDROLOGY, AND GEOCHEMISTRY | 62 |
| 14.0 | ACKNOWLEDGMENTS AND CONTRIBUTIONS..... | 62 |
| 15.0 | REFERENCES..... | 63 |

Appendixes

- Appendix A Diagram of Site Activities Related to Progress
- Appendix B Modifications to Work Plans
- Appendix C Borehole Log
- Appendix D Descriptions of Geologic Samples
- Appendix E Moisture and Matric-Potential Results
- Appendix F Westbay™ MP55 Well Components Installed in R-31
- Appendix G Summary of Schlumberger Borehole Geophysical Data (on CD, back cover)
- Appendix H Borehole Video of R-31 (on CD, back cover)

List of Figures

| | | |
|---------------|--|----|
| Figure 1.0-1 | Map showing the location of well R-31, in the southeastern portion of the Laboratory, with regional water table contours | 2 |
| Figure 4.0-1 | As-built well construction diagram for R-31 | 14 |
| Figure 4.3-1 | Well development data obtained by airlifting at screen #3 in R-31 | 17 |
| Figure 4.3-2 | Well development data obtained by pumping at screen #4 in R-31 | 17 |
| Figure 5.0-1 | Straddle-packer assembly used for hydrologic testing at the R-31 site | 19 |
| Figure 7.0-1 | Geodetic survey points at well R-31 | 23 |
| Figure 8.0-1a | Predicted and as-drilled stratigraphy at R-31 | 25 |
| Figure 8.0-1b | Details of as-drilled stratigraphy at the R-31 site..... | 26 |
| Figure 8.0-2 | Locations of R-31, other boreholes, outcrop control points, and interpretive geologic sections..... | 27 |
| Figure 8.0-3 | Interpretive north-south geologic section from O-4 through R-31 to Chaquehui Canyon..... | 28 |
| Figure 8.0-4 | Interpretive northwest-southeast geologic section from DT-9 through R-31 to the east side of the Rio Grande..... | 29 |
| Figure 8.2-1 | Stratigraphy and natural gamma properties of the upper 285 ft of R-31 | 31 |
| Figure 8.4-1 | Relations between Cerros del Rio stratigraphy, natural gamma signal, SiO ₂ contents, Mg/(Mg+Fe) ratios, K ₂ O/P ₂ O ₅ ratios, and contents of selected trace elements (Sr, Cr, Ni) at R-31..... | 33 |
| Figure 8.5-1 | Relationships between Puye Formation stratigraphy, natural gamma signal, Si/Al cation ratios, ratios of quartz to all silica minerals [quartz/(quartz + tridymite + cristobalite)], and glass alteration indices [(clays + zeolites)/(clays + zeolites + glass)] at the R-31 site..... | 38 |
| Figure 10.1-1 | Variation in moisture content of samples from the surface to the 355-ft depth in R-31 ... | 47 |
| Figure 10.1-2 | Matric potential of samples from the surface to the 355-ft depth in R-31..... | 47 |
| Figure 11.1-1 | Vertical distributions of bromide, oxalate, and phosphate in core and cuttings from R-31 | 52 |
| Figure 11.1-2 | Vertical distributions of chloride, fluoride, nitrate, and sulfate in core and cuttings from R-31 | 54 |
| Figure 11.1-3 | Vertical distributions of $\delta^{18}\text{O}$ and δD in core samples from R-31 | 55 |

List of Tables

| | | |
|-------------|---|----|
| Table 3.0-1 | Shift Information for Operations at the R-31 Site..... | 3 |
| Table 3.1-1 | Production Statistics for Well R-31 | 5 |
| Table 3.1-2 | Drilling Performance Statistics by Stratigraphy for Well R-31 | 6 |
| Table 3.3-1 | Footage Intervals Drilled Dry or with Lubricating Slurry, in Well R-31..... | 9 |
| Table 4.1-1 | Well Casing Used in Well R-31..... | 15 |
| Table 4.2-1 | Annular Fill Materials Used in Well R-31 | 15 |
| Table 4.3-1 | Summary of Final Development of R-31 by Pumping | 18 |
| Table 6.0-1 | Depths of Key Westbay TM MP55 System Components in Well R-31 | 21 |

| | | |
|---------------|---|----|
| Table 7.0-1 | Geodetic Data for Well R-31 | 23 |
| Table 8.3-1 | ³⁹ Ar/ ⁴⁰ Ar Ages of Cerros del Rio Basalt Samples from R-31 | 31 |
| Table 8.4-1 | XRF Analyses of Cerros del Rio Lavas from R-31 | 34 |
| Table 8.4-2 | X-Ray Diffraction (XRD) Analyses of Sediments from R-31 (Weight %)..... | 35 |
| Table 8.5-1 | XRF Analyses of Puye Formation Sediments from R-31 | 39 |
| Table 9.0-1 | Laboratory and Schlumberger Geophysical Logging Runs Performed in Well R-31 | 41 |
| Table 9.2-1 | Statistical Parameters of Natural Gamma Signals (Laboratory Tool) for Different Lithologies at R-31 (Raw Counts, Unsmoothed) | 45 |
| Table 10.2-1 | Summary of Straddle-Packer/Injection Testing at the R-31 Site | 49 |
| Table 11.1-1 | Anion Data from Vadose-Zone Pore Waters at the R-31 Site..... | 53 |
| Table 11.1-2 | Stable Isotope Data from Vadose-Zone Pore Waters at the R-31 Site..... | 55 |
| Table 11.2-1a | Anion and Cation Hydrochemistry of Regional Aquifer Samples from R-31 (Filtered and Nonfiltered Samples)..... | 57 |
| Table 11.2-1b | Radionuclide, Cyanide, Total Organic Carbon, and Stable Isotope Hydrochemistry of Regional Aquifer Samples from R-31 (Nonfiltered Samples)..... | 58 |

List of Acronyms and Abbreviations

| | |
|-------|--|
| APS | accelerator porosity sonde |
| ASTM | American Society for Testing and Materials |
| BGO | bismuth germanate |
| bgs | below ground surface |
| cpm | counts per minute |
| cps | counts per second |
| cu | capture unit |
| DL | detection limit |
| DOE | U.S. Department of Energy |
| DR | dual rotation |
| DTW | depth to water |
| DX | Dynamic Experimentation (Division) |
| EM | electromagnetic |
| EPA | U.S. Environmental Protection Agency |
| ER | Environmental Restoration (Project) |
| ESH | Environmental Safety and Health (Division) |
| ETT | electromagnetic thickness tool |
| FIMAD | Facility for Information Management, Analysis, and Display |
| FIP | Field Implementation Plan |
| FMU | Field Management Unit |

| | |
|--------|--|
| FSF | Field Support Facility |
| GPS | Global Positioning System |
| GR | gross gamma radiation (tool) |
| H | size of tremie rod |
| HE | high explosive |
| HNGS | hostile natural gamma spectroscopy (tool) |
| HSA | hollow-stem auger |
| ICPES | inductively coupled plasma emission spectroscopy |
| I.D. | inner diameter |
| IR | Ingersoll Rand |
| JMML | Jemez Mountains meteoric line ($\delta D - \delta^{18}O$ correlation) |
| K | hydraulic conductivity |
| LANL | Los Alamos National Laboratory |
| Ma | million years ago |
| MFC | multi-finger caliper (tool) |
| MOU | Memorandum of Understanding |
| MP | multi-port |
| N | size of tremie rod |
| NAD | North American Datum |
| NDA | no detectable activity |
| NMED | New Mexico Environment Department |
| NTU | nephelometric turbidity unit |
| O.D. | outer diameter |
| PLF | low-frequency phase output |
| PPE | personal protective equipment |
| QA | quality assurance |
| QXRD | quantitative x-ray diffraction |
| RC | reverse circulation |
| SAIC | Science Applications International Corporation |
| SBDC | Stewart Brothers Drilling Company |
| SSHASP | Site-Specific Health and Safety Plan |
| TA | Technical Area (of the Los Alamos National Laboratory site) |
| TD | total depth |
| TOC | total organic carbon |
| WCSF | waste characterization strategy form |
| WGS | World Geodetic System |

WLS weighted least-squares
 XRD x-ray diffraction
 XRF x-ray fluorescence

Metric to English Conversions

| Multiply SI (Metric) Unit | by | To Obtain US Customary Unit |
|--|------------|--|
| kilometers (km) | 0.622 | miles (mi) |
| kilometers (km) | 3281 | feet (ft) |
| meters (m) | 3.281 | feet (ft) |
| meters (m) | 39.37 | inches (in.) |
| centimeters (cm) | 0.03281 | feet (ft) |
| centimeters (cm) | 0.394 | inches (in.) |
| millimeters (mm) | 0.0394 | inches (in.) |
| micrometers or microns (μm) | 0.0000394 | inches (in.) |
| square kilometers (km^2) | 0.3861 | square miles (mi^2) |
| hectares (ha) | 2.5 | acres |
| square meters (m^2) | 10.764 | square feet (ft^2) |
| cubic meters (m^3) | 35.31 | cubic feet (ft^3) |
| kilograms (kg) | 2.2046 | pounds (lb) |
| grams (g) | 0.0353 | ounces (oz) |
| grams per cubic centimeter (g/cm^3) | 62.422 | pounds per cubic foot (lb/ft^3) |
| milligrams per kilogram (mg/kg) | 1 | parts per million (ppm) |
| micrograms per gram ($\mu\text{g/g}$) | 1 | parts per million (ppm) |
| liters (L) | 0.26 | gallons (gal.) |
| milligrams per liter (mg/L) | 1 | parts per million (ppm) |
| degrees Celsius ($^{\circ}\text{C}$) | $9/5 + 32$ | degrees Fahrenheit ($^{\circ}\text{F}$) |

CHARACTERIZATION WELL R-31 COMPLETION REPORT

by

David Vaniman, Jon Marin, William Stone, Brent Newman, Patrick Longmire, Ned Clayton, Rick Lewis, Richard Koch, Stephen McLin, Giday WoldeGabriel, Dale Counce, David Rogers, Rick Warren, Emily Kluk, Steve Chipera, David Larssen, William Kopp

ABSTRACT

Characterization well R-31 is located in the north fork of Ancho Canyon, within Technical Area (TA) 39 of Los Alamos National Laboratory (LANL or the Laboratory). This well is the fifth of approximately 32 wells being installed in the regional aquifer as part of the implementation of the Laboratory's "Hydrogeologic Workplan" (LANL 1998, 59599). Well R-31 was funded by the Laboratory's Nuclear Weapons Infrastructure, Facilities, and Construction Program and installed by the Environmental Restoration (ER) Project. R-31 was designed to provide hydrogeologic, water-quality, and water-level data for potential intermediate-depth perched zones and for the regional aquifer at a site downgradient of disposal and explosives-testing sites at TA-39. When R-31 was sited, it was anticipated that the drill hole would provide information on the thicknesses, contact depths, and hydrogeologic properties of the lower Bandelier Tuff (Otowi Member), Cerros del Rio lavas, Puye Formation sediments (fanglomerates and river gravels), and Santa Fe Group sediments. All of these units except the Santa Fe Group were encountered at the R-31 site, albeit not at the depths and in most cases not in the thicknesses expected. The Otowi Member of the Bandelier Tuff was ~200 ft thicker than anticipated, placing the Cerros del Rio lavas (present at the expected thickness of ~400 ft) at a lower elevation than predicted. Beneath the Cerros del Rio lavas, the expected 560 ft of Puye Formation fanglomerates was only 70 ft, leading to an encounter with Puye Formation river gravels ("Totavi") at an elevation much higher than expected (5600 ft above mean sea level versus 5350 ft) and with greater thickness (over 320 ft of gravels, versus only 80 ft). Drilling did not penetrate through these gravels at the R-31 site, leaving in question the nature of the subgravel lithology (possibilities include more Puye Formation fanglomerates, Santa Fe Group sediments, or Miocene basalt).

R-31 was drilled in two phases. Phase I was conducted from September 9 to October 1, 1999, and consisted of drilling to 250 ft to collect core from Otowi Member ash flows with a hollow-stem auger (HSA) drill rig. Phase II drilling was conducted from January 6 to February 8, 2000, using air-rotary drilling methods that included a combination of open-hole and casing-advance techniques. During Phase II, R-31 was drilled to a total depth (TD) of 1103 ft, close to the planned depth of 1100 ft. Construction, development, and testing of a five-screen well was completed between February 8 and April 3, 2000.

New data gathered during the drilling and completion of R-31 affect the hydrogeologic conceptual model of the southeastern part of the Laboratory. The saturated zone at the R-31 site includes basalt- and Puye Formation-hosted waters with no evidence of contamination. The occurrence of the regional water table within Cerros del Rio lavas rather than within Puye Formation fanglomerates and the unexpected thickness of Puye Formation river gravels are both new components in the conceptual model for this area. The extensive occurrence of river gravels provides access to large amounts of a highly transmissive lithology that extends to depths below the present Rio Grande. The model for the Laboratory has been improved with new data for hydrologic conductivity in fractured basalt and in the river-gravel facies of the Puye Formation; variability of this parameter within the river gravels is as yet unexplained.

1.0 INTRODUCTION

This report describes drilling, well installation, and testing activities and provides a preliminary interpretation of the data for characterization well R-31. R-31 is located in the north fork of Ancho Canyon within TA-39 in the southeastern portion of the Laboratory (Figure 1.0-1). The drill site chosen for R-31 is within the TA-39 storage area locally referred to as the "boneyard." R-31 was installed by the ER Project with funding support from the Nuclear Weapons Infrastructure, Facilities, and Construction Program. The well was installed pursuant to the "Hydrogeologic Workplan" (LANL 1998, 59599) in support of the Laboratory's "Groundwater Protection Management Program Plan" (LANL 1995, 70215).

The role of R-31 in the Groundwater Protection Management Program is to provide water-quality, geologic, hydrologic, and geochemical data for perched zones and for the regional aquifer downgradient of potential release sites in the north fork of Ancho Canyon, or connected through cross-canyon flow to release sites in the main channel of Ancho Canyon or in Water Canyon. The likeliest sources of contamination are within the north fork of Ancho Canyon, where TA-39 activities have included open-air testing of high explosives, landfill disposal, and use of several septic systems. The history of activities at TA-39, including potential sources of contamination, known releases and discharges, and previous investigations, is provided in the "RFI Work Plan for Operable Unit 1132" (LANL 1993, 15316).

This report consists of two parts. Part I is a chronological presentation of preparatory, drilling, well construction, well development, testing, and completion activities. Part II summarizes initial interpretations of the geologic, hydrologic, geochemical, and geophysical data collected during and immediately following the activities described in Part I. A more thorough treatment of the data collected awaits supporting data that will be obtained through other hydrogeologic characterization wells and related field studies. Although R-31 is primarily a characterization well, its design also meets the requirements of a monitoring well as described in Module VIII of the Laboratory's Hazardous Waste Facility Permit.

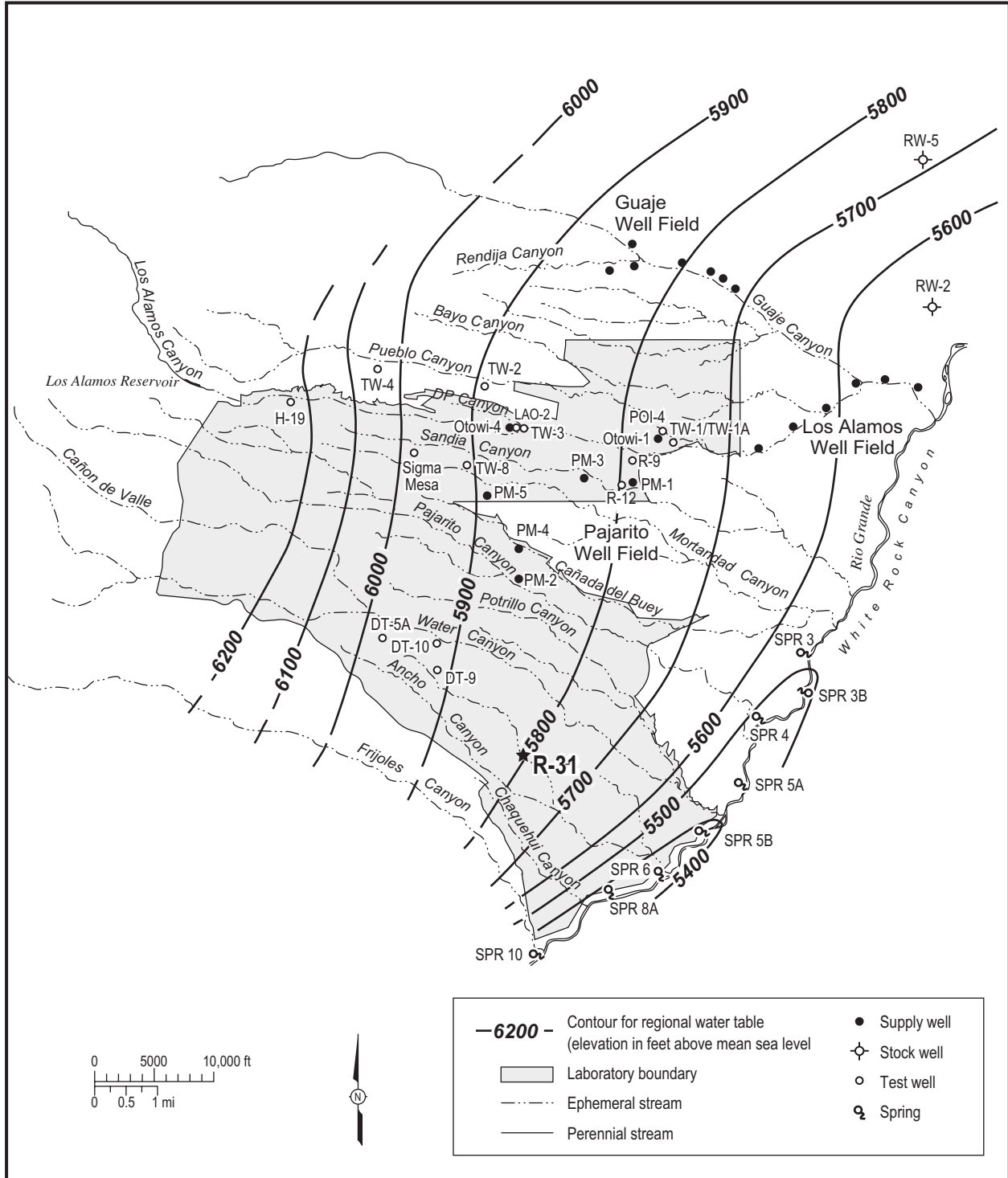
PART I: SITE ACTIVITIES

Project activities related to the installation of well R-31 included administrative preparation, Phase I drilling and site preparation for Phase II, Phase II drilling, well construction, insertion of annular fill, well development, wellhead completion, hydrologic testing, installation of the Westbay™ multi-port sampling system, and final site waste management and survey tasks. A graphic depiction of project history to accompany the text below is presented in Appendix A. The following text sections are arranged in chronological order.

2.0 PREPARATORY ACTIVITIES

Preparatory work for R-31 occurred from February to September 1999. Field preparation requirements for Phase I drilling were minimal and consisted of a site radiation survey conducted in June 1999.

Science Applications International Corporation (SAIC) was authorized to begin administrative preparation on February 11, 1999. As part of this preparation, Group ESH-5 at the Laboratory developed a site-specific health and safety plan (SSHASP) for work at the R-31 site. SAIC prepared a waste characterization strategy form (WCSF) and outlined drilling and sampling plans in the R-31 field implementation plan (FIP) to guide field activities. The host facility, FMU-67, implemented a memorandum of understanding (MOU) with the ER Project to provide access and security control for the R-31 project.



Source: Purtymun 1984, 6513

Figure 1.0-1. Map showing the location of well R-31, in the southeastern portion of the Laboratory, with regional water table contours

All administrative documents, permits, agreements, and plans were assembled for an ER Readiness Review Meeting on May 20, 1999. The Canyons Focus Area Project Leader signed the Readiness Review checklist on June 1, 1999, giving authorization to begin field activities. On June 30, 1999, further work on R-31 was placed on hold pending funding resolutions. Work resumed on September 9, 1999.

Before Phase I drilling activities began at the R-31 site, a radiological control technician conducted a surface radiological survey on June 2, 1999. Alpha, beta, and gamma measurements were collected, and statistical analyses were performed to calculate background values. The survey consisted of 19 points on a grid projected over the work area. Each point was surveyed using direct-reading alpha and beta/gamma meters. Alpha radiation was measured using a Ludlum 139 with an air proportional probe, and beta/gamma was measured using an ESP-1/HP-260. Calculated background values for the drill site showed no detectable activity (NDA) for alpha and 171 counts per minute (cpm) for beta/gamma.

3.0 DRILLING

Drilling of borehole R-31 was completed in two phases. Phase I drilling was conducted during September 1999, using an HSA drill rig for installation of surface conductor casing and collection of core samples. Phase II drilling was conducted from early January to early February 2000 using an air-rotary system with reverse circulation to provide cuttings samples. Table 3.0-1 lists the number of shifts and dates for all R-31 field activities, from Phase I through well completion.

Table 3.0-1
Shift Information for Operations at the R-31 Site

| Operations Category | Dates | Number of Shifts |
|--|--------------------------------------|------------------|
| Phase I drilling/site preparation for Phase II | September 9 – October 1, 1999 | 14 10-hr |
| Phase II drilling | January 6 – February 8, 2000 | 39 12-hr |
| Well design | February 9 – February 15, 2000 | 6 12-hr |
| Well installation | February 16 – February 19, 2000 | 6 12-hr |
| Insertion of annular fill | February 19 – March 5, 2000 | 28 12-hr |
| Well development/hydrologic testing | March 8 – March 27, 2000 | 17 12-hr |
| Well completion tasks | April 3 and December 1, 2000 | 2 10-hr |
| Total Shifts | September 9, 1999 – December 1, 2000 | 112 |

3.1 Phase I Drilling

A kickoff meeting was held at the Field Support Facility (FSF) on September 9, 1999, to initiate Phase I drilling and site preparation activities for Phase II at the R-31 site. The primary goal of Phase I drilling was to install surface conductor casing and to collect core samples for moisture-content and anion analyses. Phase I operations were conducted by Stewart Brothers Drilling Company (SBDC) from September 9 through October 1, 1999, using a CME-750 HSA drill rig. The HSA drilling method is relatively inexpensive and efficient, capable of drilling through the nonwelded Otowi Member but difficult to use for deeper drilling. In conjunction with preparation of a hole in which to set the surface conductor casing, core samples were collected to characterize the upper vadose zone at the R-31 site (Section 11.1 of this report). Phase I operations were conducted in one 10-hr shift per day, Monday through Friday, including mobilization and demobilization of equipment.

3.1.1 Phase I Drilling Chronology

Phase I drilling began on September 9, 1999, and progressed to a depth of 250 ft below ground surface (bgs) using a 4 1/4-in.-inner diameter (I.D.) Truspin™ auger and a Moss™ wireline continuous-core retrieval system. From September 20 to 22, using the in-place Truspin™ auger string as a guide, the borehole was then over-reamed using an 11-in.-I.D. HSA to a depth of 37 ft bgs. As the Truspin™ auger string was withdrawn, the borehole was backfilled with cuttings from 250 to 37 ft. After the 11-in.-I.D. HSA was removed on September 22, two 18-in.-diameter, 20-ft-long steel casing joints were welded together and lowered to a depth of 37 ft bgs, leaving a stickup of 3 ft above ground surface. A cement slurry was tremied to 37 ft and rose approximately 11 ft (to 26 ft bgs) inside and outside the casing. The casing was repeatedly raised and lowered to achieve a homogeneous cement seal. After curing overnight, the upper part of the borehole annular space around the casing was cemented to approximately 10 ft bgs on September 23. A detailed chronology of Phase I operations is provided in Appendix A.

3.1.2 Phase I Drilling Summary

Phase I drilling operations and site preparation activities for Phase II at the R-31 site required 14 shifts from September 9 through October 1, 1999. Six of these shifts were drilling shifts, conducted September 14 to 17, 20, and 22; the remaining eight shifts were used for mobilization and setup (September 9 to 10 and September 13 to 14), demobilization (September 23), and site preparation for Phase II drilling (September 24 and 27, and October 1).

The total footage drilled during Phase I by HSA methods was 287 ft. Of that total, 250 ft were drilled with a 4 1/4-in.-I.D. Truspin™ HSA at an average rate of 15.2 ft/hr, and 37 ft were over-reamed with an 11-in.-I.D. HSA at an average rate of 6.5 ft/hr. Phase I performance statistics are summarized in Tables 3.1-1 and 3.1-2.

3.2 Site Preparation for Phase II Drilling

During Phase I, Parker Construction began site preparation tasks for Phase II drilling. In addition, pad leveling and grading required 3 operator days, after the Phase I drilling equipment was withdrawn from the site and surface casing installation was completed. Appendix A provides a chronology of the site preparation activities.

After the surface casing was set and the grade of the pad was established with a bulldozer, a backhoe and hand tools were used to excavate a pit approximately 8 ft by 10 ft by 5 ft deep around the surface casing. At the bottom of the pit, a reinforced concrete pad 6 ft by 8 ft by 1 ft thick was cast around the surface casing. This pad required approximately 90 bags of Portland cement, which was poured into a wooden form holding half-inch rebar at the base of the excavation. A steel box (4 ft by 6 ft by 4.1 ft deep), open on the top and bottom, was lowered over the surface casing to the cement pad at the base of the excavation. The steel box would house hydraulic casing jacks required for Phase II drilling. Once the steel box was positioned on the pad, base-course gravel was tamped in 2-ft lifts to backfill the excavation around the box. The box extended approximately 1 in. above grade. The tamped gravel was designed to provide a foundation for the Phase II drill-rig jacks.

**Table 3.1-1
Production Statistics for Well R-31**

| Drilling Systems/ Casings in Order of Use → | Phase I | | | Phase II | | | | Total |
|--|--------------------------------|--------------------|-----------------------------|-------------------------------------|--------------------------------------|-------------------------------------|------------------------------------|---------------|
| | 4 1/4-in.- I.D. HSA Core | 11-in.-I.D. HSA | 18-in. Surface Casing | 13 3/8-in. Casing ^{a,b} | 12 1/4-in. Tricone ^{c,d} | 11 3/4-in. Casing ^{e,f} | 9 5/8-in. Casing ^{g,h} | |
| Bandelier Tuff footage (ft) ⁱ | 250.0 | 37.0 | | 259.0 | | | | 546.0 |
| <i>Bandelier Tuff rate (ft/hr)^j</i> | 15.6 | 7.2 | | 20.6 | | | | 17.4 |
| Basalt footage (ft) ^j | | | | | 418.0 | | | 418.0 |
| <i>Basalt rate (ft/hr)^j</i> | | | | | 17.4 | | | 17.4 |
| Puye clastics footage (ft) ^k | | | | | 79.0 | | 326.0 | 405.0 |
| <i>Puye clastics rate (ft/hr)^k</i> | | | | | 16.1 | | 19.1 | 18.5 |
| Total footage drilled (ft) ^l | 250.0 | 37.0 | | 259.0 | 497.0 | | 326.0 | 1369.0 |
| <i>Total footage rate (ft/hr)^l</i> | 15.2 | 6.5 | | 20.6 | 17.1 | | 19.1 | 17.7 |
| Trip-in footage (ft) ^m | | | 37.0 | 26.0 | 290 | 710.0 | 2412.0 | 3475 |
| <i>Trip-in rate (ft/hr)^m</i> | | | 37.0 | 156.0 | 145.0 | 110.1 | 211.0 | 182.6 |
| Trip-out footage (ft) ^m | 250.0 | 37.0 | | 575.0 | 787.0 | 650.0 | 3129.0 | 5428 |
| <i>Trip-out rate (ft/hr)^m</i> | 76.9 | 44.4 | | 57.0 | 295.1 | 166.0 | 119.8 | 141.6 |
| Life-of-hole TD (ft bgs) ⁿ | 250.0 | 37.0 | 37.0 | 285.0 | 787.0 | 325.0 | 1103.3 | |

^a 13 3/8-in. casing used a Holte 3-wing under-reamer, SD-12 hammer, and 7-in. reverse circulation (RC) rods.

^b From the surface to 26 ft, the 13 3/8-in. casing was tripped into the 18-in. surface casing.

^c 12 1/4-in. tricone bit used 7-in. RC rods.

^d From the surface to 285 ft, the 12 1/4-in. tricone open-borehole drill system was tripped into the 13 3/8-in. casing.

^e 11 3/4-in. casing used a Holte 3-wing under-reamer, SD-12 hammer, and 7-in. RC rods.

^f From the surface to 285 ft, the 11 3/4-in. casing was tripped into the 13 3/8-in. casing, and from 285 ft to 325 ft, the 11 3/4-in. casing was tripped into the 12 1/4-in. open borehole. No new footage was drilled with the 11 3/4-in. casing system.

^g 9 5/8-in. casing used Mitsubishi 2-wing eccentric under-reamer, IR 380 hammer, and 7-in. RC rods.

^h From the surface to 285 ft, the 9 5/8-in. casing was tripped into the 13 3/8-in. casing, and from 285 ft to 777 ft, the 9 5/8-in. casing was tripped into the 12 1/4-in. open borehole.

ⁱ Bandelier Tuff footage and rate include surface alluvium, Otowi Member including Guaje Pumice Bed, cement in surface casing, and sediment atop Cerros del Rio lavas.

^j Basalt footage and rate include subunits of Cerros del Rio lavas (low, moderate, and high natural gamma) and intercalated deposits consisting of sediments, alluvial scoria, flow-base breccia, and flow-base sediments.

^k Puye footage and rate include Puye Formation fanglomerates and river gravels.

^l Total footage and rate compile all drilling in borehole and do not connect time and trip-in/out footage. Borehole TD is 1103 ft. Total cored footage (250 ft) is 23% of borehole TD (1103 ft) and 18% of total footage drilled (1369 ft).

^m Trip-in/out footages and rates compile statistics for respective casings/drill systems including extra trips in/out for system repair/maintenance.

ⁿ Life of hole TD is the maximum depth of the respective casing or drill system.

**Table 3.1-2
Drilling Performance Statistics by Stratigraphy for Well R-31**

| Drilling Systems | | | Phase I | | Phase II | | | Total |
|--|------|-----|--------------------------------|---------------------|-------------------------------------|--------------------------------------|------------------------------------|-------|
| | | | 4 1/4-in.- I.D. HSA Core | 11-in.- I.D. HSA | 13 3/8-in. Casing ^{a,b} | 12 1/4-in. Tricone ^{c,d} | 9 5/8-in. Casing ^{e,f} | |
| Stratigraphy | From | To | | | | | | |
| Alluvium (ft) | 0 | 24 | 24.0 | 24.0 | | | 48.0 | |
| <i>Rate of penetration (ft/hr)^g</i> | | | 9.0 | 8.7 | | | 8.9 | |
| Otowi Member (ft) | 24 | 264 | 226.0 | 13.0 | 227.0 | | 466.0 | |
| <i>Rate of penetration (ft/hr)^g</i> | | | 16.4 | 4.5 | 19.0 | | 17.3 | |
| Cement (ft) | 26 | 37 | | | 11.0 | | 11.0 | |
| <i>Rate of penetration (ft/hr)^g</i> | | | | | 44.0 | | 44.0 | |
| Guaje Pumice Bed (ft) | 264 | 280 | | | 16.0 | | 16.0 | |
| <i>Rate of penetration (ft/hr)^g</i> | | | | | 24.0 | | 24.0 | |
| Sediment (ft) | 280 | 285 | | | 5.0 | | 5.0 | |
| <i>Rate of penetration (ft/hr)^g</i> | | | | | 33.3 | | 33.3 | |
| Basalt (low gamma) (ft) | 285 | 444 | | | | 154.0 | 154.0 | |
| <i>Rate of penetration (ft/hr)</i> | | | | | | 15.9 | 15.9 | |
| Sediment (ft) | 444 | 450 | | | | 6.0 | 6.0 | |
| <i>Rate of penetration (ft/hr)^g</i> | | | | | | 27.7 | 27.7 | |
| Basalt (high gamma) (ft) | 450 | 473 | | | | 23.0 | 23.0 | |
| <i>Rate of penetration (ft/hr)^g</i> | | | | | | 17.3 | 17.3 | |
| Flow-top rubble (ft) | 473 | 484 | | | | 11.0 | 11.0 | |
| <i>Rate of penetration (ft/hr)^g</i> | | | | | | 10.2 | 10.2 | |
| Basalt (moderate gamma) (ft) | 484 | 513 | | | | 29.0 | 29.0 | |
| <i>Rate of penetration (ft/hr)^g</i> | | | | | | 32.8 | 32.8 | |
| Basalt (high gamma) (ft) | 513 | 534 | | | | 21.0 | 21.0 | |
| <i>Rate of penetration (ft/hr)^g</i> | | | | | | 27.4 | 27.4 | |
| Basalt (low gamma) (ft) | 534 | 596 | | | | 62.0 | 62.0 | |
| <i>Rate of penetration (ft/hr)^g</i> | | | | | | 16.8 | 16.8 | |
| Alluvial scoria (ft) | 596 | 626 | | | | 30.0 | 30.0 | |
| <i>Rate of penetration (ft/hr)^g</i> | | | | | | 17.1 | 17.1 | |
| Basalt (low gamma) (ft) | 626 | 693 | | | | 67.0 | 67.0 | |
| <i>Rate of penetration (ft/hr)^g</i> | | | | | | 8.2 | 8.2 | |
| Flow-base breccia (ft) | 693 | 703 | | | | 10.0 | 10.0 | |
| <i>Rate of penetration (ft/hr)^g</i> | | | | | | 35.3 | 35.3 | |
| Flow-base sediments (ft) | 703 | 710 | | | | 7.0 | 7.0 | |
| <i>Rate of penetration (ft/hr)^g</i> | | | | | | 30.0 | 30.0 | |

Table 3.1-2 (continued)

| Drilling Systems | | | Phase I | | Phase II | | | Total |
|--|------|------|--------------------------------|---------------------|-------------------------------------|--------------------------------------|------------------------------------|--------|
| | | | 4 1/4-in.- I.D. HSA Core | 11-in.- I.D. HSA | 13 3/8-in. Casing ^{a,b} | 12 1/4-in. Tricone ^{c,d} | 9 5/8-in. Casing ^{e,f} | |
| Stratigraphy | From | To | | | | | | |
| Puye fanglomerate (ft) | 710 | 745 | | | | 35.0 | | 35.0 |
| Rate of penetration (ft/hr) ^g | | | | | | 18.5 | | 18.5 |
| Puye fanglomerate (ft) | 745 | 780 | | | | 35.0 | 3.0 | 38.0 |
| Rate of penetration (ft/hr) ^g | | | | | | 16.2 | 25.7 | 17.0 |
| Puye river gravels (ft) | 780 | 900 | | | | 7.0 | 120.0 | 127 |
| Rate of penetration (ft/hr) ^g | | | | | | 3.2 | 21.8 | 20.8 |
| Puye fanglomerate (ft) | 900 | 935 | | | | | 35.0 | 35.0 |
| Rate of penetration (ft/hr) ^g | | | | | | | 26.3 | 26.3 |
| Puye river gravels (ft) | 935 | 1103 | | | | | 168.0 | 168.0 |
| Rate of penetration (ft/hr) ^g | | | | | | | 15.5 | 15.5 |
| Total footage drilled (ft) ^h | | | 250.0 | 37.0 | 259.0 | 497.0 | 326.0 | 1369.0 |
| Rate of penetration (ft/hr) ^g | | | 15.2 | 6.5 | 20.6 | 17.1 | 19.1 | 17.7 |

Note: Excludes 18-in. casing in Phase I and 11 3/4-in. casing in Phase II; no new footage was drilled with these.

^a 13 3/8-in. casing used a Holte 3-wing under-reamer, SD-12 hammer, and 7-in. RC rods.

^b From the surface to 26 ft, the 13 3/8-in. casing was tripped into the 18-in. surface casing.

^c 12 1/4-in. tricone bit used 7-in. RC rods.

^d From the surface to 285 ft, the 12 1/4-in. tricone open-borehole drill system was tripped into the 13 3/8-in. casing.

^e 9 5/8-in. casing used a Mitsubishi 2-wing eccentric under-reamer, IR 380 hammer, and 7-in. RC rods.

^f From the surface to 285 ft, the 9 5/8-in. casing was tripped into the 13 3/8-in. casing, and from 285 ft to 777 ft, the 9 5/8-in. casing was tripped into the 12 1/4-in. open borehole.

^g Rate does not include connect time or trip-in/out footage.

^h Total footage compiles all drilling in borehole. Borehole TD was 1103 ft. Total footage drilled (1369 ft) minus borehole TD (1103 ft) represents borehole footage (266 ft) where the borehole was over-reamed or redrilled with another drill system.

In mid October 1999, the U.S. Department of Energy (DOE) suggested that the proposed Phase II drilling technique (air-rotary casing advance with wet fluid assist) be replaced by mud-rotary drilling as a more cost-effective method than air-rotary drilling. This change in scope required that administrative documents (SSHASP, FIP, WCSF, MOU) be modified for management of drilling mud. SBDC visited the R-31 site to prepare a drilling plan that would make use of available mud-rotary equipment. In December 1999, however, drilling plans reverted to air-rotary casing advance with wet fluid assist because of concern that any contamination in perched groundwater zones encountered during mud-rotary drilling might be spread along with the mud-based fluids.

3.3 Phase II Drilling

A kickoff meeting was held on January 6, 2000, for the Phase II activities. Air-rotary methods were used for the Phase II drilling at the R-31 site to provide access to depths and lithologies that could not be reached by HSA methods. In particular, penetration of the Cerros del Rio lava flows could not have been

accomplished using an HSA drill rig. The completion of Phase II drilling by air-rotary methods, with reverse circulation, allowed access to the depths necessary to meet the data collection and well-emplacement goals for R-31.

To conduct the Phase II drilling, Dynatec Drilling Company, Inc. (formerly Tonto Drilling Company) mobilized a rented Foremost™ dual rotation (DR)-24 drill rig, a dust suppression system, and ancillary support equipment such as a diesel generator and a core logging trailer to the R-31 site. Dynatec provided a drilling supervisor, drilling crews, crew vehicles including 1-ton flatbed trucks, drilling rods, hammers, bits, a 5000-gal. water truck, a fuel truck, construction lights, an auxiliary air compressor, and a 5-ton boom truck for handling casing, drill rods, and heavy support apparatus such as casing jacks. The ER Project's FSF provided drill casings, drilling bits, a small front-end loader (Bobcat™), a dust suppression system, water containment tanks, depth-to-water meters, water sampling bailers, a sample filtration trailer, a diesel-powered electric generator, core boxes, chip trays, and an industrial sink for borehole material washing. The ER Project also provided escort vehicles, a laptop computer, a cellular telephone, equipment to measure water sample field parameters, a filtering apparatus, and a core-logging microscope. The Sample Management Office provided sample collection and shipping containers. ESH-18 provided the borehole geophysics trailer and a downhole pressure transducer and electronic data logger. The facility host (the Dynamic Experimentation Division [DX]) provided radio communication and a site security plan to comply with DX requirements.

From initial mobilization on January 12 to January 16, activities were conducted on a work schedule of one 12-hr shift per day. Starting on January 16, with the exception of down time for equipment repairs, cement curing, and facility shutdowns, drilling progressed on a work schedule of two 12-hr shifts per day, 7 days per week.

3.3.1 Phase II Drilling Chronology

Phase II drilling began on January 17, when a 13 3/8-in. retractable casing and under-reamer bit were tripped into the 18-in. surface casing to the cement at 26 ft bgs. As this system drilled through the cement plug at the base of the surface casing, the casing packoff blew out, requiring repair to control dust emissions. From January 17 through January 18, the 13 3/8-in. casing was advanced from 26 ft bgs to the former borehole TD of 250 ft reached during Phase I drilling. During the night shift of January 18 to 19, the 13 3/8-in. casing penetrated the Guaje Pumice Bed of the Otowi Member of the Bandelier Tuff from 264 to 280 ft, a sediment from 280 to 283 ft, and weathered Cerros del Rio basalt from 283 to 285 ft. During the next day shift on January 19, the 13 3/8-in. casing became stuck in the basalt at 285 ft. As Dynatec prepared to pull the 13 3/8-in. casing back up above the Guaje Pumice Bed, status lights indicated a malfunction of the diesel power source.

On January 21, a mechanic from Cummins Diesel visited the R-31 site to diagnose and repair the rented DR-24 drill rig. During the down time for drill rig repair, a decision was made to change to an open-borehole drilling system. Upon resuming drilling activities, the 13 3/8-in. casing was back-reamed until free at 282 ft, and the casing advance under-reamer bit was tripped out to the surface. During this effort, one of the two hydraulic rams in the drill rig mast broke.

The hydraulic ram failure did not require immediate repair, so during the night shift of January 21 to 22, the 12 1/4-in. tricone system was tripped in to 290 ft, and the borehole was advanced to 345 ft in moist, slightly vesicular basalt.

As of the night shift on January 21 to 22 and down to a depth of 345 ft, only air had been used as a drilling fluid. On January 22, the drilling crew started mixing TORKease® polymer and EZ-MUD® (polyacrylamide-polyacrylate copolymer) with municipal water obtained from a Los Alamos County fire-

protection hydrant located within the city limits of White Rock. The polymer slurries were used to improve drilling progress. During Phase II drilling, a total of five truckloads of municipal water (approximately 15,000 gal.) were transported to the R-31 site for use in mixing slurries. Footage intervals for which lubricating slurry was used are indicated in Table 3.3-1.

**Table 3.3-1
Footage Intervals Drilled Dry or with Lubricating Slurry, in Well R-31**

| Order of Use | Drilling Technique/Tools | Footage Intervals Drilled Dry (ft) | Footage Intervals Drilled with Lubricating Slurry (ft) |
|--------------|---|------------------------------------|--|
| 1 | HSA/4 1/4-in. I.D. | 0–250 | |
| 2 | HSA/11-in. I.D. | | 0–37 |
| 3 | Air rotary/13 3/8-in. casing | 26–285 | |
| 4 | Air rotary/open-hole 12 1/4-in. tricone | 290–345 | 345–787 |
| 5 | Air rotary/11 3/4-in. casing | | 285–325 |
| 6 | Air rotary/9 5/8-in. casing | | 777–1103 |

With the introduction of TORKease® and EZ-MUD® polymer slurry on January 22, drilling with an open-borehole tricone bit progressed to a depth of 485 ft in slightly vesicular basalt. Based on the amount of water return and pressure gauges on the drill rig, the driller noted possible formation water at this depth, although positive identification was difficult because of the use of water-based slurry to aid drilling. The borehole was rested while the drill rig and support equipment were refueled, but the water in the borehole had dissipated by the time measurements were again taken.

During the night shift of January 22 to 23, drilling with the open-borehole tricone bit and polymer slurry advanced to a depth of 545 ft in vesicular basalt. The driller noted groundwater based on the volume of water return. Initial return flow was approximately 25 gal./min, decreasing to approximately 10 gal./min. Field support personnel notified the appropriate Technical Team leaders that groundwater had been encountered. At this time, the borehole was rested, and field support personnel prepared to collect an airlifted groundwater screening sample from 545 ft bgs. This attempt produced only 2 gal. of water. Open-borehole drilling with the tricone bit and polymer slurry was resumed to a depth of 625 ft in moderately vesicular basalt. The borehole was rested while the drill rig and support equipment were refueled prior to shift change.

After the morning shift change on January 23, field support personnel measured water inside the drill string at 533.6 ft bgs using an electronic depth-to-water meter. Field support personnel notified the Technical Team leaders of the definite presence of groundwater and prepared to collect a screening sample from 625 ft bgs. After personnel on-site had airlifted for approximately 5 min to purge the drill system, the borehole produced several hundred gallons of murky red groundwater laden with oxidized scoriaceous basaltic cobbles. Field support personnel collected 25 gal. of groundwater from 625 ft bgs and transported the groundwater to the sample processing trailer at the FSF. After personnel had airlifted the groundwater screening sample, open-borehole drilling resumed with the tricone bit and polymer slurry to a depth of 635 ft in highly vesicular to scoriaceous basalt and to a depth of 685 ft in massive basalt. Based on the volume of water returned, the driller reported enhanced groundwater flow at 671 ft bgs.

During the night shift of January 23 to 24, the tricone bit was advanced with polymer slurry to a depth of 693 ft in massive basalt, 710 ft in flow-base deposits, and 765 ft in the fanglomerate facies of the Puye Formation. From 755 to 760 ft, no cuttings were recovered due to lost circulation. Open-borehole drilling

with the tricone bit and polymer slurry then progressed to a depth of 780 ft in the fanglomerate facies and 785 ft in the "Totavi Lentil" river gravels of the Puye Formation. Within the river gravels, the drilling rate decreased to approximately 1 ft/hr as the bit encountered loose quartzite sand, gravel, and cobbles.

During the day shift of January 24, open-borehole drilling with the tricone bit and polymer slurry advanced to a depth of 787 ft; at this depth, the loose formation caved constantly due to a lack of matrix induration. Because of the caving formation and poor borehole condition, it was decided to change from the open-borehole drilling system to a casing-advance system using the 11 3/4-in. casing. The changing out of the drilling system provided an opportunity to log the open borehole prior to advancing the 11 3/4-in. casing. The FSF dispatched the ESH-18 geophysical logging trailer to the R-31 site. Prior to logging, field support personnel measured the depth to water (DTW) in the open borehole at 528.1 ft bgs. Field support personnel then ran a caliper log of the open borehole to a depth of 680 ft, attempted to calibrate the natural gamma tool, and detected a faulty electrical connection in the gamma tool. The ESH-18 geophysical logging trailer was demobilized to the FSF for repair.

During the night shift of January 24 to 25, the 13 3/8-in. casing was worked free to ensure recovery of the casing following completion of the borehole. The crew then tripped in the 11 3/4-in. casing to 190 ft. During the day shift of January 25, field support personnel measured the DTW at 534.3 ft bgs. FSF personnel remobilized the repaired ESH-18 geophysical logging trailer to the R-31 site.

During the night shift of January 25 to 26, field support and FSF personnel performed downhole video logging to a depth of 725 ft and natural gamma logging to 720 ft, after which the ESH-18 geophysical logging trailer was demobilized to the FSF. For the rest of the shift, drilling personnel repositioned the drill rig to plumb over the borehole casings and tripped in the 11 3/4-in. casing from 190 to 285 ft bgs.

During the day shift of January 26, it was determined that the 11 3/4-in. casing would not pass through the casing shoe on the 13 3/8-in. casing, so the 11 3/4-in. under-reamer was repositioned, and the packoff was set between the two retractable casings.

During the night shift of January 26 to 27, TORKease® polymer slurry was used to work the 11 3/4-in. casing through the casing shoe on the 13 3/8-in. casing. The 11 3/4-in. casing was then advanced to 325 ft, at which depth progress was halted due to intense friction with the 13 3/8-in. casing. The 11 3/4-in. under-reamer drill system was then tripped out of the hole.

All field activities were suspended on January 27, due to host facility operations.

During the day shift of January 28, all 11 3/4-in. casing was tripped out of the hole and 9 5/8-in. casing was hauled from the FSF to the R-31 site.

During the night shift of January 28 to 29, the 9 5/8-in. casing was tripped in to 250 ft, the drill rig was repositioned over the borehole casings, and the 9 5/8-in. casing was advanced to 777 ft.

During the day shift of January 29, an Ingersoll Rand (IR) 380 hammer and a Mitsubishi 2-wing eccentric under-reamer bit for the 9 5/8-in. casing were tripped in to 777 ft. (The borehole had caved in from the former TD of 787 to 777 ft.) The 9 5/8-in. casing was advanced to 787 ft in quartzite-cobble-rich river gravels and to 827 ft in sand and gravel with quartzite. A large volume of sand and gravel was returned from this interval by the drilling circulation system and managed as drill cuttings.

During the night shift of January 29 to 30, the 9 5/8-in. casing was advanced to 847 ft in Puye Formation sand and gravel with quartzite. The high volume of gravel cuttings produced wore a hole in the side of the cyclone. The casing became tight in the borehole, so the 9 5/8-in. casing and drill system were pulled back to 827 ft. All field activities were suspended on January 30 due to host facility operations.

During the day shift of January 31, field support personnel measured the DTW at 532.05 ft bgs inside the drill system. The 9 5/8-in. casing was worked until free in the borehole and reamed back to 847 ft. The hole in the cyclone was repaired, and the 9 5/8-in. casing was advanced to 887 ft in sand and gravel with quartzite.

During the night shift of January 31 to February 1, the under-reamer drill system was tripped out for inspection. The bit was found to be in good condition.

During the day shift of February 1, the under-reamer drill system was tripped back into the 9 5/8-in. casing to a depth of 885 ft. Sheared bolts in the upper travel block head were repaired, and the 9 5/8-in. casing was advanced to 890 ft in sand and gravel with quartzite and to 893 ft in more dacite-rich gravels. At this time it was found that the drill rig was overheating. The rig was shut down to cool, after which the 9 5/8-in. casing was advanced to 897 ft. Drilling was again suspended pending diagnosis and repair.

During the day shift of February 2, the Cummins Diesel mechanic returned to the R-31 site and determined that the overheating problem was due to erroneous electrical signals in the diesel engine's computer sensors. He reset or turned off the appropriate sensors, and the 9 5/8-in. casing was advanced to 922 ft in the gravel deposits. At this depth, the casing became stuck, and the circulation system plugged with sand and gravel. At the end of the shift, the cyclone was disconnected so that a new one could be installed.

During the day shift of February 3, the new cyclone was installed, borehole circulation was unplugged, and the 9 5/8-in. casing was advanced to 1007 ft in quartzite-bearing gravels. All available water storage containers onsite had been filled to capacity, and drilling was halted until more storage could be obtained. In the interim, on February 4, a new fan belt was installed on the DR-24 diesel engine.

During the day shift of February 5, field support personnel measured the DTW at 525.1 ft bgs inside the drill system. The 9 5/8-in. casing was advanced to 1096 ft in quartzite-bearing gravels. Enhanced water returns were observed at 1090 ft, and additional tanks were obtained for water storage.

During the day shift of February 6, circulation was lost, and the casing became stuck. After the casing was worked free, it was advanced to 1103 ft in gravels. Drilling was halted at this point because of the difficulty in making further progress and the danger of losing tools; the TD of the R-31 borehole was 1103 ft at the end of shift number 51.

3.3.2 Phase II Drilling Summary

During Phase II, the DR-24 drill rig was mobilized to the R-31 site on January 12, 2000, and demobilized on April 28, 2000. Drilling production at another deep borehole (CdV-R15-3) required switching out the less powerful leased DR-24 drill rig at that site with the DR-24 rig from the R-31 site. Phase II operations, from kickoff meeting to the beginning of well completion activities, required 38 total shifts (Table 3.0-1). Drilling operations were typically conducted in two 12-hr shifts per day, 7 days per week, but were periodically suspended due to host-facility work restrictions. A detailed chronology of Phase II operations is provided in Appendix A.

Drilling techniques used during Phase II consisted of air-rotary under-reamer advance of two retractable casing strings (13 3/8-in. and 9 5/8-in.) and open-borehole drilling using a 12 1/4-in. tricone carbide button bit. The total footage drilled during Phase II by the various drilling techniques was 1082 ft. Of that footage, total footage drilled by the 13 3/8-in. casing advance system was 259 ft at an average rate of 20.6 ft/hr (Table 3.1-1)(not including 26 ft of open hole inside the 18-in. surface casing at that time). The footage drilled using the open-borehole drilling system was 497 ft at an average rate of 17.1 ft/hr (not including

285 ft of open hole inside the 13 3/8-in. casing at that time). The footage drilled using the 9 5/8-in. casing advance system was 326 ft at an average rate of 19.1 ft/hr (not including 777 ft of open hole inside the 13 3/8-in. casing and 12 1/4-in. open borehole at that time). The total Phase II footage does not include regular conditioning of the borehole or tripping drill systems to regain circulation and/or change bits. The compiled totals and rates for tripping tools into and out of the borehole include intervals within existing casings or open borehole, tremie pipes, and the well casing (in only). The total trip-in footage was 3475 ft at an average rate of 182.6 ft/hr, and the total trip-out footage was 5428 ft at an average rate of 141.6 ft/hr. Phase II performance statistics are summarized in Tables 3.1-1 and 3.1-2.

3.3.2.1 Casing Advancement (13 3/8 in.)

During Phase II, 13 3/8-in. retractable casing and an under-reamer drill system were tripped into the 18-in. surface casing to a depth of 26 ft and then advanced from 26 to 285 ft using air as the drilling fluid. The 13 3/8-in. casing was advanced within the Otowi Member of the Bandelier Tuff and associated units from 26 to 285 ft (259 ft total) at an average rate of 20.6 ft/hr (Table 3.1-1). The 13 3/8-in. casing drilled out the cement plug within the 18-in. surface casing from 26 to 37 ft, the Otowi Member ignimbrite from 37 to 264 ft, the Guaje Pumice Bed from 264 to 280 ft, and a sediment from 280 to 285 ft (Table 3.1-2). Advancement of the 13 3/8-in. retractable casing was terminated at 285 ft bgs because the casing became stuck in the Cerros del Rio lavas.

3.3.2.2 Open-Borehole Drilling

Open-borehole drilling using a 12 1/4-in. tricone bit was used to drill a total of 497 ft from 290 to 787 ft bgs. (The under-reamer bit used with the casing advance system to 285 ft drills 5 ft ahead of the casing.) Dynatec drilled a total of 418 ft from 290 to 708 ft bgs in Cerros del Rio lavas and intercalated deposits at an average rate of 17.4 ft/hr and a total of 79 ft from 708 to 787 ft bgs in the Puye Formation fanglomerate and quartz-poor and quartz-rich paleo-river gravels at an average rate of 16.1 ft/hr. (Table 3.1-2 provides a more detailed breakout of drilling rates.) Open-borehole drilling was suspended at a depth of 787 ft because the unconsolidated river gravels began to cave into the borehole.

3.3.2.3 Casing Advancement (11 3/4 in.)

After the open-borehole drilling, 11 3/4-in. retractable casing and an under-reamer drill system were tripped into the 13 3/8-in. casing to a depth of 285 ft. Due to deviation in the open borehole below the 13 3/8-in. casing, the 11 3/4-in. casing was tripped in with difficulty from 285 to 325 ft inside the 12 1/4-in. open borehole drilled in Cerros del Rio lavas. Use of the 11 3/4-in. casing was stopped at 325 ft due to binding between the casings.

3.3.2.4 Casing Advancement (9 5/8 in.)

Following the abandoned attempt to use the 11 3/4-in. casing, 9 5/8-in. retractable casing and an under-reamer drill system were tripped into the 13 3/8-in. casing and open borehole to a depth of 777 ft. The 9 5/8-in. casing was advanced 10 ft (from 777 to 787 ft bgs) in borehole slough and 316 ft (from 787 to 1103 ft bgs) in fanglomerates and river gravels at an average rate of 19.1 ft/hr (Table 3.1-2).

3.4 Overall Summary of Drilling Performance

The great variability of lithologies at the R-31 site had significant impact on drilling performance. Entirely different drilling systems were used for the Otowi Member of the Bandelier Tuff (HSA) versus the Cerros del Rio lavas and Puye Formation fanglomerates with river gravels (air-rotary). In addition, modifications

to bit and casing use were required for the different units drilled with the air-rotary system. Table 3.3-1 summarizes the shift information for all activities at the R-31 site. The total number of shifts for all activities was 112, but the shifts required for drilling were 6 for Phase I and 39 for Phase II. The total footage drilled during Phase I was 287 ft. During Phase II, the total footage drilled was 1082 ft (including redrilled fill). Although the percentage of drilling accomplished by HSA methods was 21% of shift time while the percentage of drilling shifts for air-rotary drilling was only 13%, the increased difficulty of drilling at greater depth accounts for much of this difference in performance. Overall, the drilling rates in all lithologies at the R-31 site varied between 15 and 21 ft/hr with the exception of the large (11-in.-I.D.) HSA, which was advanced at about half that rate (~7 ft/hr).

4.0 WELL CONSTRUCTION

The design for well R-31 was completed on February 10, 2000, using information from video logs, gamma logs, cuttings analysis, and driller observations. The design called for five screens: one at a possible perched horizon within the Cerros del Rio lavas, one spanning the regional water table, one within a fractured and potentially transmissive interval within the Cerros del Rio lavas, and two in likely transmissive gravels below the lavas (Figure 4.0-1).

4.1 Production Casing

Well construction consisted of installing stainless steel and carbon steel well casing as preparation for the multi-port Westbay™ sampling apparatus specified in the well design (Section 6.0). Dynatec installed the well casing from February 16 to 19, 2000, in six shifts. Table 4.1-1 lists the well casing materials installed from a temporary stickup above the ground surface of 6.0 ft to the bottom of the well at 1077.7 ft bgs. Steel centralizers were attached to the mild carbon steel well casing at 50-ft intervals. From 10 to 50 ft, steel tabs were welded to the mild carbon steel well casing at 10-ft intervals to provide well stabilization in the near-surface concrete annular fill. Stainless steel centralizers were attached to the well casing above and below each screened interval and spaced evenly at no greater than 50-ft intervals in blank casing sections between screens. Figure 4.0-1 illustrates the final well casing configuration and depths below the ground surface for each well component.

4.2 Annular Fill

Steel tremie pipe of 1 3/4-in. outer diameter (O.D.) and 1 3/8-in. I.D. was used to deliver annular materials at the specified design depths. Because of problems with flowing sand in the Puye Formation river gravels below 280 ft, a modified annular fill of natural slough plus coarse-sand amendment was specified at screens #4 and #5. The annular fill was installed from February 19 through March 5, 2000, in 28 shifts (Appendix A). Sands were emplaced at screened intervals to provide access to formation waters and to alleviate backfill slough; the sands were tremied into the annular space using municipal water to make a fluid slurry. Bentonite was emplaced between screened intervals to seal the annular space and prevent cross communication; the bentonite was delivered using EZ-MUD® mixed with municipal water as a fluid slurry. Portland cement (mixed at a ratio of 5 gal. water for each 100-lb bag of cement) was used to provide foundations for the annular fill and for wellhead protection of the annular space in the upper 67 ft of the borehole. During the emplacement of annular fill, a total of 13 truckloads of municipal water (approximately 39,000 gal.) were transported to the R-31 site.

Drawing Not to Scale

All depths in feet below ground surface

Steel tabs
At 10, 20, 30, 40,
and 50 ft

Centralizers
Every 50 ft and
above/below each
screen

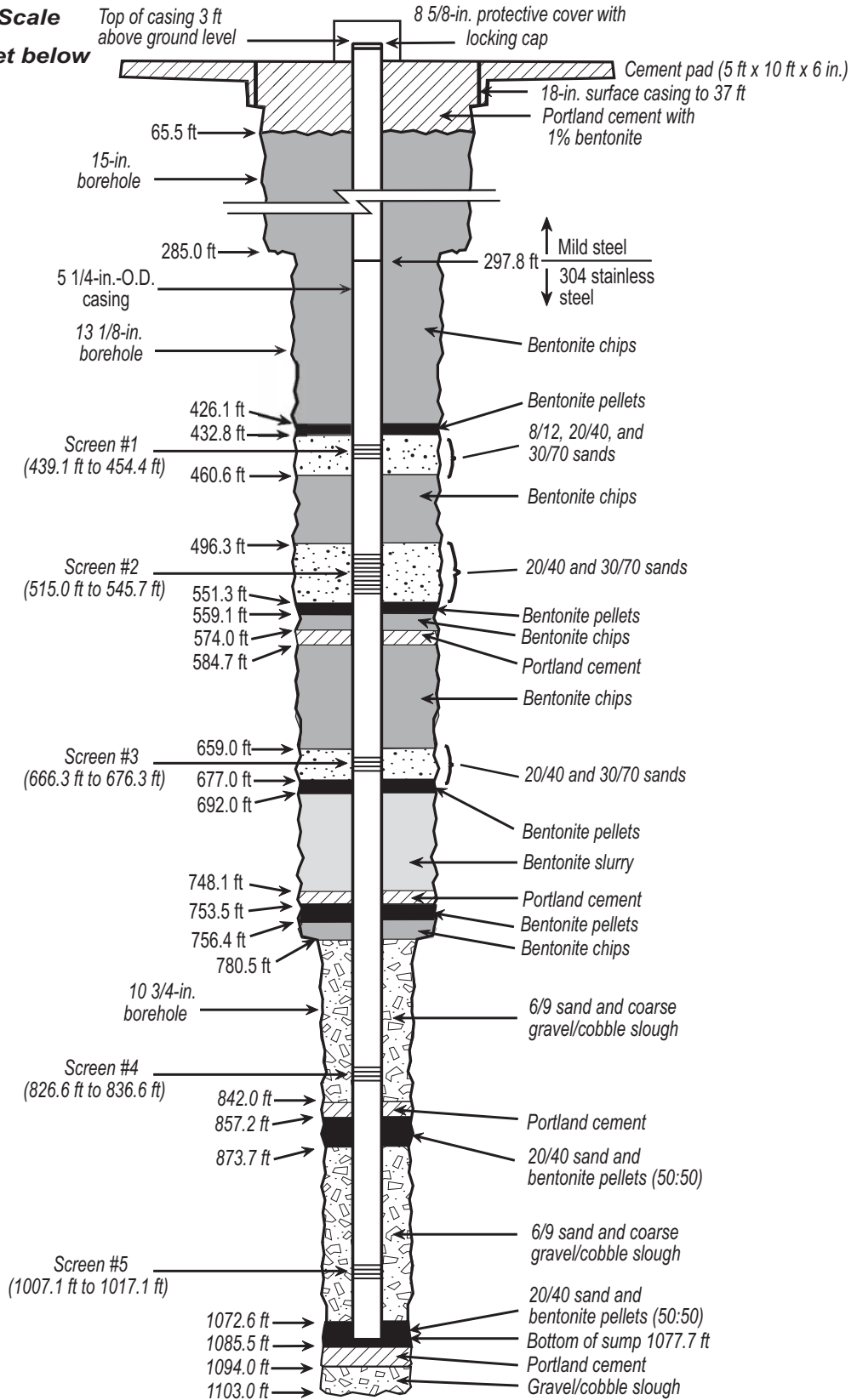


Figure 4.0-1. As-built well construction diagram for R-31

**Table 4.1-1
Well Casing Used in Well R-31**

| Component | Length (ft) | Casing Material | Depth bgs (ft) |
|-----------|-------------|--|-----------------------------------|
| Casing | 300.8 | Mild carbon steel plus 5' union | 3.0 above ground surface to 297.8 |
| Casing | 141.3 | Stainless steel | 297.8 to 439.1 |
| Screen #1 | 15.3 | Stainless steel 0.010 slot with one blank interval from 444.1 to 444.5 ft | 439.1 to 454.4 ^a |
| Casing | 60.6 | Stainless steel | 454.4 to 515.0 |
| Screen #2 | 30.7 | Stainless steel 0.010 slot with two blank intervals from 535.3 to 535.7 ft and 524.9 to 525.3 ft | 515.0 to 545.7 ^a |
| Casing | 120.6 | Stainless steel | 545.7 to 666.3 |
| Screen #3 | 10.0 | Stainless steel 0.010 slot | 666.3 to 676.3 ^a |
| Casing | 150.3 | Stainless steel | 676.3 to 826.6 |
| Screen #4 | 10.0 | Stainless steel 0.010 slot | 826.6 to 836.6 ^a |
| Casing | 170.5 | Stainless steel | 836.6 to 1007.1 |
| Screen #5 | 10.0 | Stainless steel 0.010 slot | 1007.1 to 1017.1 ^a |
| Sump | 60.6 | Stainless steel with end cap | 1017.1 to 1077.7 |

Note: All screens are rod-based, wire-wrapped. All casing is 5 1/4-in. O.D.

^a Screen depths are slotted intervals.

Table 4.2-1 provides a summary of the annular fill materials used. The final configuration of the annular materials is also illustrated in Figure 4.0-1.

**Table 4.2-1
Annular Fill Materials Used in Well R-31**

| Material | Amount | Unit |
|---|--------|---------|
| 20/40 sand ^a | 160 | bags |
| 30/70 sand ^b | 39.5 | bags |
| 6/9 sand ^c | 181 | bags |
| 8/12 sand ^c | 72 | bags |
| Benseal® bentonite ^d | 34.5 | bags |
| Holeplug® bentonite chips ^e | 711 | bags |
| Pelplug® bentonite pellets ^f | 100.5 | buckets |
| Portland cement ^g | 53 | bags |

^a 20/40 sand is medium-grained and used to pack screened intervals.

^b 30/70 sand is fine-grained and used to separate screen packs from bentonite.

^c 6/9 and 8/12 sands are coarse and used to plug formation fractures and matrix pores.

^d Benseal® is granular bentonite that produces a bentonite slurry when mixed with water.

^e Holeplug® bentonite is 3/8-in. angular and unrefined bentonite chips.

^f Pelplug® bentonite is 1/4-in. by 3/8-in. refined elliptical pellets.

^g Portland cement was mixed with municipal water at a ratio of 5 gal. water for each 100-lb bag of cement.

4.3 Well Development

During a first attempt at hydrologic testing, it was learned that the well had not been developed in accordance with the FIP. Screens #2, #3, #4, and #5 had only been “washed and jetted.” (Screen #1 was dry.) Furthermore, field parameters (temperature, specific conductance, turbidity, and pH) had not been monitored to verify the effectiveness of development. As this did not follow the planned procedure, the well was redeveloped after this first attempt at hydrologic testing. The well development data discussed below were gathered during the redevelopment effort. The total cycle of development and testing extended over a period of 20 days, from March 8 to March 27, 2000 (Appendix A). Surging and airlifting were used for preliminary development. Final development was accomplished by pumping. (The well was retested after completion of development, as specified in the FIP.)

4.3.1 Surging

A steel ball-float surge block was run through each screened interval by wireline, starting with screen #2 and working down. (Screen #1 was dry and hence could not be developed.) The surge block was lowered to the bottom of each screen, then slowly raised through each 1- to 2-ft length of screen a minimum of five times. When this process had been completed for all screens, the surge block was pulled out of the well. As no water was discharged in this process, the impact of surging on field parameters could not be checked.

4.3.2 Airlifting

In order to remove as much suspended material as possible prior to development by pumping, the well was cleaned by airlifting. First, the depth to fill accumulated in the sump was determined. Then, a dual-rod system (using H and N rods) was run to the sump, and it was cleared of sediment by airlifting. Next, each screened interval, in ascending order, was cleaned by airlifting. As this process produced water, the impact on field parameters was checked at regular intervals. This phase of development was halted when specific conductance and pH had leveled off and turbidity measurements were repeatedly <5 nephelometric turbidity units (NTU) or could not be improved.

Airlifting at screen #2 was not productive. However, 1 hr of airlifting reduced turbidity to <5 NTU at screen #3 (Figure 4.3-1) and to 5.5 NTU at screen #4. Airlifting was not very effective at screen #5. Turbidity actually increased during the first hour of airlifting, and after nearly 2 hr, turbidity was still at 60 NTU.

4.3.3 Pumping

Final development consisted of pumping each screened interval, in descending order, until turbidity was <5 NTU or could not be improved and other field parameters had leveled off. This was accomplished by operating a 10-hp submersible pump placed just below each screened interval. After the well had been allowed to rest for a brief period (approximately 15 minutes), the pumping and monitoring process was repeated to see if field parameters could be improved or at least reproduced. This was repeated three times (for a total of four episodes of pumping and monitoring). When field parameters were reproduced or could not be improved, pumping, and thus development, was halted. Results for the pumping stage of development at screen #4 are typical of the results for screens #2, #3, and #5 (Figure 4.3-2). Field-parameter readings throughout the pumping phase of well development are given in Table 4.3-1.

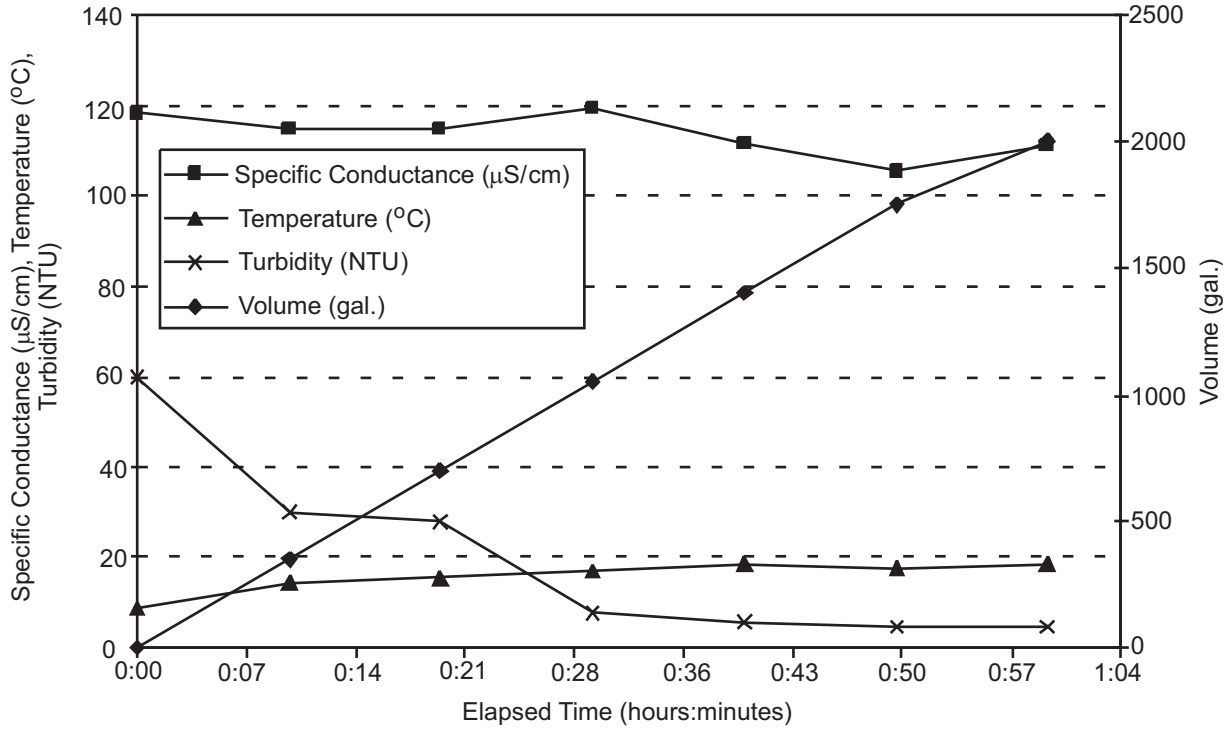


Figure 4.3-1. Well development data obtained by airlifting at screen #3 in R-31

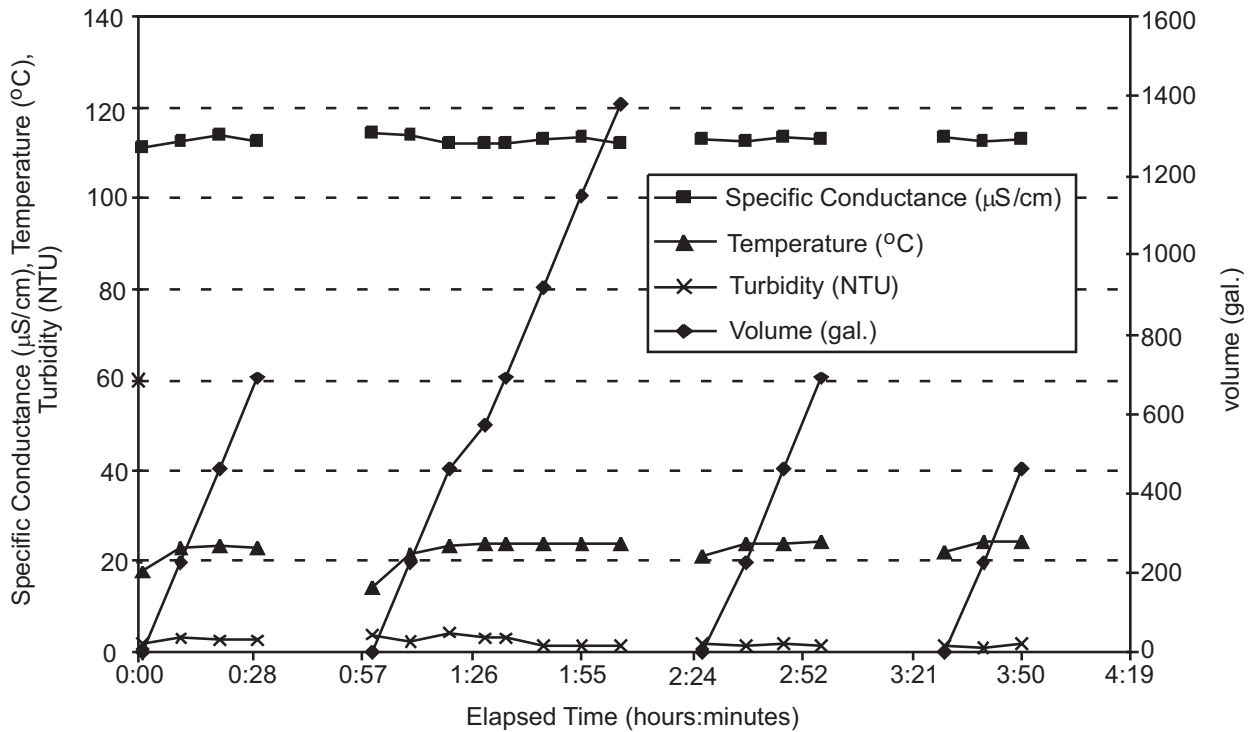


Figure 4.3-2. Well development data obtained by pumping at screen #4 in R-31

**Table 4.3-1
Summary of Final Development of R-31 by Pumping**

| Screen # | Elapsed Time (min) ^b | Water Produced (gal.) | Range of Field Parameters | | | |
|----------|---------------------------------|-----------------------|-------------------------------|---|-------------------------|-----------------------|
| | | | Temperature (°C) ^a | Specific Conductance (µS/cm) ^a | Initial Turbidity (NTU) | Final Turbidity (NTU) |
| 2 | 140 | 3400 | 16.3–22.6 | 180.9–112.5 | 86 | 0.89 |
| 3 | 230 | 5430 | 15.7–23.7 | 117–111.8 | 2.4 | 1.1 |
| 4 | 146 | 3220 | 17.9–24.5 | 111–112.9 | 1.9 ^c | 1.9 ^c |
| 5 | 154 | 2880 | 19.5–23.5 | 114–110.7 | 1.7 ^c | 2.7 ^c |

^a Presented in order of value at beginning, then value at end of pumping.

^b Time devoted to pumping only; not total time spent on final development.

^c Turbidity of water from both of these screens rose to as high as 4.5 NTU during pumping, then came back down to final value shown.

4.3.4 Well Development Issues

Three issues were raised concerning well development during the activities at the R-31 site. First, a discrepancy between the field development operations and those called for in the FIP was first identified at this site. No one was assigned the responsibility of ensuring that specified development procedures were being followed. To prevent that problem from happening again, the hydrology task leader was assigned the additional task of overseeing well development.

The second issue concerned well development methods. Surging removes fines from a screened interval by causing water to move both into and out of the formation. Normally, surging is accomplished by means of a block attached to steel rods. Use of a surge block on a wireline eliminates the opportunity to move water into the formation on the down stroke. A wireline was used at R-31 because of the potential that the strong down stroke provided by connection to rods could cause the annular fill to settle and possibly place bentonite opposite a screen. Experience at R-31 indicates that this potential disruption of annular fill is unlikely and is outweighed by the benefits of rigorous development.

The third issue concerned targeting of individual screens during development. Isolating screened intervals for at least the final stage of development (pumping) would be ideal. However, this isolation was not possible because an apparatus for pumping between straddle packers was not available. Thus, the source of the water produced in the pumping phase of development was uncertain. Nonetheless, based on monitoring of field parameters, each screened interval appeared to be adequately developed by the three-phase scheme that was used.

4.4 Wellhead Completion

Wellhead completion involved pouring a reinforced 5 ft by 10 ft by 6 in.-thick cement pad around the well casing to ensure long-term structural integrity of the well. In addition, the concrete pad was designed to support a small lockable steel housing for well instrumentation. The concrete pad was poured by Buschman Construction on December 1, 2000. A brass survey pin labeled R-31 was installed in the northwest corner of the concrete pad. In addition, four removable steel bumper posts were installed at the corners of the concrete pad to prevent vehicular disturbance.

5.0 HYDROLOGIC TESTING

Hydrologic testing was conducted at the R-31 site to obtain information on aquifer properties. As the well was completed with multiple screens, only straddle-packer/slug-injection tests were possible. Two rounds of testing were required because the well had been inadequately developed prior to the first round. During the first round, tests were performed for all five screened intervals. After more thorough well development (three phases, as described in Section 4.3), a second round of testing was conducted. Only screens #3 and #4 were retested. Screen #1 was omitted because it was dry, and retesting of screen #2 was deemed inappropriate because it straddles the top of the regional zone of saturation, with a portion of the screen lying above the water table. In the interest of time, Screen #5 was not retested. (The rig was needed at the next site.)

Hydrologic testing at the R-31 site involved the slug-injection of municipal water at a constant rate for a brief period and monitoring of the water-level response for 30 to 60 minutes. Water-level recovery was monitored for a similar period of time. Injection was accomplished by means of the straddle-packer/injection assembly shown in Figure 5.0-1. The water level was monitored by means of a transducer placed within the water-filled rod to which the packer assembly was attached. The data obtained from well testing are discussed in Section 10.2.2.

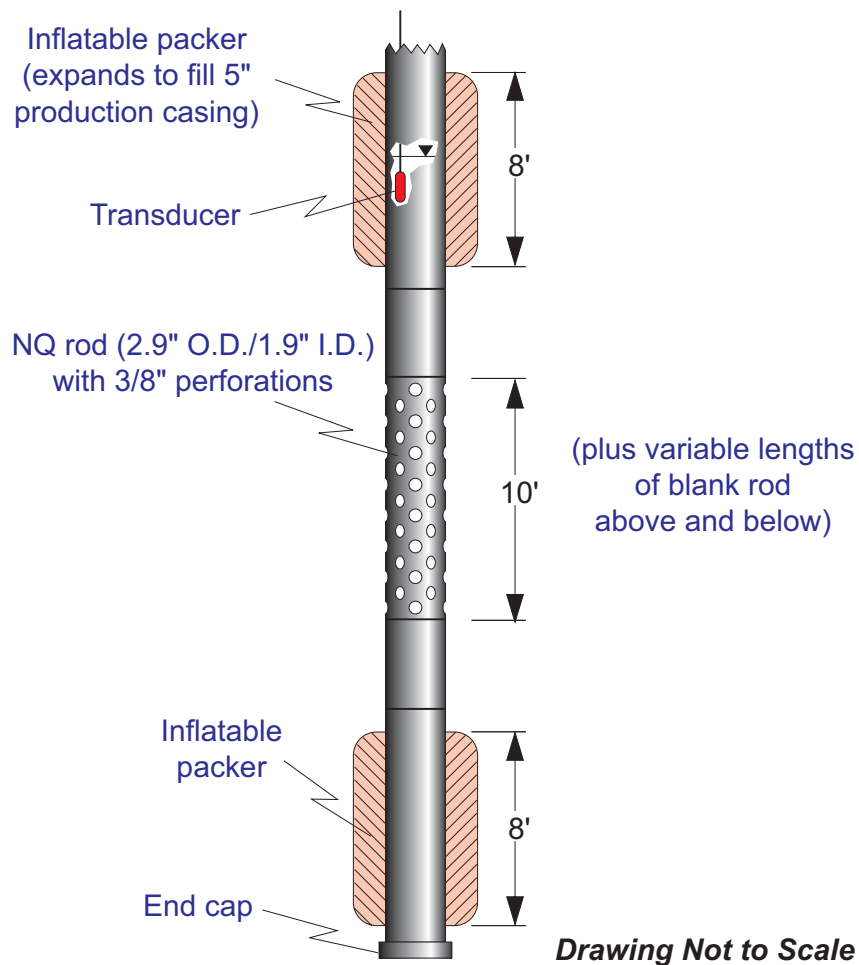


Figure 5.0-1. Straddle-packer assembly used for hydrologic testing at the R-31 site

6.0 WESTBAY™ INSTRUMENTATION

Following well development, a Westbay™ MP55 system for groundwater monitoring was installed in the steel-cased well. Model 2523 MOSDAX System sampler probe equipment is used to collect groundwater samples from the completed well.

A Multi-Port (MP) Casing Installation Log, which specifies the location of each Westbay™ well component, was prepared in the field by Westbay™ in consultation with the Laboratory. The log was based on a draft of the well completion diagram. Available geophysics and an as-built video taken inside the steel well casing were also reviewed before MP55 measurement ports, pumping ports, and packers were sited within the well. The Laboratory approved the final version of the MP Casing Installation Log in the field on September 26, 2000, prior to installation of Westbay™ components. The approved MP Casing Installation Log was used as the installation guide in the field.

The stainless steel well casing arrangement included a 10-ft length of blank casing above each screen section instead of the usual 20-ft length. As a result, the pair of packers immediately above each screened interval was shifted up by 10 ft to position the packers in a single, continuous, 20-ft length of stainless steel casing.

A measurement-port coupling and associated magnetic location collar were included in each primary monitoring zone to provide the capability to measure fluid pressures and collect fluid samples. A pumping port coupling was also included in the screened zones to provide purging, sampling, and hydraulic conductivity testing capabilities. Additional measurement port couplings were included below the pumping ports for monitoring hydraulic tests.

Measurement port couplings were included in quality assurance (QA) zones (QA zones for testing Westbay™ MP55 system integrity) to provide QA testing capabilities. The QA measurement ports were positioned below each of the packers to permit routine operation of the squeeze relief venting with the packer inflation equipment during the inflation process.

The MP casing components were set out in sequence according to the MP Casing Installation Log on racks near the borehole. Casing lengths were numbered in order, beginning with the lowermost, as an aid in confirming the proper sequence of components. The sequential MP casing component numbers are given on the MP Casing Installation Log and are used in the following text to identify selected MP casing components (packers and ports).

The appropriate coupling was attached to each piece of MP casing. Magnetic location collars were attached 2.5 ft below the measurement ports in each of the primary monitoring zones and 2.5 ft below coupling No. 128 near the top of the well. The length of each MP casing section was measured with a steel tape to confirm nominal lengths, and the data were entered on the field copy of the MP Casing Installation Log.

The MP casing components were lowered into the well in sequence with a Smeal work-over rig provided by the Laboratory. Each casing joint was tested with a minimum internal pressure of 300 psi for one minute to confirm hydraulic seals. Commercially available de-ionized water purchased by Westbay™ was used for the joint tests. A record of each successful joint test and the placement of each MP casing component was made on the field copy of the MP Casing Installation Log.

The suspended weight of the MP casing components was monitored during lowering to confirm that the operating limits of the MP System casing components were not exceeded. Lowering of the MP casing to the target position was successfully completed on April 4, 2000.

After the MP casing was lowered into the borehole, the water level inside the MP casing was left at a depth of more than 871 ft below the top of the MP casing to confirm hydraulic integrity. The open-hole water level was 524 ft below the top of the 5.5-in.-O.D. stainless steel well casing. With this differential pressure acting on the MP casing string, the water level inside the MP casing was stable overnight, indicating that the MP casing was water-tight.

After the components were lowered into the well and the hydraulic integrity of the MP casing had been confirmed, the MP casing string was positioned as shown on the MP Casing Installation Log. The datum for the borehole was ground level. The MP casing string was supported with the top of coupling No. 129 at a depth of 0.13 ft.

The packers were inflated on April 5 and 6, 2000, using de-ionized water. The packers were inflated in sequence beginning with the lowermost. All of the packers were inflated successfully, and QA tests showed that all of the packer valves were closed and sealed.

After lowering and final positioning of the MP casing were carried out, the tensile load at the top of the MP casing was 900 lb. Westbay's™ standard procedure for de-stressing the MP casing was carried out. The MP casing was lowered before inflation of packers No. 9 and 5 to distribute some of the weight of the MP casing to the packers. The final load at the top of the MP casing was 500 lb. During the de-stressing, the top of coupling No. 129 was lowered from the starting point of 0.13 ft to a final depth of 0.63 ft. A sketch of the as-built top of the MP casing and of the final positions of the MP casing components is provided in Appendix F. Table 6.0-1 summarizes depth information for key components.

**Table 6.0-1
Depths of Key Westbay™ MP55 System Components in Well R-31**

| Zone No. ^a | Screen Interval ^b (ft) | Sand Pack Interval ^b (ft) | MP Casing No. (from MP Log) | Packer No. | Packer Serial No. (0612) | Nominal Packer Position ^c (ft) | Magnetic Collar Depth (ft) | Measurement Port Depth ^c (ft) | Pumping Port Depth ^c (ft) | Port Name ^a |
|-----------------------|--------------------------------------|--|--------------------------------|------------|-----------------------------|---|-------------------------------|--|--|------------------------|
| | | | 87 | 1 | 022 | 414.8 | | | | |
| SQA1 | | | 86 | | | | None | 419.2 | | SQA1 |
| | | | 85 | 2 | 013 | 424.6 | | | | |
| Zone 1 | 439.1 to 454.4 | 432.8 to 460.6 | 81 | | | | 456.3 | 453.8 | | MP1A |
| | | | 80 | | | | | 459.2 | PP1 | |
| | | | 79 | | | | | 464.8 | MP1B | |
| | | | 78 | 3 | 017 | 468.5 | | | | |
| LQA1 | | | 77 | | | | 473.0 | | LQA1 | |
| | | | 75 | 4 | 018 | 488.2 | | | | |
| SQA2 | | | 74 | | | | | 492.7 | | SQA2 |
| | | | 73 | 5 | 023 | 498.1 | | | | |
| Zone 2 | 515.0 to 545.7 | 496.3 to 551.3 | 69 | | | | 534.7 | 532.2 | | MP2A |
| | | | 68 | | | | 544.0 | 542.5 | | MP2B |
| | | | 67 | | | | | | 547.9 | PP2 |
| | | | 66 | | | | | | 553.5 | MP2C |
| | | | 65 | 6 | 027 | 557.2 | | | | |

Table 6.0-1 (continued)

| Zone No. ^a | Screen Interval ^b (ft) | Sand Pack Interval ^b (ft) | MP Casing No. (from MP Log) | Packer No. | Packer Serial No. (0612) | Nominal Packer Position ^c (ft) | Magnetic Collar Depth (ft) | Measurement Port Depth ^c (ft) | Pumping Port Depth ^c (ft) | Port Name ^a |
|-----------------------|--------------------------------------|--|--------------------------------|------------|-----------------------------|--|-------------------------------|---|---|------------------------|
| LQA2 | | | 64 | | | | | 561.7 | | LQA2 |
| | | | 56 | 7 | 016 | 641.1 | | | | |
| SQA3 | | | 55 | | | | | 645.6 | | SQA3 |
| | | | 54 | 8 | 020 | 650.9 | | | | |
| Zone 3 | 666.3 to 676.3 | 659.0 to 677.0 | 51 | | | | 672.8 | 670.3 | | MP3A |
| | | | 50 | | | | | 675.6 | | PP3 |
| | | | 49 | | | | | 681.3 | | MP3B |
| | | | 48 | 9 | 028 | 685.0 | | | | |
| LQA3 | | | 47 | | | | | 689.5 | | LQA3 |
| | | | 35 | 10 | 021 | 801.7 | | | | |
| SQA4 | | | 34 | | | | | 806.2 | | SQA4 |
| | | | 33 | 11 | 026 | 811.6 | | | | |
| Zone 4 | 826.6 to 836.6 | natural fill plus sand | 30 | | | | 833.4 | 830.9 | | MP4A |
| | | | 29 | | | | | 836.3 | | PP4 |
| | | | 28 | | | | | 841.9 | | MP4B |
| | | | 27 | 12 | 014 | 845.6 | | | | |
| LQA4 | | | 26 | | | | | 850.1 | | LQA4 |
| | | | 12 | 13 | 015 | 982.2 | | | | |
| SQA5 | | | 11 | | | | | 986.6 | | SQA4 |
| | | | 10 | 14 | 025 | 992.0 | | | | |
| Zone 5 | 1007.1 to 1017.1 | natural fill plus sand | 7 | | | | 1013.8 | 1011.3 | | MP5A |
| | | | 6 | | | | | 1016.7 | | PP5 |
| | | | 5 | | | | | 1022.3 | | MP5B |
| | | | 4 | 15 | 019 | 1026.0 | | | | |
| LQA5 | | | 3 | | | | | 1030.5 | | LQA5 |

^a LQA = long quality assurance zone or port, SQA = short quality assurance zone or port, MP = measurement port, PP = pressure port.

^b All depths are with respect to ground level. Depths of sand pack and screened intervals are from Figure 4.0-1.

^c All depths of MP casing components are the depth to the top of the respective coupling.

After packer inflation was completed, fluid pressures were measured at each measurement port. The fluid pressure profile measurements were taken on April 7, 2000. At that time, the in-situ formation pressures may not have recovered from the pre-installation and installation activities. Longer term monitoring may be required to establish representative fluid pressures.

A plot of the piezometric levels in all zones, including QA zones, based on the April 7 pressure measurements, was examined to confirm proper operation of the measurement ports and to check on the presence of annulus seals between adjacent monitoring zones. All of the measurement ports operated

normally. Each of the packers was supporting a differential hydraulic pressure, a finding that confirmed the integrity of the packer seals.

7.0 GEODETIC SURVEY OF COMPLETED WELL

Well R-31 was geographically surveyed on February 13, 2001, using the Global Positioning System (GPS). A Trimble 4000 SSE dual-frequency base receiver was set up and initialized over control monument B3902 in TA-39 to conduct a real-time kinematic survey. Coordinate values for the control were from the 1992/1993 GPS survey establishing the Laboratory control network. The datum for the horizontal control network is the North America Datum of 1983 (NAD-83). Results are summarized in Table 7.0-1.

**Table 7.0-1
Geodetic Data for Well R-31**

| Description | Easting | Northing | Elevation (feet above mean sea level) |
|----------------------------------|-----------|-----------|--|
| Brass monument in R-31 pad | 1637353.8 | 1745648.4 | 6362.5 |
| Top of plate on Westbay™ casing | 1637356.3 | 1745642.3 | 6363.7 |
| Top of collar on Westbay™ casing | 1637356.3 | 1745642.1 | 6364.1 |

The receiver provided position data relative to the World Geodetic System (WGS) 1984 ellipsoid, and algorithms within the survey controller transformed the WGS-84 position to the New Mexico State Plane coordinate system using the NAD-1983. Measurements are referenced to the National Geodetic Vertical Datum of 1929 (NGVD 1929). The Facility for Information Management, Analysis, and Display (FIMAD) location identification number for characterization well R-31 is AN-00001. Figure 7.0-1 illustrates the positions of surveyed reference points at the R-31 site.

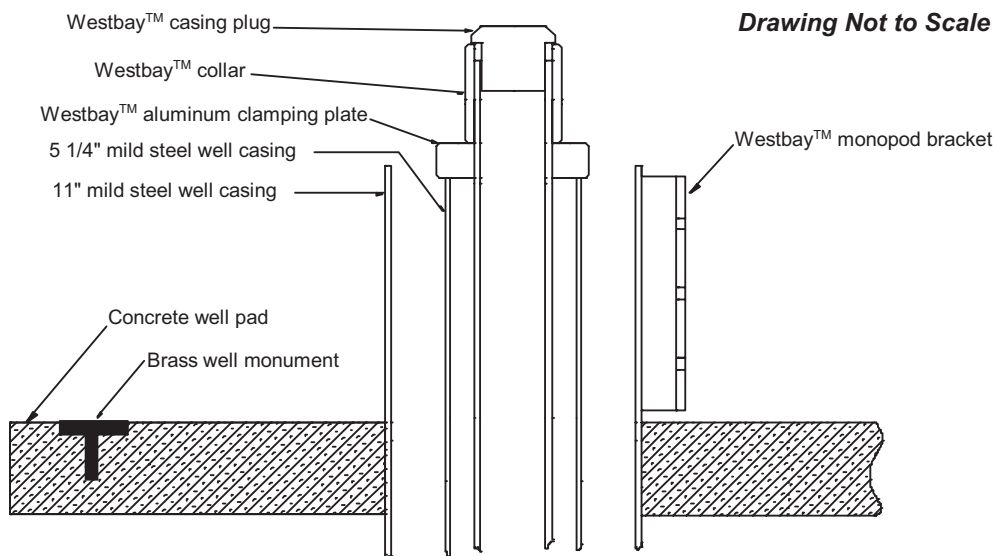


Figure 7.0-1. Geodetic survey points at well R-31

PART II: ANALYSES AND INTERPRETATIONS

8.0 GEOLOGY

Geologic units encountered in R-31 consist of, in descending order: alluvium; the Otowi Member of the Bandelier Tuff including the basal Guaje Pumice Bed; sediment beneath the Bandelier Tuff; lavas, interflow units, and subflow deposits of the Cerros del Rio volcanic field; and deposits of the Puye Formation including both fanglomerates and river gravels. Depths and elevations of the contacts between these units are shown in Figures 8.0-1a and 8.0-1b, with a comparison to the predicted stratigraphy based on the 3-D geologic model available at the time drilling began (Figure 8.0-1a). Notable differences between the predicted and as-drilled stratigraphy are the greater thickness of the Otowi Member of the Bandelier Tuff, the correspondingly deeper base of the Cerros del Rio lava sequence, and the much greater abundance of "Totavi"-like river gravels relative to fanglomerates within the Puye Formation. Throughout this section the term "Totavi" is used in quotes because of a published constraint requiring >80% quartzite and other resistant lithologies from northern New Mexico (plutonic and metamorphic lithologies) to qualify for this designation (Dethier 1997, 49843). The Puye Formation river gravels in R-31 contain fewer quartzite and granitic clasts (averaging ~34%, based on data in Appendix C) but are nevertheless related to the Totavi in origin, deposited by through-going river systems.

A brief summary of unit characteristics is given in the following sections, and a lithologic log is provided in Appendix C. A model of the topography on top of the Cerros del Rio lavas is shown in Figure 8.0-2. Interpretive geologic sections through existing boreholes are shown in Figures 8.0-3 (north to south) and 8.0-4 (northwest to southeast). These interpretive sections emphasize the two units that differed most notably from predicted depth or thickness at the R-31 site: Cerros del Rio lavas and "Totavi" river gravels. In both cross sections, the exceptional thickness of Puye river gravels ("Totavi") stands out at the R-31 site. These gravels extend well below the present level of the Rio Grande. The cross sections also show that the regional water table is within the Cerros del Rio lavas throughout much of the southern and eastern Laboratory site.

Descriptions of geologic units are based on examination of cuttings, geophysical logs, drilling information, and laboratory examination of borehole materials. Core was collected through most of the Otowi Member of the Bandelier Tuff (to the 250-ft depth), but samples of the Otowi Member were not collected for detailed geologic characterization because this unit is better known than those at greater depth. Cuttings were collected during Phase II drilling to TD. The cuttings were collected by reverse circulation, minimizing the admixture of materials from upper portions of the borehole.

Cuttings samples were used to gather petrographic, mineralogic, and geochemical data from units beneath the Bandelier Tuff. These data are primarily used to define and identify the units that compose the Laboratory's 3-D geologic model. Additional information provided by these data include the presence or absence of alteration that affects hydrogeologic properties, particularly the occurrence of clay alteration and evidence of water-rock interaction. Petrographic data were obtained both by binocular microscope examination of cuttings at the site and by petrographic microscope using thin sections prepared from representative cuttings samples (Appendix D). Mineralogic data were obtained by quantitative x-ray diffraction (QXRD). Geochemical data were collected from cuttings samples by x-ray fluorescence (XRF). In addition, $^{39}\text{Ar}/^{40}\text{Ar}$ ages were determined for the uppermost and lowermost Cerros del Rio lavas to aid in stratigraphic correlation.

Figure 8.0-1b shows the locations of well screens in R-31 in relation to the stratigraphy. Knowledge of the lithologies at screen locations is particularly important for relating geochemistry, petrology, mineralogy, and sedimentology to the interpretation of waters sampled from the screened intervals.

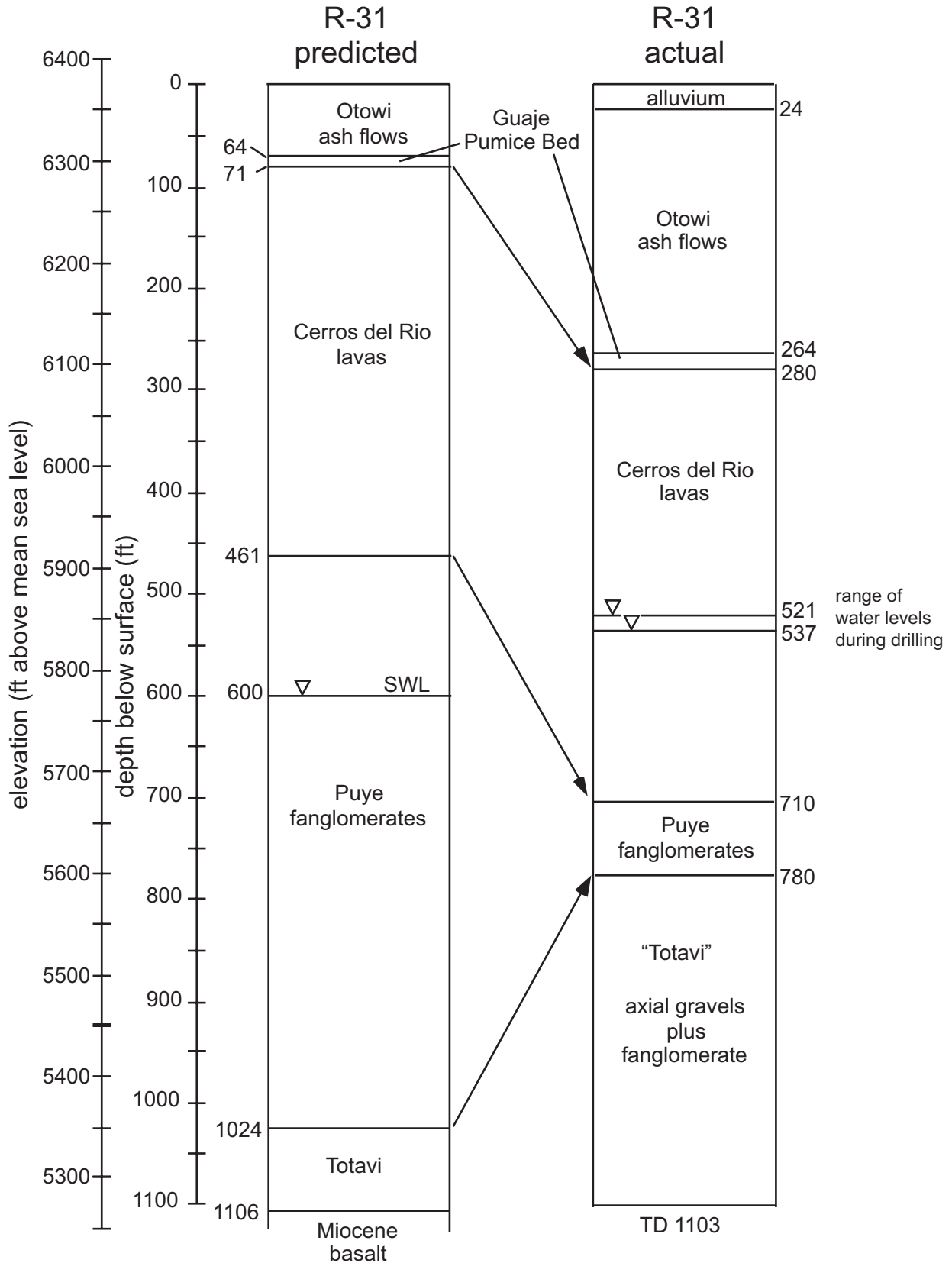


Figure 8.0-1a. Predicted and as-drilled stratigraphy at R-31

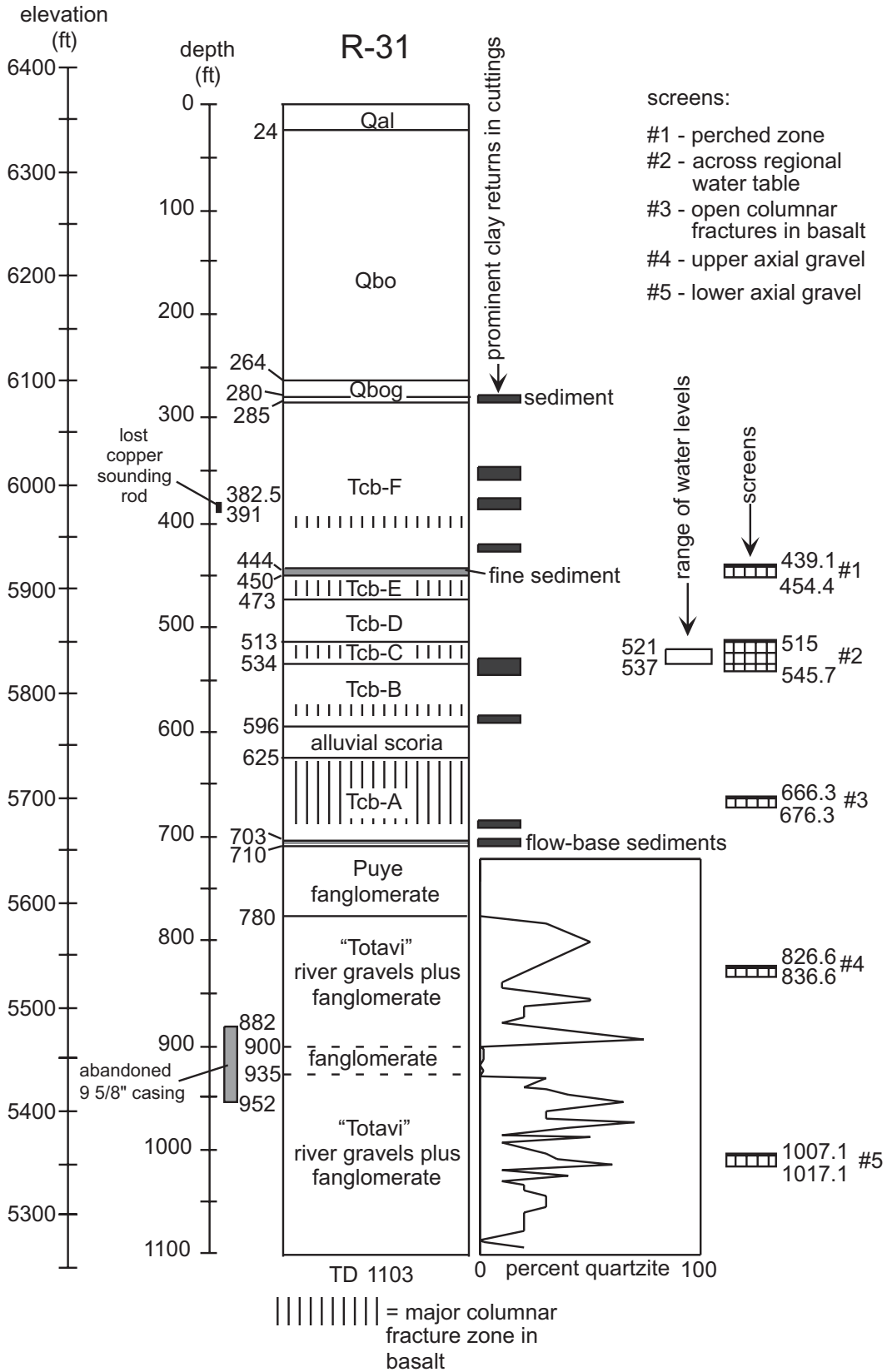
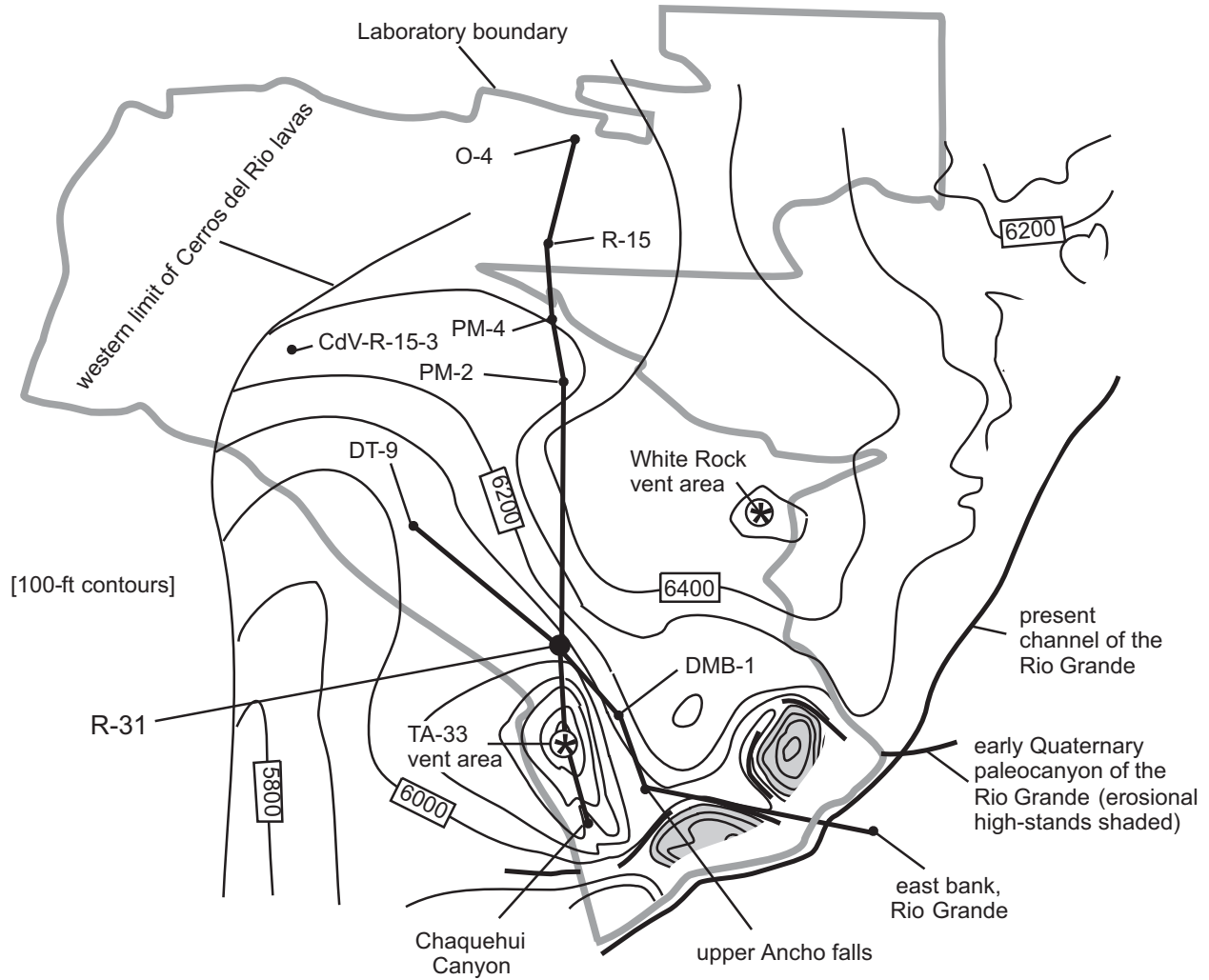
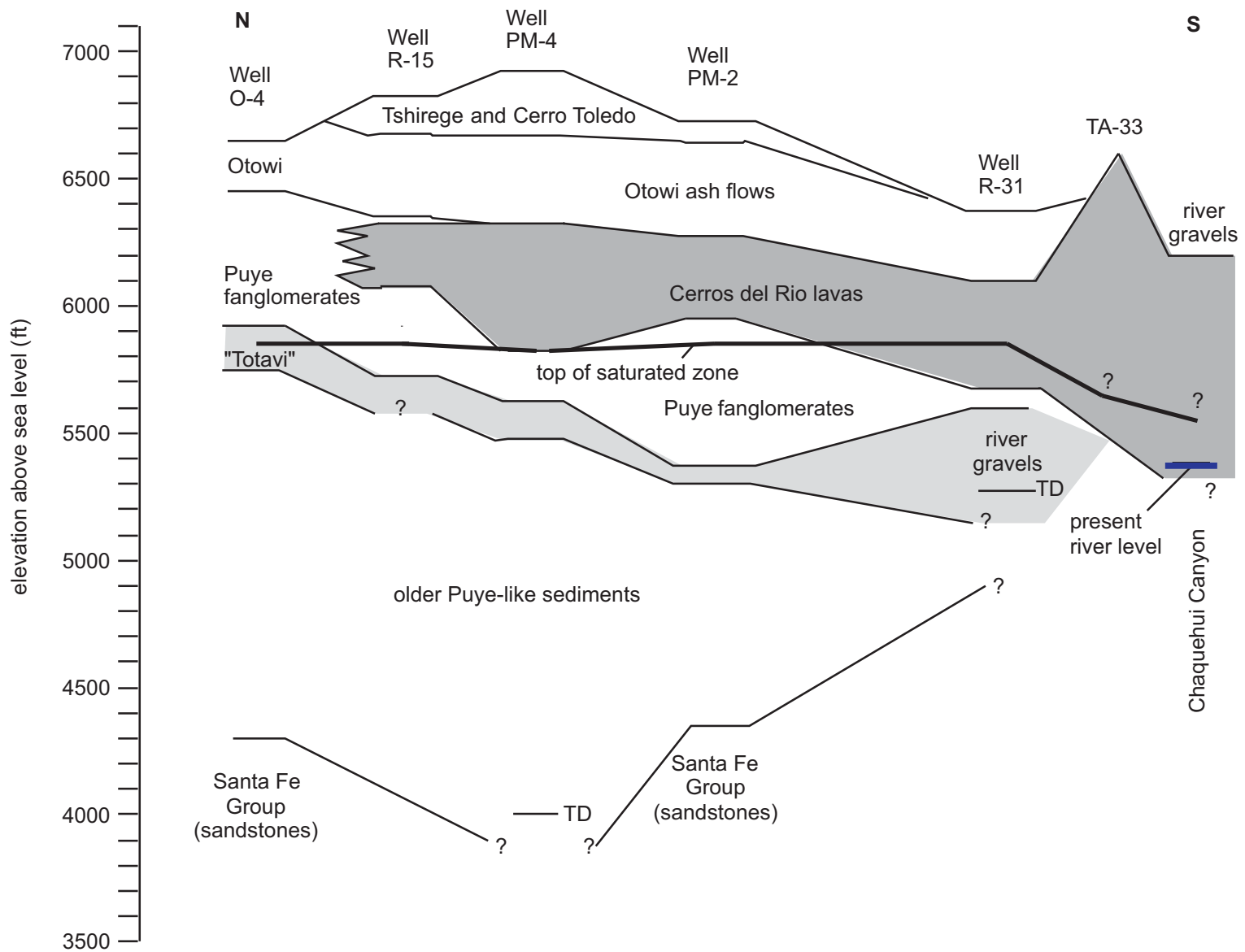


Figure 8.0-1b. Details of as-drilled stratigraphy at the R-31 site



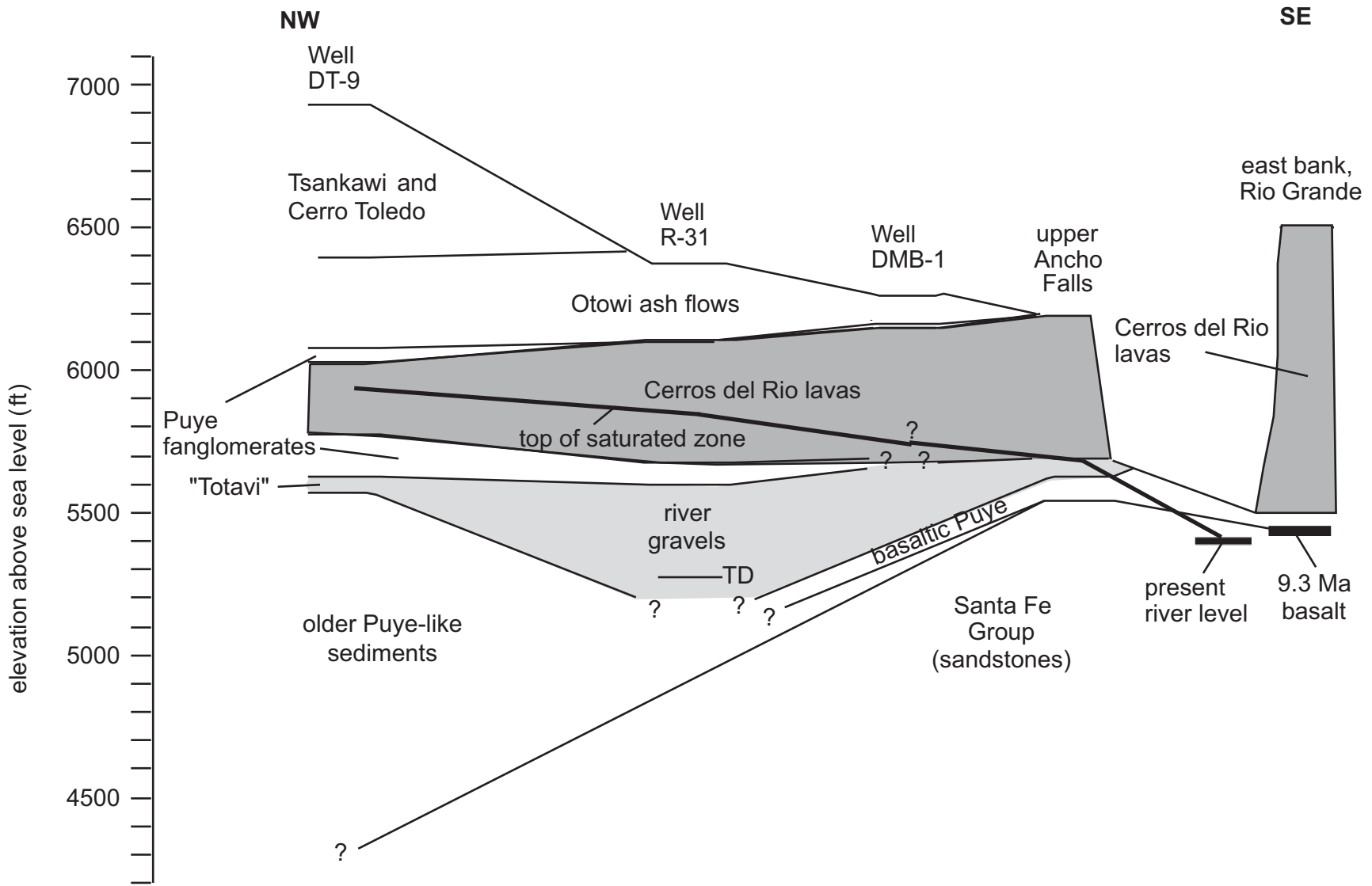
Note: Contours show interpretive elevation at the top of the Cerros del Rio lavas; high-stands in the Cerros del Rio lavas are either vent areas (asterisks) or high points isolated by paleocanyons at the Rio Grande (shaded).

Figure 8.0-2. Locations of R-31, other boreholes, outcrop control points, and interpretive geologic sections



Note: Question marks indicate contacts or water levels that have not yet been confirmed through drill-hole evidence.

Figure 8.0-3. Interpretive north-south geologic section from O-4 through R-31 to Chaquehui Canyon



Note: Question marks indicate contacts or water levels that have not yet been confirmed through drill-hole evidence.

Figure 8.0-4. Interpretive northwest-southeast geologic section from DT-9 through R-31 to the east side of the Rio Grande

In the sections that follow, emphasis is placed on those chemical, mineralogic, petrographic, and age data needed to constrain unit identification and correlation with the 3-D geologic model. The presence or absence of particular alteration minerals (e.g., carbonates and clays) is also discussed because of the influence such minerals have on groundwater movement and composition. Mineralogy is also a factor in understanding reactive transport.

8.1 Alluvium (0- to 24-ft depth)

During Phase I drilling, samples collected by HSA showed that alluvium (Qal) in R-31 extended to the 24-ft depth. The alluvium consists of detritus derived from the Bandelier Tuff and from lava domes of predominantly dacitic composition in the Tschicoma Formation. No samples of alluvium were selected for more detailed analysis.

8.2 Bandelier Tuff (Ash Flows of the Otowi Member, 24- to 264-ft depth; Guaje Pumice Bed of the Otowi Member, 264- to 280-ft depth)

Prior to drilling at the R-31 site, the 3-D geologic model of the site geology placed the bottom of the Bandelier Tuff at ~6300 ft above sea level. The as-drilled thickness of lower Bandelier Tuff (Otowi Member) is much greater than anticipated, and the unit has a basal elevation of 6082 ft. Core samples collected from the Otowi Member ash flows (Qbo) down to the 250-ft depth were analyzed for moisture and anion/stable-isotope content; the results of these measurements are summarized in Sections 10.1 and 11.1, respectively.

Core samples of the Otowi Member ash flows consist of nonwelded vitric tuff with abundant phenocrysts of feldspar and bipyramidal euhedral quartz. The ash flows contain a few percent of intermediate-composition volcanic lithic clasts. The Guaje Pumice Bed (Qbog) is a vitric pumice airfall with pumice sizes generally ~1–2 cm but ranging up to ~5–8 cm. Natural gamma logging through the Otowi Member ash flows and the Guaje Pumice Bed is summarized in Figure 8.2-1. The consistent rise in natural gamma signal through the ash flows with increasing depth is typical of this unit. The higher natural gamma signal in the Qbog unit is observed in many but not all boreholes. Spectral gamma data (Appendix G) indicate that the increase in the natural gamma signal in the Otowi Member is related principally to an increase in the abundance of Th and U.

8.3 Sediment Beneath the Bandelier Tuff (280- to 285-ft depth)

A clay-rich sediment was encountered in the interval from 280 to 285 ft. Cuttings from this interval included abundant dark earth-brown clay, with basalt fragments. The clay coloration at this horizon differs from the reddish clays more typical of alteration within the underlying basalt units. The actual thickness of the sediment may be less than 5 ft. The radiometric $^{39}\text{Ar}/^{40}\text{Ar}$ plateau age of 2.3 million years ago (Ma) for the immediately underlying Cerros del Rio basalt (Table 8.3-1) allows a maximum of ~700,000 years for sediment accumulation between the end of Cerros del Rio volcanism and the emplacement of the 1.61 Ma Otowi Member.

Analysis by thin section shows this sediment to be an immature basaltic sand. Detrital grains in the thin section include quartz, plagioclase, amphibole, clinopyroxene, magnetite, and olivine, as well as small clasts of basaltic rock. Although the sediment is largely basaltic in nature, the presence of quartz and amphibole detritus indicates some sources other than the nearby Cerros del Rio basaltic lithologies. Oxalate concentrations suggest soil development within these sediments (Section 11.1.1).

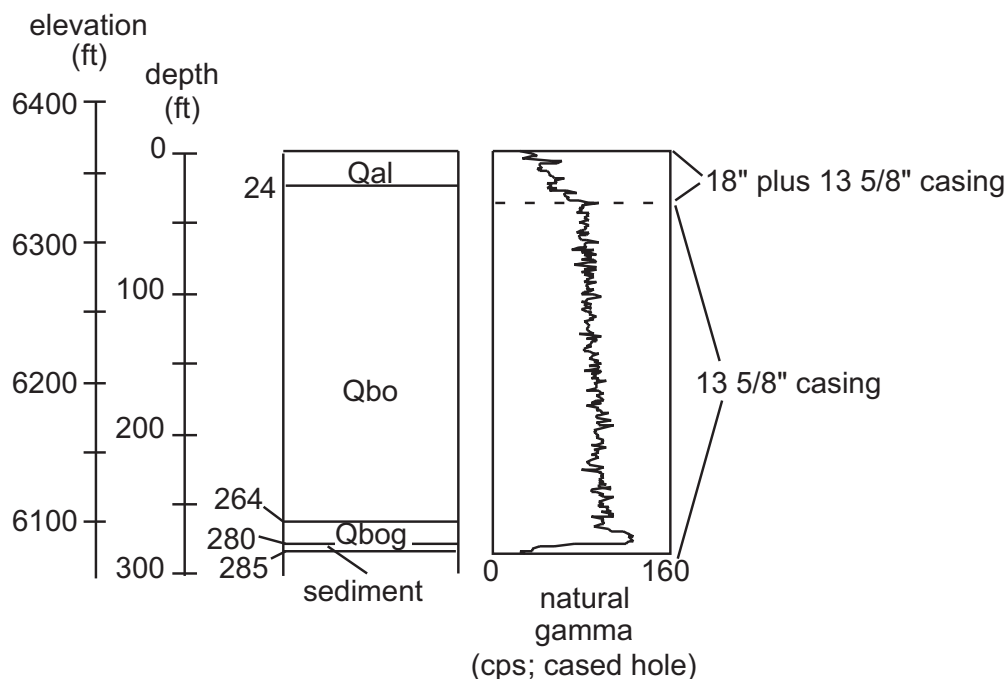


Figure 8.2-1. Stratigraphy and natural gamma properties of the upper 285 ft of R-31

8.4 Cerros del Rio Lavas, Interflow Units, and Subflow Deposits of the Cerros del Rio Volcanic Field (285- to 710-ft depth)

Lavas, interflow rubble and scoria zones, and subflow deposits of the Cerros del Rio volcanic field were encountered in the interval from 285 to 710 ft. Both video borehole logging and natural gamma information were used to define six major flow sequences (A through F) as shown in Figure 8.0-1b. (The video log can be examined in Appendix H, which is contained in the CD attached to the back cover of this report.) The video log revealed a probable soil horizon from 444 to 450 ft, and examination of cuttings and video information indicated a sequence of alluvial scoria (reworked to in-place basaltic detritus) from 596 to 625 ft. Samples representative of the uppermost and lowermost flows were selected for ³⁹Ar/⁴⁰Ar radiometric dating to constrain the timespan of Cerros del Rio volcanism at the R-31 site and to support correlations with other Cerros del Rio volcanic units. Results of ³⁹Ar/⁴⁰Ar dating are summarized in Table 8.3-1.

**Table 8.3-1
³⁹Ar/⁴⁰Ar Ages of Cerros del Rio Basalt Samples from R-31**

| Sample | Material Dated | Percent ³⁹ Ar in Plateau | Plateau Age ±2σ |
|----------------------|------------------------|-------------------------------------|-----------------|
| R-31 285-290, basalt | Groundmass concentrate | 91.5% | 2.34 ± 0.33 Ma |
| R-31 680-685, basalt | Groundmass concentrate | 71.1% | 2.69 ± 0.15 Ma |

The ³⁹Ar/⁴⁰Ar plateau ages indicate that the sequence of Cerros del Rio lavas (Tcb) at the R-31 site was emplaced within a timespan of ~350,000 years. These ages compare with ages of 2.36 to 2.48 Ma for lavas in Ancho Canyon, 2.39 to 2.54 Ma for lavas at TA-33, 2.45 to 2.78 Ma for lavas at Chaquehui Canyon, 2.39 to 2.59 Ma for lavas near Water Canyon, and 2.54 Ma on the eastern side of White Rock Canyon (WoldeGabriel et al. 1996, 54427).

Although the cuttings, video, and natural gamma data support the distinction of the six major flow sequences A through F shown in Figure 8.0-1b, chemical and petrographic data collected from the cuttings support a larger-scale grouping of flow sequences C through F that is distinct from sequences A and B. In chemical composition, the tholeiites of flow sequence F are readily related to nearby lavas, but deeper units differ from known local lavas. The regional relationships between lava types are described below. Figure 8.4-1 shows the relationships between the Cerros del Rio stratigraphy, the natural gamma signal, and several chemical parameters that illustrate the variability among Cerros del Rio lavas at the R-31 site.

8.4.1 Cerros del Rio Alkalic to Tholeiitic Lavas (285- to 534-ft depth), Including a Sedimentary Horizon (444- to 450-ft depth)

The upper 249 ft of Cerros del Rio lavas at the R-31 site is a sequence that passes from alkalic to tholeiitic composition from bottom to top. The flow series C, D, E, and F encompassed in this sequence (Figures 8.0-1b and 8.4-1) were identified through a borehole video survey (Appendix H) as discrete flow packages with distinctive flow-contact rubble zones. Although this sequence might be interpreted as a volcanic continuum, the intercalation of a 6-ft sediment horizon between flow series E and F indicates a hiatus in eruptive history. This horizon is important because it provides a clay-rich perching zone in otherwise unsaturated Cerros del Rio deposits above the regional water table.

Figure 8.4-1 shows that this alkalic-to-tholeiitic sequence passes from alkalic basalts with ~1050 to 1150 ppm Sr at the base (flow series C and D) into intermediate compositions of ~700 ppm Sr (flow series E and the base of series F) and a thick sequence of over 100 ft of tholeiitic lava (upper series F) with ~350 to 500 ppm Sr. Thin-section petrography indicates significant variability within this sequence. Flow series C includes an olivine-clinopyroxene porphyritic basalt (515- to 520-ft sample) with granular aggregates of clinopyroxene. Flow series D includes lava (495- to 500-ft sample) that is also olivine-clinopyroxene porphyritic, but the clinopyroxene phenocrysts are more abundant than olivine and are euhedral and concentrically zoned. The sample from the top of flow series E (450- to 455-ft sample) includes fragments of olivine-porphyritic basalt with olivine phenocrysts in either a vitric or fine-grained matrix. Above the sedimentary interval at the 444- to 450-ft depth, flow series F varies internally from lava with abundant (~9%) coarse (up to 2 mm) olivine phenocrysts (435- to 440-ft sample) to olivine-plagioclase porphyritic lava (390- to 395-ft depth) and olivine-porphyritic lava with subophitic pyroxene (285- to 290-ft sample). In addition to the systematic variation from top to bottom in chemical parameters such as Sr content (Figure 8.4-1), the variety of textural types in this series indicates differing crystallization histories superimposed on compositional variation.

The sediment at the 444- to 450-ft depth represents a hiatus in volcanic activity with accumulation of fine-grained detritus. Samples of this sediment were separated from basalt in the cuttings from 450 to 455 ft; the basalt portion (450-455B) is described above and in Table 8.4-1, and the mineralogic analysis of the sediment portion (450-455SS) is described in Table 8.4-2. In thin section, the sediment is a fine-grained (~20 to 30 μm) siltstone with a clay-rich matrix cementing grains of quartz, biotite, feldspar, amphibole, and muscovite. Basaltic pumices that are largely vitric adhere to some of the siltstone fragments, but the pumices were not included with the siltstone fraction (Table 8.4-2). The siltstone without pumice is the only glass-free sediment analyzed from R-31. The mineralogic analysis also shows this to be the most clay-rich sample analyzed, with the only significant content of kaolinite as well as smectite and the greatest amount of zeolite (clinoptilolite). The abundance of quartz silt grains and common muscovite in this sediment indicates distant sources unrelated to the basaltic lavas beneath and above this sediment. The fine grain size and abundance of readily-lofted mica suggest an eolian origin.

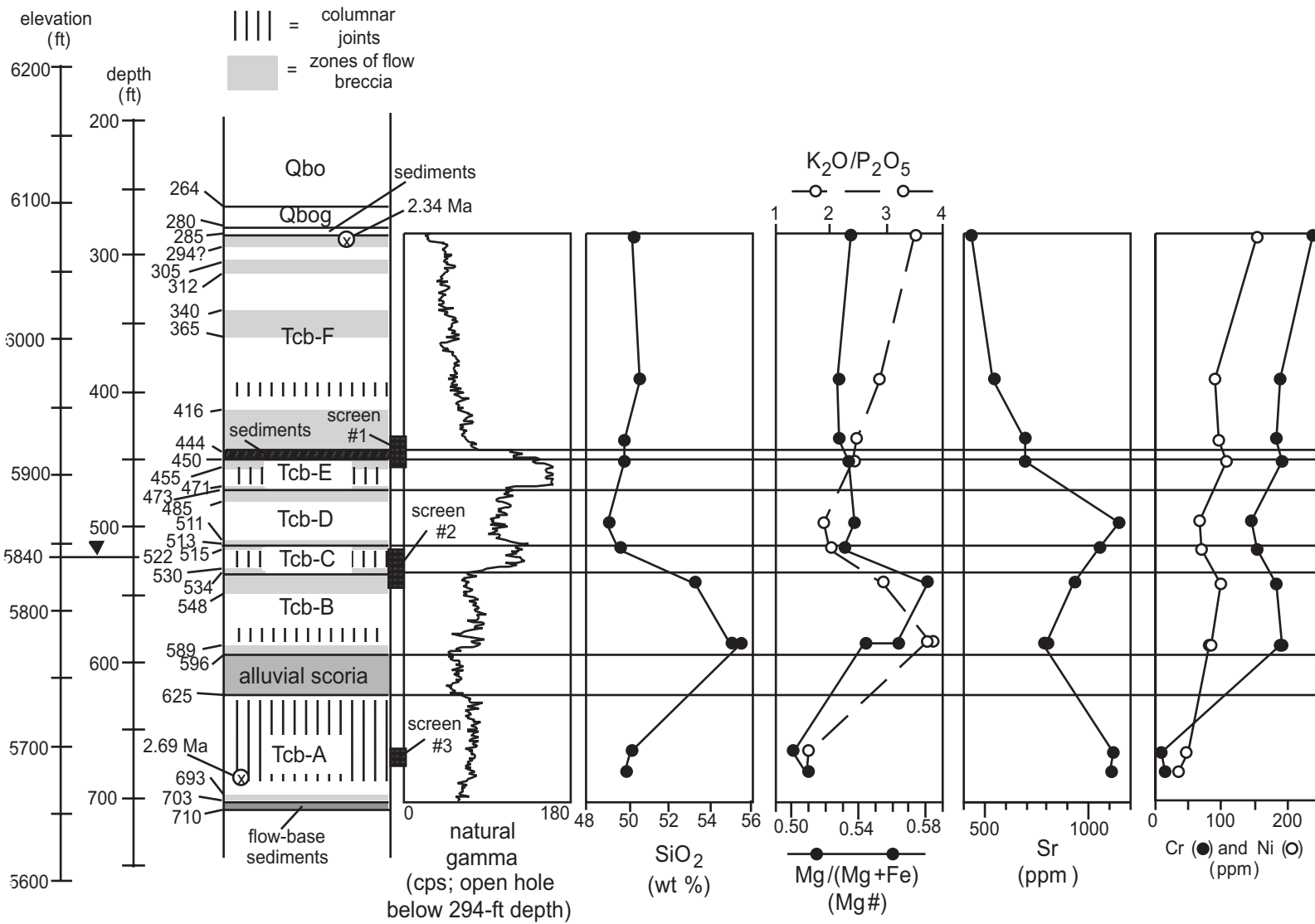


Figure 8.4-1. Relations between Cerros del Rio stratigraphy, natural gamma signal, SiO₂ contents, Mg/(Mg+Fe) ratios, K₂O/P₂O₅ ratios, and contents of selected trace elements (Sr, Cr, Ni) at R-31

Table 8.4-1
XRF Analyses of Cerros del Rio Lavas from R-31

| Sample Number ^a | R-31 285-290 | R-31 390-395 | R-31 435-440 | R-31 450-455B | R-31 495-500 | R-31 515-520 | R-31 540-545 | R-31 585-590G ^b | R-31 585-590R ^b | R-31 665-670 | R-31 680-685 |
|---|--------------|--------------|--------------|---------------|--------------|--------------|--------------|----------------------------|----------------------------|--------------|--------------|
| Flow series | F | F | F | E | D | C | B | B | B | A | A |
| Major Elements (wt %) | | | | | | | | | | | |
| SiO ₂ | 50.24 | 50.61 | 49.79 | 49.83 | 49.00 | 49.60 | 53.25 | 54.99 | 55.54 | 50.10 | 49.82 |
| TiO ₂ | 1.44 | 1.45 | 1.58 | 1.58 | 1.53 | 1.55 | 1.32 | 1.14 | 1.11 | 1.45 | 1.46 |
| Al ₂ O ₃ | 15.62 | 16.07 | 16.27 | 15.95 | 16.11 | 16.22 | 15.69 | 15.59 | 15.62 | 17.47 | 17.36 |
| FeO ^c | 8.93 | 7.01 | 4.69 | 5.57 | 5.27 | 4.87 | 4.45 | 4.21 | 2.97 | 5.21 | 5.42 |
| Fe ₂ O ₃ ^c | 2.30 | 3.57 | 5.74 | 4.94 | 4.70 | 4.99 | 3.78 | 3.75 | 4.91 | 4.65 | 4.31 |
| MnO | 0.17 | 0.17 | 0.17 | 0.17 | 0.16 | 0.16 | 0.14 | 0.13 | 0.12 | 0.15 | 0.15 |
| MgO | 7.09 | 6.40 | 6.20 | 6.44 | 6.20 | 5.93 | 6.09 | 5.48 | 4.94 | 5.28 | 5.42 |
| CaO | 8.85 | 9.00 | 9.13 | 9.07 | 9.79 | 9.58 | 7.97 | 7.42 | 7.29 | 8.56 | 8.56 |
| Na ₂ O | 3.16 | 3.37 | 3.53 | 3.50 | 3.28 | 3.47 | 3.73 | 3.70 | 3.76 | 4.24 | 4.09 |
| K ₂ O | 1.04 | 1.12 | 1.37 | 1.35 | 1.47 | 1.52 | 1.94 | 1.95 | 1.89 | 1.24 | 1.24 |
| P ₂ O ₅ | 0.30 | 0.39 | 0.56 | 0.56 | 0.79 | 0.77 | 0.66 | 0.51 | 0.51 | 0.78 | 0.80 |
| LOI ^d | -0.51 | -0.26 | -0.06 | -0.10 | 0.50 | 0.23 | 0.05 | 0.19 | 0.30 | -0.37 | 0.03 |
| Total | 99.12 | 99.16 | 99.05 | 98.96 | 98.30 | 98.66 | 99.01 | 98.86 | 98.67 | 99.12 | 98.64 |
| Trace Elements (ppm) | | | | | | | | | | | |
| V | 189 | 187 | 191 | 179 | 192 | 203 | 154 | 143 | 115 | 172 | 165 |
| Cr | 237 | 190 | 183 | 193 | 144 | 153 | 183 | 191 | 189 | <8 | 15 |
| Ni | 154 | 90 | 96 | 108 | 68 | 69 | 100 | 85 | 82 | 48 | 35 |
| Zn | 101 | 93 | 85 | 90 | 83 | 94 | 74 | 74 | 69 | 90 | 104 |
| Rb | 22 | 19 | 22 | 22 | 23 | 23 | 38 | 35 | 36 | 16 | 18 |
| Sr | 432 | 537 | 696 | 692 | 1145 | 1049 | 923 | 797 | 776 | 1121 | 1099 |
| Y | 41 | 38 | 28 | 33 | 30 | 24 | 34 | 29 | 35 | 31 | 16 |
| Zr | 147 | 167 | 191 | 203 | 224 | 233 | 235 | 208 | 197 | 226 | 224 |
| Nb | 17 | 17 | 30 | 25 | 36 | 26 | 30 | 24 | 27 | 32 | 36 |
| Ba | 358 | 508 | 711 | 711 | 1005 | 1004 | 1040 | 997 | 1037 | 818 | 773 |

Note: Values reported in weight percent or parts per million. Analytical errors (2σ) are SiO₂, 0.7; TiO₂, 0.01; Al₂O₃, 0.2; FeO and Fe₂O₃, 0.06; MnO, 0.01; MgO, 0.08; CaO, 0.1; Na₂O, 0.1; K₂O, 0.05; P₂O₅, 0.01; V, 10; Cr, 8; Ni, 10; Zn, 12; Rb, 5; Sr, 25; Y, 6; Zr, 30; Nb, 7; and Ba, 50.

^a Number ranges indicate depth ranges of cuttings in feet.

^b Sample from 585-590 was analyzed as separate red (R) and gray (G) subsamples.

^c Ferrous/ferric ratio determined by digestion and titration.

^d LOI = loss on ignition; negative numbers indicate oxidation of ferrous iron during ignition.

Table 8.4-2
X-Ray Diffraction (XRD) Analyses of Sediments from R-31 (Weight %)

| Sample ^a | Smectite | Kaolinite | Clinoptilolite | Mordenite | Tridymite | Cristobalite | Quartz | Alkali Feldspar | Plagioclase | Glass | Hematite | Mica | Hornblende | Augite | Olivine | Dolomite | Total |
|---|----------|-----------|----------------|----------------|-----------|--------------|--------|-----------------|-------------|-------|----------|------|------------|--------|---------|----------|-------|
| Sediment between basalt flows | | | | | | | | | | | | | | | | | |
| R-31 450-455SS | 36.1 | 1.0 | 2.7 | — ^b | — | — | 29.6 | 6.4 | 22.8 | — | 0.3 | 3.2 | 0.2 | — | — | — | 102.5 |
| Alluvial scoria between basalt flows | | | | | | | | | | | | | | | | | |
| R-31 600-605 | 5.0 | — | — | — | — | — | — | 3.6 | 53.0 | 20.3 | 2.1 | — | — | 11.8 | 5.1 | — | 100.9 |
| Sediment below lavas (sandstone component) | | | | | | | | | | | | | | | | | |
| R-31 705-710 | 31.6 | — | 1.1 | — | 0.8 | 0.9 | 12.2 | 5.1 | 30.5 | 21.3 | 0.3 | 0.2 | — | — | — | — | 104.0 |
| Puye sediments | | | | | | | | | | | | | | | | | |
| R-31 730-735 fanglomerate | 7.4 | — | 0.5 | — | 4.0 | 4.8 | 3.0 | 6.7 | 31.1 | 35.1 | 0.4 | 0.5 | 0.5 | 2.3 | — | 0.8 | 97.2 |
| R-31 760-765 fanglomerate | 5.7 | — | — | — | 4.0 | 6.7 | 1.4 | 9.5 | 32.9 | 29.8 | 0.6 | 0.6 | 0.1 | 4.0 | — | — | 95.3 |
| R-31 830-835 river gravel | 4.8 | 0.1 | — | — | 2.0 | 4.3 | 28.9 | 11.6 | 34.6 | 10.9 | 0.4 | 1.2 | 0.1 | — | — | — | 99.0 |
| R-31 920-925 fanglomerate | 1.4 | — | 0.6 | — | 8.2 | 11.5 | 2.2 | 20.9 | 36.6 | 17.7 | 0.6 | 1.3 | 0.1 | — | — | — | 101.1 |
| R-31 1005-1010 river gravel | 2.6 | — | — | 0.5 | 2.5 | 4.3 | 7.6 | 8.5 | 25.1 | 46.2 | 0.6 | 1.2 | 0.7 | — | — | 0.8 | 100.7 |
| R-31 1010-1015 river gravel | 3.7 | — | — | — | 4.7 | 6.9 | 7.3 | 12.7 | 32.3 | 27.4 | 0.5 | 2.3 | 0.5 | — | — | — | 98.2 |
| R-31 1095-1100 river gravel | 1.0 | — | — | — | 4.9 | 7.0 | 15.8 | 14.1 | 31.3 | 20.4 | 0.7 | 2.1 | 0.1 | — | — | — | 97.4 |

Note: Values are reported in weight percent. Analytical errors (2σ) are ~5% of the amount reported for abundances >10% and ~10% of the amount reported for abundances <10%.

^a Number ranges indicate depth ranges of cuttings in feet.

^b Dashes indicate that the phase was not detected; detection limits are ~0.1%.

Well screen #1 at R-31 (439.1- to 454.4-ft depth) is placed across this clay-rich sediment. Evidence from the borehole video indicated accumulation of water above the sediment and flow along the borehole wall where it passed through the sediment. If the clay-rich sediment is a perching horizon, screen #1 is situated to obtain water samples that may accumulate at the base of tholeiitic Cerros del Rio flow sequence F in R-31.

Screen #2 (515.0- to 545.7-ft depth) straddles the contact between alkalic-basalt flow sequence C and the basaltic andesites of flow sequence B (Section 8.4.2, below). This screen was placed to contain the regional water table. The borehole video examination indicated a rubble zone at a depth of 514 to 517 ft, massive lava at 517 to 529 ft, and rubblely vesicular lava from 529 to 547 ft.

8.4.2 Cerros del Rio Basaltic Andesite Lavas (534- to 596-ft depth)

Flow series B at the R-31 site is a 62-ft thick basaltic andesite (geochemical classification; 53% to 56% SiO₂) distinct from the basaltic lavas (49% to 51% SiO₂) above and below. Petrographic examination classifies this flow series as a mugearite (Appendix D). The two depth intervals examined in thin section

differ petrographically, with the upper sample (540- to 545-ft sample) being an olivine-porphyrritic lava with quartz xenocrysts, and the lower sample (585- to 590-ft sample) being an olivine-plagioclase porphyritic lava with sieved and resorbed plagioclase phenocrysts. Two separate samples of the lava from the 585- to 590-ft depth were analyzed chemically and in thin section: one split of gray-colored lava (585-590G), and one split of red-colored lava (585-590R). Petrographically, the gray lava is a mixed sample, including both olivine-rich basalt and mugearite (Appendix D). This mixed sample is more Mg-rich and has a higher ratio of ferrous to ferric iron; otherwise the chemical analysis differs little from the red sample (Table 8.4-1). The red lava sample (585-590R) is the best representative of a "pure" mugearite from this flow series.

8.4.3 Alluvial Scoria Within the Cerros del Rio Lavas (596- to 625-ft depth)

A sequence of 29 ft of alluvial scoria separates flow sequences A and B at the R-31 site. This material is considered to be alluvial because of the rounding of scoria fragments that were obtained as cuttings. A sample of the alluvial scoria from the 600- to 605-ft depth was analyzed by QXRD and in thin section. Although apparently transported, the detritus is almost all basaltic scoria, and quartz is entirely absent (Table 8.4-2). The absence of foreign detritus such as quartz indicates local reworking of a Cerros del Rio scoria unit. In thin section, the scoria fragments consist of various olivine-porphyrritic basalts, some in a vitric matrix. The thin section includes one fragment of muscovite-bearing, clay-cemented siltstone of probable eolian origin, similar to the siltstone from the 444- to 450-ft depth (Section 8.4.1).

8.4.4 Cerros del Rio Low-Ni,Cr Alkalic Basalt Lavas (625- to 703-ft depth) and Flow-Base Sediments (703- to 710-ft depth)

The lowest flow sequence at the R-31 site, sequence A, includes distinctively Ni,Cr-poor alkalic basalts. Two samples of this sequence were analyzed chemically and petrographically, one from the 665- to 670-ft depth and one from the 680- to 685-ft depth. Both samples have low Ni (35 to 48 ppm) and exceptionally low Cr (15 to <8 ppm) relative to other basalts of the Cerros del Rio volcanic field (Figure 8.4-1). The more typical basalts of the Cerros del Rio volcanic field generally have >60 ppm Ni and >75 ppm Cr (WoldeGabriel et al. 1996, 54427). Petrographically, the samples from sequence A are fine-grained basalts with a texture dominated by flow-oriented feldspar laths (pilotaxitic texture). Olivine and clinopyroxene phenocrysts are small, ~0.2 mm, within the size range of the feldspathic matrix.

Well screen #3, at the 666.3- to 676.3-ft depth, is located within this flow sequence, and the lithology at this depth is represented by the sample from the 665- to 670-ft depth. Borehole video images of the low-Ni,Cr basalts show continuous columnar jointing, without evidence of clay infilling, from near the top of sequence A (~630-ft depth) to about 690 ft (Appendix H). The hydraulic conductivity of ~7 ft/day measured in this zone (Section 10.2.2) is attributed to fracture connection.

The flow-base sediments at the 703- to 710-ft depth include basaltic scoria and basaltic sandstone. A subsample of the basaltic sandstone from the 705- to 710-ft cuttings run was analyzed in thin section and by QXRD for mineralogy. A separate subsample of scoria from this interval was analyzed in thin section. The scoria consists of varied olivine-porphyrritic basalts, but most have similar mineralogy (Appendix D) and are probably related to flow sequence A. The basaltic sandstone is fine-grained, grading to siltstone, with detritus dominated by basaltic lithic fragments plus grains of quartz and amphibole, fragments of volcanic glass, and rare microcline and chert. There are only rare plutonic or metamorphic lithic fragments and no dacitic detritus that would indicate Tschicoma Formation sources typical of Puye Formation sediments.

8.5 Puye Formation Sediments: Fanglomerates and River Gravels (710-ft depth to TD of 1103 ft)

The Puye Formation extends from 710 ft to the TD of 1103 ft at the R-31 site. A major transition from fanglomerate deposits to river gravels occurs at the 780-ft depth. However, the river gravels include

intercalated horizons of fanglomerate deposition, particularly at the depth interval from 900 to 935 ft. The intercalation of dacite-dominated fanglomerates and dispersal of dacitic detritus within the river gravels indicates intermixture of local volcanic debris from the west with plutonic and metamorphic detritus from distant northern sources. Figure 8.5-1 shows the stratigraphy of Puye Formation sediments in the lower part of R-31 with hand-sample estimates of total percentages of quartzite (Appendix C), the natural gamma log obtained through drill casing (9 5/8-in. casing to 1067 ft), the cation ratio of Si to Al in 2- to 4-mm sediment samples, the ratio of quartz/(quartz + tridymite + cristobalite) determined from QXRD analysis of the 2- to 4-mm sediment samples, and the glass alteration index of the 2- to 4-mm sediment samples. This last parameter is the ratio of (clays + zeolites)/(clays + zeolites + glass), a number that is near zero if there has been little glass alteration within the sediment and that approaches one where alteration is extreme. Chemical analyses of the Puye Formation sediments are listed in Table 8.5-1. The mineralogic data used to construct the last two columns of Figure 8.5-1 are from Table 8.4-2. The Si/Al ratio rises in those sedimentary horizons where quartzites predominate over all other rock types (volcanic, granitic, and metamorphic rocks other than quartzite). The quartz/(quartz + tridymite + cristobalite) ratio rises in sedimentary horizons where granitic and metamorphic rocks (including quartzite) predominate over volcanic rocks. For comparative purposes, the mineralogic data for the Cerros del Rio flow-base sediments (basaltic sandstone) at the 703- to 710-ft depth are included in Figure 8.5-1.

The principal marker of transition from fanglomerates into river gravels at the 780-ft depth is the abrupt appearance of quartzite clasts at this depth. The natural gamma signal throughout the Puye Formation rises gradually with depth but drops near the fanglomerate-to-river-gravel transition depth. The cause of this drop in the gamma signal is not known to be directly related to any specific feature but may reflect a K, U, and Th-poor quartzite component. The Si/Al ratio and the ratio of quartz/(quartz + tridymite + cristobalite) are only poorly correlated, reflecting the absence of a simple bivariate mixing system (e.g., quartzite and granite) and the presence of at least three major contributing components (granitic lithologies, quartzites, and dacitic volcanic rocks). Of note is the very low glass alteration index in all of the sediments beneath the basaltic sandstone. This lack of glass alteration places limits on the exposure of these sediments to alteration conditions and rules out hydrothermal alteration of the Puye Formation sediments at the R-31 site.

8.5.1 Puye Formation Fanglomerates (710- to 780-ft depth)

The Puye Formation at the 710- to 780-ft depth consists of volcanogenic fanglomerates. The clasts consist entirely of volcanic lithologies, and the matrix includes glassy shards and pumice derived from volcanic sources. Clay (smectite) occurs in abundances of 5% to 7% in the two samples of 2- to 4-mm fanglomerate clasts analyzed by XRD, and traces of zeolite (clinoptilolite) and dolomite were detected in one representative sample (730- to 735-ft depth, Table 8.4-2). The secondary minerals detected by XRD were unrecognized in thin section due to the combination of their fine grain size and low concentration. Many lithics within both samples are vitric, so that glass constitutes a significant fraction of the deposit.

Petrographic analysis reveals scarce felsic crystals (phenocrysts or fragments of phenocrysts) within the matrix of the Puye Formation in R-31. Felsic phenocrysts within both samples are derived primarily from volcanic sources, a characteristic that distinguishes the Puye Formation from Santa Fe Group sediments. Within the Puye Formation, fanglomerates are also distinguished from quartzite-bearing river gravels by a low ratio of quartz to all silica minerals (quartz + tridymite + cristobalite). This ratio is typically <0.3 in the fanglomerates because the silica polymorphs tridymite and cristobalite are common in the matrices of dacitic lavas that constitute these deposits. The ratio is typically >0.3 where long-range alluvial transport has preserved only the more resistant quartz and the transported detritus is from plutonic and metamorphic sources where quartz is the predominant silica mineral.

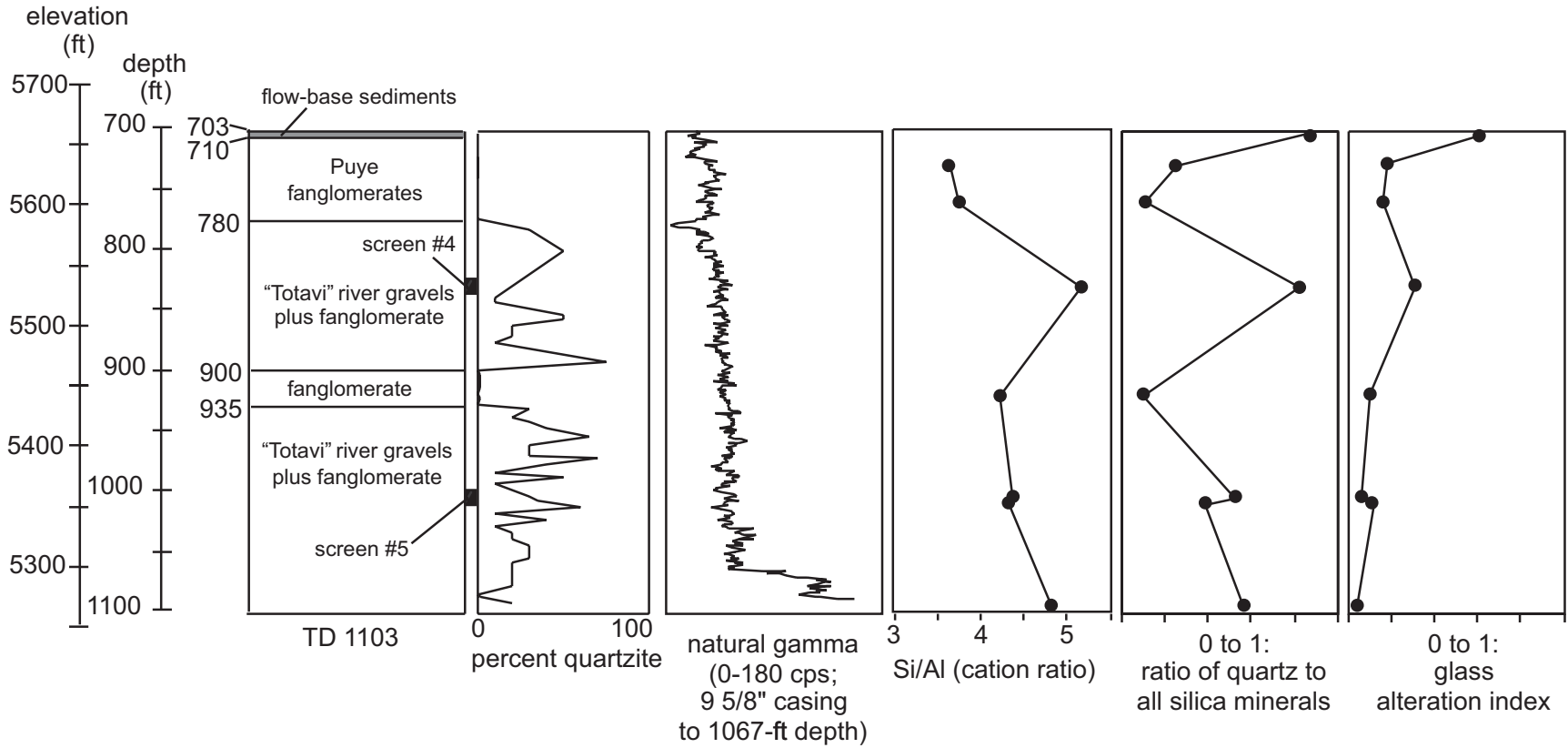


Figure 8.5-1. Relationships between Puye Formation stratigraphy, natural gamma signal, Si/Al cation ratios, ratios of quartz to all silica minerals [quartz/(quartz + tridymite + cristobalite)], and glass alteration indices [(clays + zeolites)/(clays + zeolites + glass)] at the R-31 site

Table 8.5-1
XRF Analyses of Puye Formation Sediments from R-31

| Sample Number ^a | R-31 730-735 | R-31 760-765 | R-31 830-835 | R-31 920-925 | R-31 1005-1010 | R-31 1010-1015 | R-31 1095-1100 |
|--------------------------------|--------------|--------------|--------------|--------------|----------------|----------------|----------------|
| Type | fanglomerate | fanglomerate | river gravel | fanglomerate | river gravel | river gravel | river gravel |
| Major Elements (wt %) | | | | | | | |
| SiO ₂ | 65.45 | 65.45 | 73.56 | 70.36 | 70.24 | 70.39 | 72.68 |
| TiO ₂ | 0.57 | 0.71 | 0.38 | 0.42 | 0.38 | 0.37 | 0.39 |
| Al ₂ O ₃ | 15.22 | 14.78 | 12.08 | 14.12 | 13.59 | 13.81 | 12.78 |
| Fe ₂ O ₃ | 4.05 | 4.74 | 3.20 | 3.01 | 2.80 | 2.75 | 2.71 |
| MnO | 0.07 | 0.08 | 0.05 | 0.06 | 0.06 | 0.06 | 0.05 |
| MgO | 1.90 | 1.80 | 0.71 | 1.10 | 1.07 | 1.04 | 0.83 |
| CaO | 3.38 | 3.50 | 2.21 | 2.13 | 2.10 | 2.19 | 1.99 |
| Na ₂ O | 3.21 | 3.44 | 2.87 | 3.73 | 3.10 | 3.36 | 3.40 |
| K ₂ O | 3.08 | 3.03 | 3.20 | 3.85 | 3.93 | 3.79 | 3.42 |
| P ₂ O ₅ | 0.21 | 0.23 | 0.14 | 0.11 | 0.13 | 0.13 | 0.14 |
| LOI ^b | 1.95 | 1.31 | 0.65 | 0.70 | 1.90 | 1.21 | 0.76 |
| Total | 97.15 | 97.77 | 98.40 | 98.89 | 97.40 | 97.88 | 98.39 |
| Trace Elements (ppm) | | | | | | | |
| V | 60 | 63 | 33 | 30 | 38 | 38 | 38 |
| Cr | 37 | 56 | 20 | 34 | 31 | 28 | 20 |
| Ni | 28 | 39 | <11 | 32 | 22 | 28 | 18 |
| Zn | 45 | 43 | 33 | 38 | 35 | 33 | 22 |
| Rb | 71 | 72 | 96 | 117 | 106 | 112 | 91 |
| Sr | 459 | 501 | 355 | 324 | 328 | 326 | 334 |
| Y | 12 | 14 | 30 | 24 | 21 | 26 | 24 |
| Zr | 178 | 183 | 137 | 159 | 157 | 140 | 165 |
| Nb | 19 | 35 | 12 | 35 | 31 | 25 | 21 |
| Ba | 775 | 1034 | 678 | 835 | 906 | 835 | 809 |

Note: Values reported in weight percent or parts per million. Analytical errors (2σ) are SiO₂, 0.7; TiO₂, 0.01; Al₂O₃, 0.2; Fe₂O₃, 0.06; MnO, 0.01; MgO, 0.08; CaO, 0.1; Na₂O, 0.1; K₂O, 0.05; P₂O₅, 0.01; V, 10; Cr, 8; Ni, 10; Zn, 12; Rb, 5; Sr, 25; Y, 6; Zr, 30; Nb, 7; and Ba, 50.

^a Number ranges indicate depth ranges of cuttings in feet.

^b LOI = loss on ignition.

The fanglomerate samples from the 730- to 735-ft and 760- to 765-ft depths contain lithics that characteristically occur within the Puye Formation. The low abundance of basalt clasts contrasts markedly with the abundance of basalt clasts in the Old Alluvium (Broxton et al. 2001, 66599), and the complete absence of lithics with Precambrian provenance contrasts markedly with the river gravels that occur below 780 ft. About one third of the lithics within the 760- to 765-ft sample are included within a clast group that probably represents rhyodacite of Rendija Canyon, dated by K/Ar at 4.55 ± 0.44 Ma (2σ) by

F. W. McDowell (Broxton 1987, 71428). Although total felsic phenocryst contents are lower than those known from hand samples of this rhyodacite, a highly distinctive assemblage of features is identical. Like the rhyodacite of Rendija Canyon, these lithics are mafic-poor and contain very strongly resorbed plagioclase phenocrysts, prominent quartz phenocrysts, sphenes, and acicular groundmass pyroxene, mostly orthopyroxene. Felsic phenocrysts, which are often the same size as the lithic fragments analyzed, are probably preferentially lost from lithics due to transport abrasion; this loss probably also accounts for the relatively high content of quartz grains derived from volcanic sources. Lithics of this rhyodacite are absent within the shallower sample, which consists mostly of pyroxene-phyric lithics possibly derived from the upper dacite of Pajarito Mountain, accompanied by colorless, mostly hornblende-phyric pumice possibly derived from the dacite of Sawyer Dome. The upper dacite of Pajarito Mountain has $^{39}\text{Ar}/^{40}\text{Ar}$ dates of 2.91 ± 0.06 Ma and 3.07 ± 0.07 Ma (Broxton 1999, 71429).

The stratigraphic succession within the 710- to 780-ft deep Puye Formation fanglomerates at the R-31 site is similar to the succession at the R-25 site but differs from those to the north at the R-9 and R-12 sites, and from that within outcrop samples that represent the southernmost exposure of the Puye Formation mapped within the White Rock quadrangle between elevations of 5400 to 5460 ft, 2 km southeast from R-31 (Dethier 1997, 49843). However, within the outcrops southeast of R-31, the upper portion of the Puye Formation is similar to the rhyodacite-bearing sample from the 760- to 765-ft depth in R-31.

8.5.2 Puye Formation River Gravels (“Totavi”) and Intercalated Fanglomerates (780-ft depth to TD of 1103 ft)

Quartzite-bearing river gravels of the Puye Formation, interspersed with fanglomerate-type dacitic detritus, occur from 780 ft to the TD of 1103 ft in R-31. Many of the lithics in this interval are derived from Precambrian quartzite and granite sources, distinct from the Puye Formation fanglomerates at the 710- to 780-ft depth, which contain no such lithics. Many lithics within the river gravels are vitric, so that glass constitutes a significant fraction (~11% to 46%) of all of these sediments (Table 8.4-2). This widespread glass component is represented in thin section by both vitric dacitic pumices and by fragments of dacitic lavas with glassy matrices.

In thin section, lithic clasts derived from the rhyodacite of Rendija Canyon and other dacites of the Tschicoma Formation occur within the sample of river gravel from the 830- to 835-ft depth, in proportions nearly identical to the proportions within the deeper (760- to 765-ft depth) of the two samples of Puye Formation fanglomerate described in the previous section. Moreover, the other dacite types are quite similar between the two samples. This similarity indicates that the river gravels below 780 ft in R-31 might include clasts derived by erosion of such Puye Formation fanglomerates upstream, or that fans from the same volcanic sources were active during deposition of the river gravels, or both.

The detritus in the river gravels includes a variety of metamorphic and granitic lithologies. Most abundant and distinctive are quartzites, including quartzites with strained and unstrained or annealed fabrics, muscovite quartzites, and single crystals of quartz derived from quartzites. Other metasedimentary lithologies occur but are less common than granitic fragments, often showing evidence of metamorphism or hydrothermal alteration (recrystallized, strained, or having reaction to muscovite within alkali feldspars). Microcline is common in the granitic fragments.

An interval of fanglomerates with dominantly dacitic to rhyodacitic composition occurs from 900 to 935 ft in R-31, interspersed between thick sequences of predominantly riverine detritus. This interval is represented by a sample from the 920- to 925-ft depth. In thin section, this sample contains a variety of dacitic lavas, some of which are quartz-bearing and most of which contain hydrous phenocrysts

(amphibole and/or biotite). The 35-ft interval of fanglomerates represented by this sample is exceptionally prominent because of the very low abundance of plutonic and metamorphic detritus in seven sequential cuttings runs (35 ft), but other, thinner fanglomerate deposits may occur throughout the river gravels.

Two well screens were emplaced within the river gravels of the Puye Formation in R-31. Screen #4 (826.6- to 836.6-ft depth) is represented by the sample from the 830- to 835-ft depth. This sample contains an abundance of quartzite and muscovite-quartzite, granitic fragments, and dacitic lavas with both anhydrous (clinopyroxene) and hydrous (amphibole, biotite) phenocrysts. Of all of the river-gravel samples analyzed, this one has the highest quartz/(quartz + tridymite + cristobalite) ratio, the highest Si/Al ratio, and the lowest abundance of volcanic glass (~11%, Table 8.4-2), making it the best sample from R-31 of riverine gravels dominated by distant plutonic and metamorphic sources.

Screen # 5 (1007.1- to 1017.1-ft depth) crosses a more variable section of the riverine-gravel deposits and is represented by two samples from the 1005- to 1010-ft and 1010- to 1015-ft depths. The upper sample has the highest glass abundance (~46%, Table 8.4-2) of all Puye Formation samples from R-31, including the fanglomerates. The lower sample has less glass (~27%) than the upper sample, but the abundance is still beyond the range of glass abundances in other river-gravel samples (~11% to 20%). Both samples contain quartzites and granitic clasts, but dacitic lithologies are more abundant and account for much of the glass content. Both samples, but particularly the upper sample, contain dacitic pumices with plagioclase and amphibole phenocrysts.

9.0 BOREHOLE GEOPHYSICS

Borehole geophysical surveys were conducted in R-31 before and after well installation. The Laboratory natural gamma and caliper tools were run through borehole cased to 290 ft and open to 787 ft on January 25–26, 2000. A borehole video survey was completed down to 725 ft, and a natural gamma log was completed to 720 ft. The Laboratory natural-gamma tool was again run, through borehole cased to 1067 ft and open to 1094 ft, on February 10. Schlumberger ran borehole geophysical surveys on February 9, 2000, through cased borehole and on March 6 and 17, 2000, through the completed well. The borehole geophysical logging runs are summarized in Table 9.0-1.

**Table 9.0-1
Laboratory and Schlumberger Geophysical Logging Runs Performed in Well R-31**

| Date of Logging | Logging Organization | Borehole Status | Tools ^a | Depth Interval (ft) |
|---------------------|----------------------|---|--------------------|--|
| January 25–26, 2000 | Laboratory | Cased (9 5/8-in. I.D.) to 290-ft depth, open hole below | GR, caliper | 0–720 ft |
| February 9, 2000 | Schlumberger | Cased w/ temporary casing (9 5/8-in. I.D.), no annular fill | HNGS, APS | HNGS: 66–1070 ft APS: 66–1080 ft |
| February 10, 2000 | Laboratory | Cased w/ temporary casing (9 5/8-in. I.D.), no annular fill | GR | 0–1094 ft (casing ended at 1067 ft) |
| March 6, 2000 | Schlumberger | Cased (5-in. I.D.) and completed; annular fill present | GR, MFC, ETT | 31–1077 ft |
| March 17, 2000 | Schlumberger | Cased (5-in. I.D.) and completed; annular fill present | GR, MFC, APS, HNGS | HNGS: 76–1052 ft APS: 76–1066 ft GR, MFC: 31–1077 ft |

^a GR = gross gamma radiation, HNGS = hostile natural gamma spectroscopy, APS = accelerator porosity sonde, MFC = multi-finger caliper, ETT = electromagnetic thickness tool.

The Laboratory borehole video tools include a fixed downward-view camera and a larger camera capable of downward and side views. The larger camera was used to image the cased and open borehole, and the smaller camera was used to examine the interior of the completed well at R-31. These video systems are not considered geophysical tools, but their use supplements the data obtained by borehole geophysical surveys. (The video collected on January 25–26 with the larger camera can be viewed from the CD in Appendix H.)

9.1 Borehole Geophysical Survey Methods

The tools used for borehole geophysical surveys are described below. These descriptions are provided here because tools with similar names may have different capabilities or constraints. Further detail on the Schlumberger tools is provided in Appendix G.

9.1.1 Gross Gamma Radiation (Laboratory Tool)

The GR tool uses a scintillation detector to measure the gross gamma activity within a formation or within annular-fill materials. This information is useful for determining lithologies and for correlation between different geophysical surveys. Naturally-occurring gamma radiation comes from the decay of ^{40}K and from the U and Th decay series.

9.1.2 Caliper (Laboratory Tool)

The Laboratory caliper tool is a three-arm system that provides information about effective total hole diameter. The maximum diameter measurable by this tool is 73.6 cm (29 in.). In an open borehole, this information can be useful in detecting washouts, identifying resistant beds, and distinguishing between smooth borehole in massive lavas and rough borehole in volcanic rubble zones and interbeds. This tool can also be used to locate separated drill casing and to examine the interior quality and screen integrity of a completed well.

9.1.3 Multi-Finger Caliper (MFC) Tool (Schlumberger)

The MFC tool measures internal casing/screen geometry and is used to evaluate the condition of casing joints and screens. This tool provides a detailed caliper log that measures the internal radius of casing/screens using as many as 72 caliper arms. The minimum, maximum, and average radius in each of three 120° sectors is reported. Any ovalization or pinching of the borehole is readily apparent from this log, although the orientation of any such irregularity is not recorded. The measurements obtained have an accuracy of ± 0.25 mm (0.1 in.), vertical resolution as high as 0.51 cm (0.2 in.), and radius measurement range of 9.4 to 34 cm (3.7 to 13.4 in.).

9.1.4 Accelerator Porosity Sonde (APS; Schlumberger)

The APS measures volumetric water content at several depths of investigation beyond the casing and is used to evaluate moist/porous zones and voids in annular fill. The APS measures the presence of hydrogen atoms in a formation by bombarding it with a large flux of high-energy neutrons from an electronic generator and measuring the response. The electronic neutron source generates 14-MeV neutrons in a pulsed mode at a flux rate of approximately 3×10^8 neutrons per second. This system employs four epithermal neutron detectors and one thermal neutron detector that make several lithology- and borehole-independent measurements of formation moisture content or saturated porosity at different depths of investigation, depending on source-detector spacing. The maximum depth of investigation is approximately 30 cm (12 in.) and the vertical resolution is approximately 45 cm (18 in.).

The tool provides another moisture measurement based on the time it takes for neutrons to decelerate through nuclear interactions. Two epithermal detectors measure the decay of epithermal neutrons that occurs subsequent to a neutron pulse. The decay rate is a function of the hydrogen concentration; the more hydrogen, the faster the decay. This tool function has a vertical resolution of approximately 7.5 cm (3 in.), and the depth of investigation is approximately 5 cm (2 in.).

A thermal neutron detector measures the decay rate of thermal neutrons after the neutron pulse and is used to calculate a measurement of formation sigma—the macroscopic thermal neutron absorption cross section. Sigma is a function of the types and quantities of thermal neutron absorbers present within the formation. The larger sigma is, the faster the decay of the thermal neutron population. Sigma is typically measured in "capture units" (cu), a unit related to the mass-normalized thermal neutron cross section. Quartz has a sigma of about 4 cu, fresh water has one of 22 cu. A comparison of sigma and epithermal neutron porosity can differentiate zones within the formation that contain higher concentrations of thermal neutron absorbers, independent of moisture.

The APS can be run in open or cased, water- or air-filled holes.

9.1.5 Hostile Natural Gamma Spectroscopy (HNGS) Tool (Schlumberger)

The HNGS tool measures overall and spectral natural gamma ray activity, including K, U, and Th activities. This tool is used to evaluate geology/lithology and the presence of clay versus sand annular fill.

The HNGS tool is a spectral and total passive gamma measuring sonde that can be used in either open or cased boreholes. The tool is run decentralized, with a bowspring, but receives significant input from all sides of the borehole. Average depth of investigation in typical lithologies is 7 to 9 in. The tool was designed to quantify naturally occurring radionuclides from within deep oil wells and has been optimized to provide maximum sensitivity so that typical oilfield logging speeds (1800 ft/hr; 600 m/hr) can be used while retaining effective counting statistics. To this end, the system uses two large scintillation detectors composed of bismuth germanate (BGO), with a very low activity ^{22}Na stabilization source sandwiched in between and a photomultiplier tube optically connected to each detector. BGO has a high specific gravity (approximately 7 g/cm³), which increases efficiency by promoting the capture of more gamma rays (compared to most commonly employed scintillators). Two detectors are employed to increase the sensitivity without degrading the system's vertical resolution.

The tool measures a full gamma energy spectrum that encompasses the spectral energies of K, U, and Th. A weighted least-squares processing algorithm is used to decompose the contributing source component activities. The result is a measurement of K, U, and Th components and total gamma activity that maximizes the statistical information collected by the scintillators.

9.1.6 Electromagnetic Thickness Tool (ETT; Schlumberger)

The purpose of the ETT is casing inspection. It uses nondestructive, noncontact, eddy current (induction) methods to detect areas of metal loss (or conversely, areas where metal is thicker). The ETT can evaluate multiple strings of casing, and logs can be obtained with water, mud, brine, air, or any combination thereof, in the borehole.

The ETT makes three measurements: (1) casing wall electromagnetic (EM) thickness, (2) casing inner diameter (with the EM caliper), and (3) casing EM properties. Each of these measurements is made by an independent pair of transmitter and receiver coils and associated electronic components.

To measure the EM thickness, the ETT operates at a very low frequency to sense the wall thickness indirectly by measuring the phase shift between the receiver voltage and the transmitter current. The

phase shift is directly proportional to the EM thickness of the pipe wall. The EM thickness system also measures the amplitude of the receiver voltage. The amplitude is used to determine which one of three selectable frequencies—35 Hz, 17.5 Hz, or 8.75 Hz—is appropriate for the EM thickness measurement.

The EM caliper (with the ETT operating at 65 kHz) measures the phase and amplitude of the caliper receiver voltage relative to the transmitter current to determine the inner diameter of the casing.

Two inputs are required to calculate the EM properties of the casing: (1) the voltage amplitude of the receiver coil (normalized to the transmitter current and to free space), and (2) the casing inner diameter (measured by the EM caliper). Three different frequencies of operation are used simultaneously (375 Hz, 1500 Hz, and 6000 Hz) to ensure adequate depth of investigation.

9.2 Results

The results of Laboratory gamma and caliper logging provided information regarding both the geochemical nature of the stratigraphic units, where compositional variations in K, U, and Th are significant, and the distribution of lava rubble zones where the caliper tool was in contact with uncased borehole walls. The Laboratory gamma results are particularly effective in defining the Guaje Pumice Bed and in recognizing lavas of different composition within the Cerros del Rio lava series. These gamma logs are reproduced in Figures 8.2-1, 8.4-1, and 8.5-1 to relate the natural gamma signal to stratigraphy.

The results of Schlumberger logging of the cased hole in February and of the completed well in March 2000 are summarized in Appendix G. Particularly useful are the February neutron-based analyses of water-filled porosity, with values of only 30% at screen #4 and ~50% at screen #5. This difference may have some bearing on the cause of relatively low hydraulic conductivity at screen #4 (Table 10.2-1), but full analysis of the borehole geophysical survey data and the results of hydrologic testing has yet to be completed.

Overall, most of the geophysical logs for well R-31 provide consistent, good quality data. The logs collected before the well was designed helped considerably in defining stratigraphic units and were used in determining the locations of well screens. The logs of the completed well indicate that: (1) there are a number of zones where there are air- or water-filled voids behind the casing; (2) most of the screened intervals appear to contain sand fill and are surrounded above and below by clay-rich fill; and (3) the casing and screens are geometrically intact, with some slight ovalization in the joints above screens #3 and #5.

A further result of the March 2000 logging by Schlumberger was determination of the precise location of a section of lost 9 5/8-in. drill casing and a copper sounding rod. Use of the ETT log made it possible to find them in the annulus behind the well wall. The low-frequency phase output was most sensitive to the presence of these items. This log is provided in Appendix G. The ETT log gave precise locations for the copper sounding rod at the 382.5- to 391-ft depth and the 9 5/8-in. drill casing at the 882- to 952-ft depth. The positions of these items as determined from the ETT log are shown in Figure 8.0-1b. In addition to locating the lost sounding rod and drill casing, the ETT log also determined that the depth of the 13 5/8-in. surface casing was 296 ft.

9.2.1 Stratigraphic Analysis Based on GR Logging Data (Laboratory Tool)

The Laboratory GR tool was run in both cased and open hole. Table 9.2-1 summarizes the natural gamma signal properties, by unit, for several major and minor lithologic units at the R-31 site. The natural gamma signal in counts per second (cps) has minimum and maximum values that extend beyond the range of the natural gamma plots shown in Figures 8.2-1, 8.4-1, and 8.5-1. This difference arises from the smoothing (running average) algorithm that was used to modify the curves that are shown in these

figures. Comparison of the average values shown in Table 9.2-1 with the natural-gamma curves in Figures 8.2-1, 8.4-1, and 8.5-1 shows that the average values are within the range of the curves shown.

Table 9.2-1
Statistical Parameters of Natural Gamma Signals
(Laboratory Tool) for Different Lithologies at R-31 (Raw Counts, Unsmoothed)

| Lithology ^a | Depth (ft) | Casing diameter (in.) or open hole | Minimum (cps) | Maximum (cps) | Mean (cps) | Median (cps) | Standard deviation (cps) |
|--|----------------|------------------------------------|---------------|---------------|------------|--------------|--------------------------|
| Otowi ash flows | 37–264 | 13 5/8 | 25 | 190 | 102 | 100 | 24 |
| Guaje Pumice Bed | 264–280 | 13 5/8 | 55 | 216 | 120 | 116 | 29 |
| Sediment | 280–285 | 13 5/8 | 40 | 221 | 120 | 125 | 36 |
| Cerros del Rio (F) | 285–444 | Open hole | 5 | 135 | 52 | 50 | 19 |
| Sediment | 444–450 | Open hole | 20 | 186 | 80 | 80 | 26 |
| Cerros del Rio (E) | 450–473 | Open hole | 65 | 251 | 147 | 145 | 31 |
| Cerros del Rio (D) | 473–513 | Open hole | 45 | 216 | 110 | 110 | 28 |
| Cerros del Rio (C) | 513–534 | Open hole | 55 | 231 | 121 | 120 | 25 |
| Cerros del Rio (B) | 534–596 | Open hole | 10 | 160 | 76 | 75 | 22 |
| Alluvial scoria | 596–625 | Open hole | 15 | 110 | 56 | 55 | 16 |
| Cerros del Rio (A) | 625–703 | Open hole | 20 | 145 | 72 | 70 | 20 |
| Flow-base sediments | 703–710 | Open hole | 10 | 105 | 59 | 55 | 19 |
| <i>Flow-base sediments^b</i> | <i>703–710</i> | <i>9 5/8</i> | <i>5</i> | <i>55</i> | <i>25</i> | <i>25</i> | <i>12</i> |
| Puye fanglomerate | 710–720 | Open hole | 15 | 125 | 65 | 65 | 21 |
| <i>Puye fanglomerate^b</i> | <i>710–780</i> | <i>9 5/8</i> | <i>0</i> | <i>95</i> | <i>34</i> | <i>30</i> | <i>15</i> |
| Puye river gravel | 780–900 | 9 5/8 | 0 | 100 | 41 | 40 | 17 |
| Puye fanglomerate | 900–935 | 9 5/8 | 10 | 95 | 49 | 50 | 15 |
| Puye river gravel | 935–1067 | 9 5/8 | 0 | 135 | 53 | 50 | 18 |

^a Lithologic series follows the stratigraphy illustrated in Figure 8.0-1b; letters A through F designate the six Cerros del Rio lava series shown in Figure 8.0-1b and described in Section 8.4.

^b Entries in italics indicate measurements in 9 5/8-in. cased borehole that overlap entirely or in part with open-borehole measurements in the previous line.

The highest mean natural gamma signal at R-31 (open hole) is found in the Cerros del Rio lava series E (Section 8.4.1). However, repetition of the GR logging in cased and open hole indicates that the average gamma signal in cased hole is roughly half of the signal strength in open hole. (Compare the data sets for both conditions in the flow-base sediments at the 703- to 710-ft depth and in the highest occurrence of Puye Formation fanglomerates at the 710- to 720-ft depth, Table 9.2-1.) This finding indicates that the strongest GR signal is actually produced by the Guaje Pumice Bed and the immediately underlying sediment. Moreover, the minimum signal may go to zero in cased hole where the uncased host lithology has a mean GR signal of less than ~50 cps.

10.0 HYDROLOGY

Hydrologic observations were made in both the unsaturated and saturated zones at the R-31 site. This work included determinations of both groundwater occurrence and movement.

10.1 Hydrology of Unsaturated Zones

Measurements of moisture content and of matric potential were made from core collected during Phase I HSA sampling (0- to 250-ft depth) and from cuttings collected during early Phase II drilling (250- to 355-ft depth). These data are used to constrain models of flow through the unsaturated zone. Samples from which these data were collected were sealed immediately at the drill site in preweighed and prelabeled jars. Moisture content was determined gravimetrically by drying the samples in an oven in accordance with American Society for Testing and Materials method D2216-90. Moisture contents are given as the ratio of the weight of water to the weight of the dry sample. Matric potential was determined with a chilled-mirror water activity meter (psychrometer) following the methods of Gee et al. (1992, 58717). Results of the moisture-content and matric-potential analyses are tabulated in Appendix E and summarized in the two sections below.

10.1.1 Moisture Content

Figure 10.1-1 shows the variation in moisture content of samples from the surface to the 355-ft depth in R-31. Moisture content within the alluvium in R-31 peaks at 17% at the ~7.5-ft depth and decreases to ~9% at the ~22-ft depth near the contact between the alluvium and the ash flows of the Otowi Member of the Bandelier Tuff. Within the Otowi Member ash flows, moisture content rises steadily from values of ~11% near the surface to ~15% toward the base of the ash flows. The lowest 5 to 10 ft of ash-flow deposits (samples from the 254.5- to 255-ft and 259.5- to 260-ft depths; Appendix E), above the Guaje Pumice Bed, has diminished moisture content (~8% to 10%); the Guaje Pumice Bed has a moisture content of ~15%, comparable to the ash flows above this interval of lower moisture. The cause of the diminished moisture at 255 to 260 ft might be a change in drilling technique at 250 ft from HSA core collection to air rotary; moisture was measured from cuttings instead of core below that depth. There was some chance for desiccation of the hole at the base of the cored hole between Phase I and Phase II drilling.

The sediments below the Guaje Pumice Bed are represented by one sample with a moisture content (~7%) intermediate between that of the Guaje Pumice Bed and that of the underlying Cerros del Rio lavas. The lavas, including the flow top, have a consistently low moisture content in the range of 1% to 3% with the exception of samples from the 340-ft and 350- to 355-ft depths. The borehole video shows that the 340- to 345-ft depth interval is a zone of moderate rubble development; beneath this zone, from 345 to 355 ft, is a zone of more extensive rubble development that produced abundant clay in the drill cuttings. The higher moisture content in these basalt samples is attributable to their high clay content.

10.1.2 Matric Potential

Matric potential is the measure of the capillary force (or hydrostatic pressure) with which water is held within the pores of a rock. Figure 10.1-2 illustrates the absolute value of the matric potential for samples from R-31, expressed in cm of water. ($10,200 \text{ cm H}_2\text{O} = 1 \text{ Mpa}$.) The working range for the meter is in soils drier than 0.003 water activity units (-0.4 Mpa or $-4080 \text{ cm H}_2\text{O}$) (Gee et al. 1992, 58717). This value is shown on the accompanying plots as the limit of the chilled-mirror psychrometer. The points plotted represent the same samples shown in Figure 10.1-1, and the data are listed in Appendix E. (The data represent the average of two measurements made on each sample.) The horizontal axis of the matric-potential plot is reversed so that the drier values appear to the left, corresponding to the direction of drier values in the moisture-content plot (Figure 10.1-1).

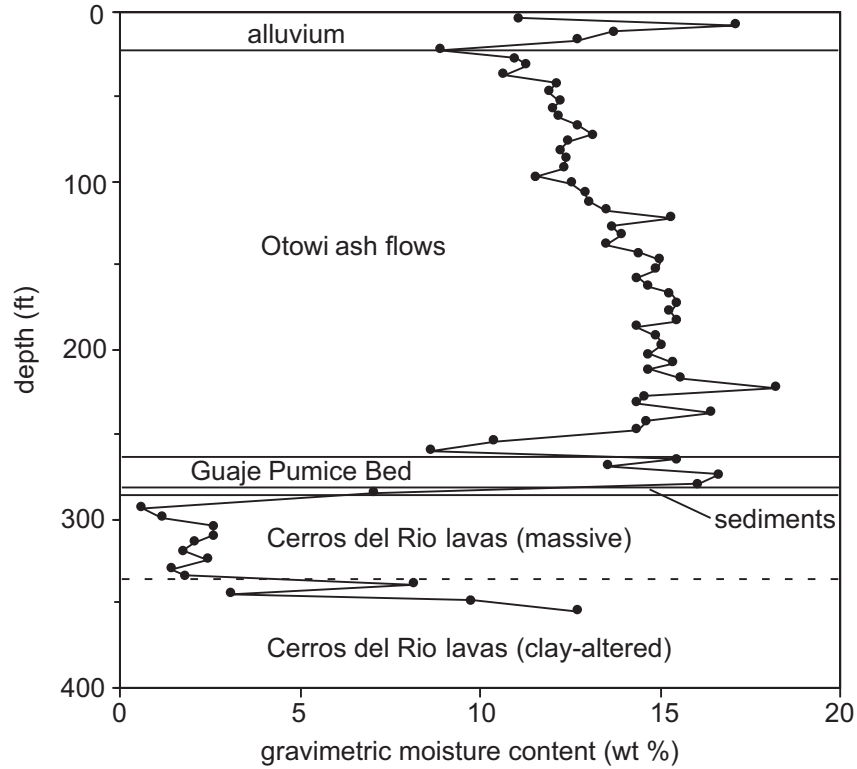


Figure 10.1-1. Variation in moisture content of samples from the surface to the 355-ft depth in R-31

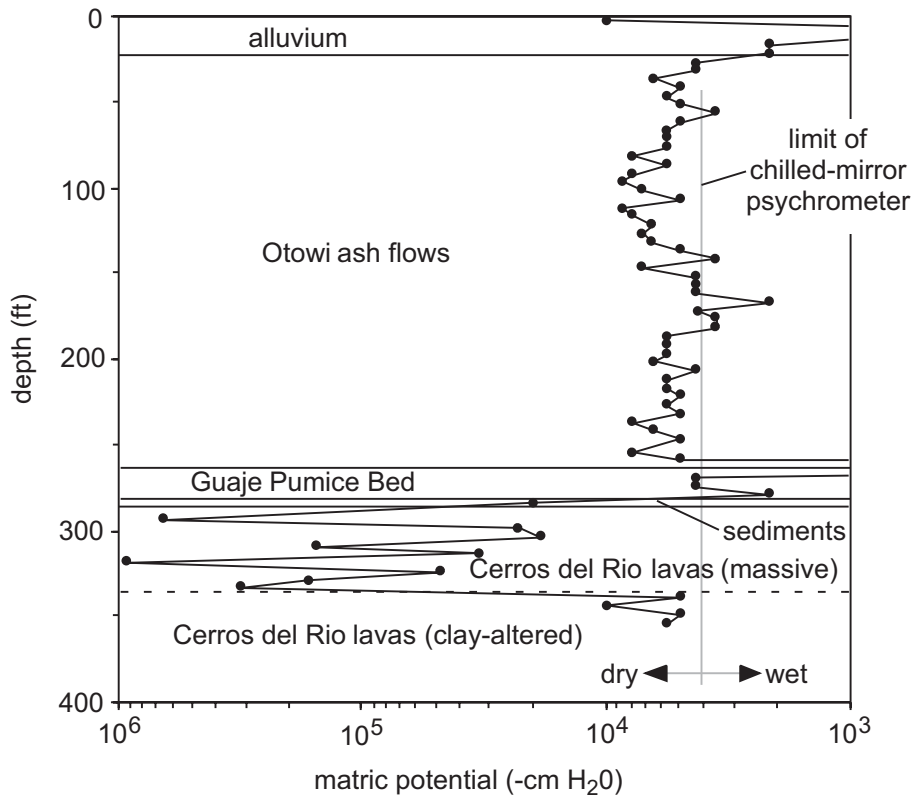


Figure 10.1-2. Matric potential of samples from the surface to the 355-ft depth in R-31

Aside from higher moisture zones at the 7.4- to 12.5-ft depth in the alluvium and at the top of the Guaje Pumice Bed (264.5 to 265.0 ft), matric potential from the surface down into the Guaje Pumice Bed is of limited range (about -3000 to -9000 cm H₂O). The sediments beneath the Guaje Pumice Bed and the basalts beneath the sediments are drier and have stronger water retention, with matric-potential values of about -11,000 to -1,000,000 cm H₂O. Matric potential returns to values in the range of -3000 to -9000 cm H₂O within the clay-rich basalts at the 339- to 355-ft depth, where the moisture content is higher and rock texture is finer grained.

10.2 Hydrology of Saturated Zones

Perched zones of saturation were anticipated in the Guaje Pumice Bed as well as in the Puye Formation or Cerros del Rio lavas. The regional water table was predicted to lie within the Puye Formation (Figure 8.0-1a).

10.2.1 Groundwater Occurrence

No water was detected in the Guaje Pumice Bed. However, first saturation may have been encountered at a depth of 485 ft in the Cerros del Rio basalt, based on water returned by the circulation system. If this was not drilling water, it represents a perched zone of saturation very near the middle of the basalt.

The regional water table was found to lie within the Cerros del Rio basalt. The depth at which the regional zone of saturation was encountered is not known, but a series of measurements at various depths provided depths to water between 521 and 537 ft (see Figure 8.0-1b). For example, on February 10, 2000, after the borehole had reached TD, but before a well had been constructed, borehole video logging showed that the camera penetrated water at a depth of 523 ft. This is a composite water-level depth, as there was a considerable length of open hole when the video log was made. Thus, the depth observed may be either deeper or shallower than the regional water table, depending on the direction of the vertical gradient.

10.2.2 Groundwater Movement

Although lateral groundwater movement is not normally determined from observations in a single well, the direction of the vertical gradient and the potential rate of lateral movement commonly are. More specifically, head measurements (static water levels at specific borehole depths converted to elevations) give a sense of the direction of the vertical gradient, and hydrologic testing provides data for evaluating hydraulic properties.

Head is normally measured in a piezometer (a pipe open at the end installed to a specific depth). Because R-31 was drilled by casing-advance methods, the casing was essentially an infinite set of piezometers whenever there was no open hole beneath the casing. In this situation, head values are determined from water-level depths obtained when the casing is screwed into the bottom (no open hole above the casing tip) and when there has been sufficient time for the water level to return to a static level after drilling activities (12 hr or more). Head values determined in this way at another well (R-25) agree very well with those obtained later by transducers in the Westbay™ MP55 system installed in R-31.

Water-level depths were measured in R-31 at borehole depths ranging from 485 to 1094 ft. However, in all but one case, there was a considerable length of open hole (31 to 476 ft). Thus, the casing was not acting as a true piezometer, and water levels obtained do not represent head. The exception is the water-level depth of 525 ft, obtained on February 5, 2000. At that time, casing was screwed into the bottom (thus, no open hole) at a borehole depth of 1007 ft, and a period of 38 hr 44 min had elapsed for the water level to recover from any drilling activity before measurement.

Head values for two or more depths give the direction of vertical hydraulic gradient. Although the vertical gradient cannot be determined from the single head value given above, a plot of all the water-level depths measured (static or otherwise) versus borehole depth indicates that the deeper the borehole, the shallower the water level, suggesting an upward gradient at the R-31 site. However, this concept was not confirmed by data from transducers deployed in the Westbay™ MP55 system installed in R-31. Head values obtained from the transducers when initially testing the isolation of zones in the Westbay™ MP55 system were nearly identical. Assuming that the zones were indeed isolated, this finding suggests either that there is a very slight downward gradient at the R-31 site or that the well was drilled more or less parallel to an isopotential and groundwater flow is essentially horizontal.

The hydraulic properties of saturated materials behind screens were determined by straddle-packer/injection tests, as described in Section 5.0. As noted there, two rounds of testing were conducted: one before final well development, and one after final well development. Data for a given screen were analyzed by the same method in both rounds of testing. The test results show that the additional development efforts improved the assessment of hydraulic properties and were therefore justified.

Only screens #3 and #4 were retested. For screen #3, positioned in basalt (Figure 8.4-1), the first round of testing (prior to final development) yielded a hydraulic-conductivity value of 3.62 ft/d; the second round of testing (after final development) yielded almost twice that value: 6.59 ft/d (Table 10.2-1). Data for screen #3 were analyzed by the Bouwer-Rice method (Bouwer and Rice 1976, 64056). For screen #4, positioned in a gravel (Figure 8.5-1), initial testing yielded a transmissivity value of 0.89 ft²/d for water-level-rise data collected during injection and 0.72 ft²/d for water-level-drop data collected during recovery; final testing yielded values of 5.50 ft²/d (for injection) and 5.90 ft²/d (for recovery). Data for screen #4 were analyzed by the Hantush-Jacob method (Hantush and Jacob 1955, 70091). Data for screen #5 were analyzed by the Bouwer-rice method.

**Table 10.2-1
Summary of Straddle-Packer/Injection Testing at the R-31 Site**

| Screen # (unit) ^a | Testing Round ^b | K ^c (ft/d) | T ^c (ft ² /d) | Average Injection Rate (gal./min) | Injection-Rate Variation (gal./min) | Test Duration (min) |
|------------------------------|----------------------------|-----------------------|-------------------------------------|-----------------------------------|-------------------------------------|---------------------|
| 3 (Tcb) | 1 | 3.62 | — | Not available | Not available | 35 |
| | 2 | 6.59 | — | 4-gal. slug | 0.0 | 20 |
| 4 (Tpt) | 1 (i) | — | 0.89 | 8.4 | 0.20 (2.4%) | 35 |
| | 1 (r) | — | 0.72 | 0.0 | 0.0 | — |
| | 2 (i) | — | 5.50 | 9.9 | 0.20 (2.0%) | 31.5 |
| | 2 (r) | — | 5.90 | 0.0 | 0.0 | — |
| 5 (Tpt) | 1 | 23.26 | — | 9.0 | 0.20 (2.2%) | 35 |

^a Screen #1 was dry, and screen #2 straddles the water table, so testing was impossible or inappropriate; Tcb = Cerros del Rio basalt, Tpt = Puye Formation "Totavi"-like gravels.

^b 1 = prefinal well development, 2 = postfinal well development; (i) = based on injection water-level data, (r) = based on recovery water-level data.

^c K = hydraulic conductivity; T = transmissivity. Text gives analytical methods applied.

These second-round transmissivity values are 6 to 8 times those obtained before complete development. However, even second-round test results seem low, especially those for the gravel behind screen #4. Three explanations have been offered for the low values obtained from analysis of first-round data for screen #4 (Stone et al. 2001, 70090). These explanations are that: (1) the screen may have been plugged;

(2) the injection rate was unable to overcome a strong upward gradient in the formation; or (3) the river gravels have a limited capacity to take on injected water because they are thin, discontinuous, or represent a small part of the section screened. The first explanation was rejected as the screen was verified to be clean by video logging. The second explanation was also rejected as no strong upward gradient exists at the R-31 site. However, the third explanation cannot be rejected as it is supported by geophysical logging evidence. Another possible explanation is that the gravel is poorly sorted. That is, hydraulic-property values would be lower than expected if the pores between pebbles are filled with finer-grained material. Unfortunately, cuttings do not provide that kind of information, so that explanation cannot be evaluated (but see the discussion of neutron-measured porosity in Section 9.2). Finally, the tests were of short duration and only involved a single well. Therefore, results may be less representative than those that might be obtained from tests of a different design and duration.

Another useful observation is the sustainable rate at which water can be extracted from a borehole or well. The regional zone of saturation seemed fairly productive during the drilling of R-31. Water was readily produced from that zone at a rate of 25 gal./min by airlifting. However, the yield eventually dropped to 10 gal./min.

11.0 GEOCHEMISTRY OF SAMPLED WATERS

Sampled waters at R-31 include pore waters leached from core or cuttings from the vadose zone and waters collected from the regional aquifer. There were preliminary indications of perched water based on water returns at ~485 ft (Section 3.3.1), but water was not present when the borehole was reentered for sampling. The likely perching horizon, based on cuttings and borehole video information, would be the fine sediments at the 444- to 450-ft depth between Cerros del Rio flow series E and F (Figure 8.0-1b). Screen #1 was situated to collect any water that might accumulate at this horizon. No water has been present at this screen interval as of the writing of this report, but samples will be obtained in the future if there is any water accumulation at this interval. In the absence of perched water samples, this section focuses on the data obtained from vadose-zone pore waters and from the regional aquifer.

11.1 Geochemistry of Vadose-Zone Pore Waters

Anion (bromide, chloride, nitrate, nitrite, phosphate, oxalate, and sulfate) and stable isotope ($\delta^{18}\text{O}$ and δD) profiles were determined from R-31 core and cuttings. As with moisture-content and matric-potential data (Section 10.1), anion and stable isotope data are used to constrain models of flow through the unsaturated zone. The samples collected for anion analyses were co-located with those collected for moisture-content and matric-potential analyses as described in this report. The sampling and analytical methods used were previously described in Broxton et al. (2001, 66599). The analytical precision of the ion chromatograph used to determine leachate concentrations was $\pm 5\%$ or less.

Pore-water anion concentrations were calculated using leachate concentrations, gravimetric moisture contents, and estimated bulk densities. Moisture-content data are reported in Section 10.1. The bulk density estimates increase the uncertainty in the pore water concentrations. However, they are not expected to introduce significant error.

The stable isotope analyses were performed on moisture-protected R-31 samples using the vacuum distillation method of Shurbaji and Campbell (1997, 64063) and the $\delta^{18}\text{O}$ and δD extraction methods of Socki et al. (1992, 64064) and Kendall and Coplen (1985, 64061), respectively. The analytical precision for the $\delta^{18}\text{O}$ and δD analyses by mass spectroscopy was better than $\pm 0.2\%$ and $\pm 4\%$, respectively.

11.1.1 Anion Results

Samples of core and cuttings obtained from the vadose zone at R-31 were analyzed to examine the vertical distributions of bromide, oxalate, nitrite, and phosphate (Figure 11.1-1; Table 11.1-1) and of chloride, fluoride, nitrate, and sulfate (Figure 11.1-2; Table 11.1-1). Several samples from R-31 had bromide, nitrate, and oxalate concentrations below the detection limit, and nitrite was not detected in any sample (Table 11.1-1). The lack of detection does not mean that these species are not present in the samples. Instead, the leaching process results in substantial dilution, and when an anion has a low concentration, the dilution can lower the concentration to a level below the detection limit. In general, the anions in R-31 samples show similar behavior with depth and have multi-peaked profiles. The spikes in anion concentrations in the alluvium and upper Otowi Member ash flows are probably related to surface evaporation processes (Figures 11.1-1 and 11.1-2). High concentrations of nitrate and phosphate may be related to microbial or other organic processes. This interpretation is supported by the absence of any corresponding chloride or bromide enrichment. The middle section of the Otowi Member has relatively low and approximately constant concentrations that are typical of the Otowi Member in other boreholes. The increase in concentrations at the bottom of the Otowi Member ash flows may be related to a decrease in moisture content. The spikes in concentrations in the Guaje Pumice Bed and basalt units appear to be related to sediments, clays, or soils. The most characteristic indicator of a paleosol constituent is the presence of oxalate, which is a common soil anion. In R-31, the highest oxalate value (~16.5 mg/L) occurs at the 295-ft depth within flow-top rubble of the Cerros del Rio, suggesting soil development at the flow surface (Section 8.3).

11.1.2 Stable Isotope Results

Both $\delta^{18}\text{O}$ and δD analyses were performed on core samples from the upper 250 ft of R-31 (Figure 11.1-3 and Table 11.1-2). Units sampled included the alluvium and the Otowi Member. Moisture-protected core samples were not available to allow examination of the Guaje Pumice Bed or Cerros del Rio basalt units. The $\delta^{18}\text{O}$ and δD results correlate, which suggests that the data are of good quality. The isotope values from the alluvium down to the middle sections of the Otowi Member show an increasing trend, and then decrease near the bottom of the Otowi Member. It may be that the larger values represent recharge of water with a different isotopic composition (possibly seasonally related) from that in the shallower or deeper parts of the profile.

11.2 Geochemistry of Regional Aquifer Waters

Three samples of regional aquifer waters in the undeveloped borehole during drilling were collected and were analyzed for a limited suite of constituents. The samples were collected primarily to determine if potential contaminants had been introduced from upper horizons into the regional aquifer during drilling operations. Potential contaminants of concern at the R-31 site include high explosive (HE) compounds and associated degradation products and, possibly, uranium and beryllium derived from firing sites in upper Ancho Canyon. The samples collected all contained some drilling fluids and thus were not representative of purely native groundwater.

The groundwater samples were obtained during active drilling, while EZ-MUD® and other additives were being used for lubricity. These additives can affect groundwater chemistry, and the analyses of R-31 water compositions reported here should be evaluated in light of this complexity. Concentrations of iron, manganese, and sulfate are all altered in the presence of EZ-MUD®. However, other constituents are not impacted by the presence of the additives used and provide useful information, including the presence or absence of mobile contaminants (tritium and nitrate). These data provide an indication of the baseline groundwater composition at various depths during drilling, against which analytical results for groundwater samples from the completed and developed well can be compared.

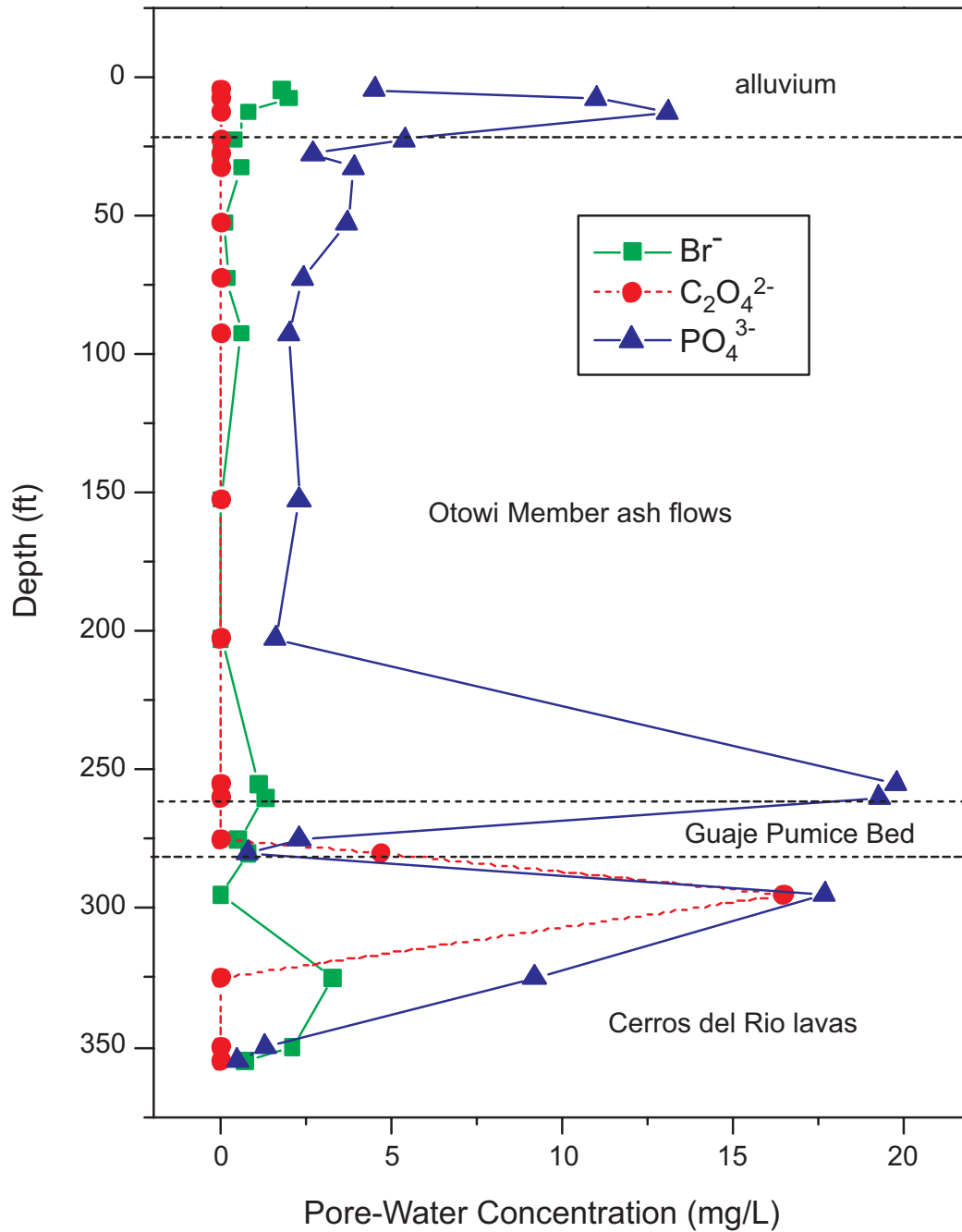


Figure 11.1-1. Vertical distributions of bromide, oxalate, and phosphate in core and cuttings from R-31

Table 11.1-1
Anion Data from Vadose-Zone Pore Waters at the R-31 Site

| Depth (ft) | Br (mg/L) | Cl (mg/L) | F (mg/L) | NO ₂ (mg/L) | NO ₃ (mg/L) | Oxalate (mg/L) | PO ₄ (mg/L) | SO ₄ (mg/L) |
|------------|-----------|-----------|----------|------------------------|------------------------|----------------|------------------------|------------------------|
| 4.5 | 1.8 | 4.0 | 19.4 | 0.0 | 0.0 | 0.0 | 4.5 | 69.1 |
| 7.5 | 2.0 | 3.8 | 13.1 | 0.0 | 7.3 | 0.0 | 11.0 | 55.6 |
| 12.5 | 0.8 | 6.5 | 12.5 | 0.0 | 40.5 | 0.0 | 13.1 | 99.1 |
| 22.5 | 0.4 | 3.7 | 20.3 | 0.0 | 99.0 | 0.0 | 5.4 | 43.1 |
| 27.5 | 0.0 | 7.7 | 12.8 | 0.0 | 147.6 | 0.0 | 2.7 | 70.2 |
| 32.5 | 0.6 | 16.4 | 12.6 | 0.0 | 115.2 | 0.0 | 3.9 | 99.2 |
| 52.5 | 0.1 | 2.4 | 15.2 | 0.0 | 0.2 | 0.0 | 3.7 | 10.2 |
| 72.5 | 0.2 | 2.8 | 8.9 | 0.0 | 19.6 | 0.0 | 2.4 | 7.7 |
| 92.5 | 0.6 | 2.6 | 13.2 | 0.0 | 21.3 | 0.0 | 2.0 | 7.2 |
| 152.5 | 0.0 | 1.7 | 14.3 | 0.0 | 7.0 | 0.0 | 2.3 | 8.4 |
| 202.5 | 0.0 | 1.8 | 30.6 | 0.0 | 19.2 | 0.0 | 1.6 | 26.4 |
| 255 | 1.1 | 98.4 | 24.8 | 0.0 | 0.0 | 0.0 | 19.8 | 312.7 |
| 260 | 1.3 | 118.0 | 28.0 | 0.0 | 0.0 | 0.0 | 19.3 | 298.1 |
| 275 | 0.5 | 98.7 | 10.0 | 0.0 | 1.7 | 0.0 | 2.3 | 68.7 |
| 280 | 0.8 | 80.2 | 10.9 | 0.0 | 0.0 | 4.7 | 0.8 | 44.6 |
| 295 | 0.0 | 33.5 | 217.6 | 0.0 | 0.0 | 16.5 | 17.7 | 65.0 |
| 325 | 3.3 | 15.5 | 75.4 | 0.0 | 0.0 | 0.0 | 9.2 | 86.4 |
| 350 | 2.1 | 7.0 | 11.3 | 0.0 | 1.1 | 0.0 | 1.3 | 13.6 |
| 355 | 0.7 | 9.7 | 12.3 | 0.0 | 3.5 | 0.0 | 0.5 | 18.1 |

Note: Values of 0.0 indicate that concentrations were below the analytical detection limit.

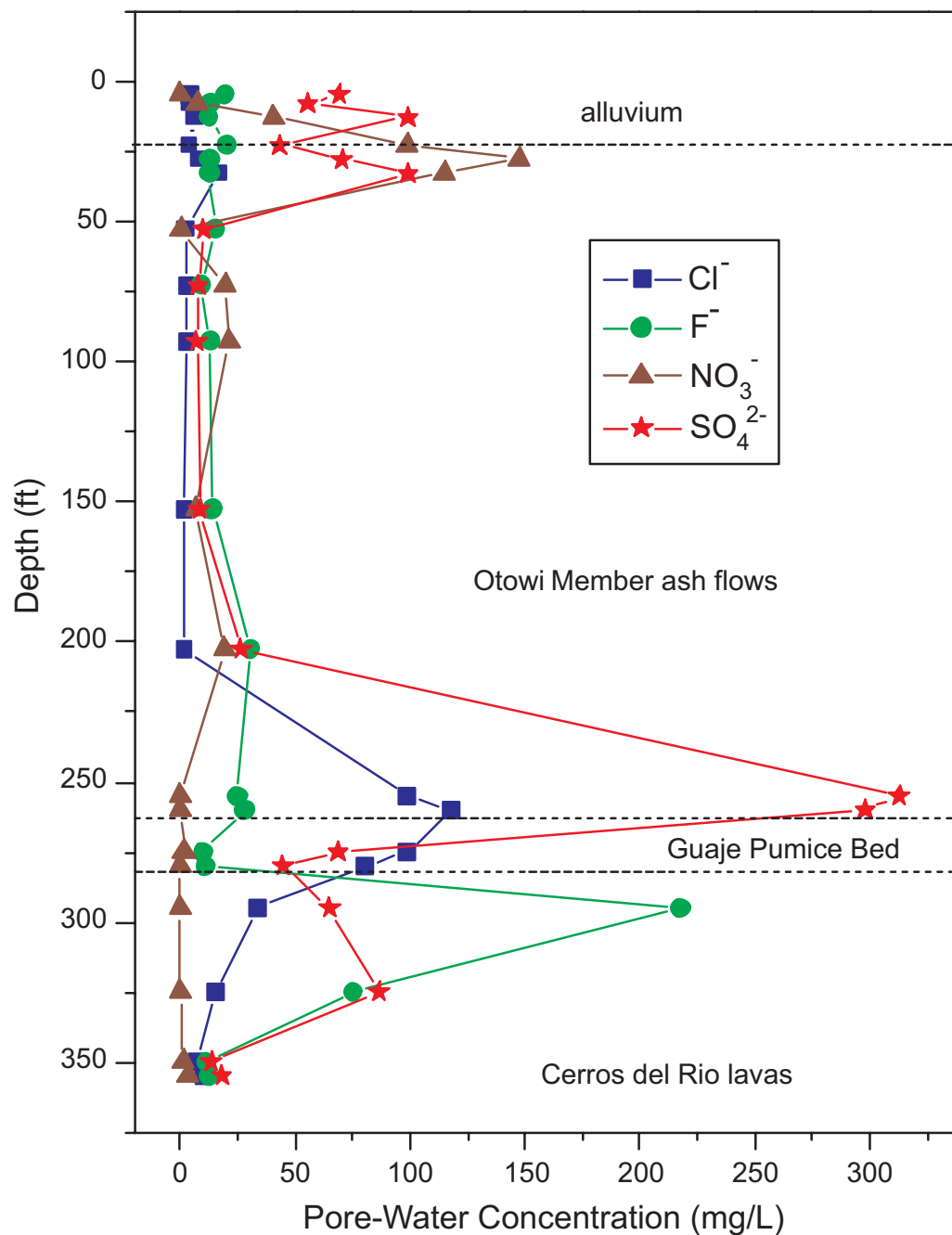


Figure 11.1-2. Vertical distributions of chloride, fluoride, nitrate, and sulfate in core and cuttings from R-31

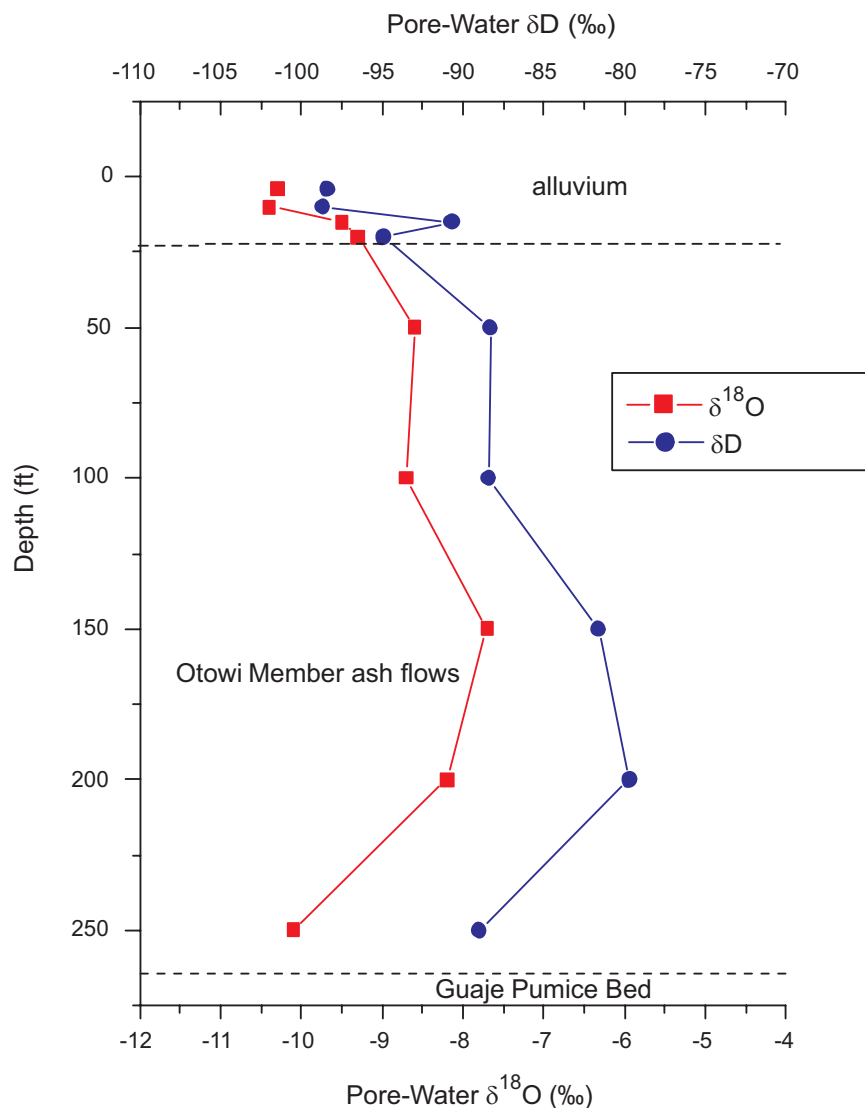


Figure 11.1-3. Vertical distributions of $\delta^{18}\text{O}$ and δD in core samples from R-31

Table 11.1-2
Stable Isotope Data from Vadose-Zone Pore Waters at the R-31 Site

| Depth (ft) | $\delta^{18}\text{O}$ (‰) | δD (‰) |
|------------|---------------------------|----------------------|
| 4 | -10.3 | -98.4 |
| 10 | -10.4 | -98.7 |
| 15 | -9.5 | -90.7 |
| 20 | -9.3 | -94.9 |
| 50 | -8.6 | -88.3 |
| 100 | -8.7 | -88.4 |
| 150 | -7.7 | -81.6 |
| 200 | -8.2 | -79.7 |
| 250 | -10.1 | -89 |

11.2.1 Methods

Groundwater samples analyzed for inorganic and organic chemicals and radionuclides were collected using a stainless-steel bailer at 545, 625, and 1087 ft in R-31. Temperature, turbidity, pH, and specific conductance were not determined on-site due to instrument malfunction. Both filtered (metals, trace elements, and major cations and anions) and nonfiltered (total organic carbon [TOC], cyanide, radionuclides, and stable isotopes of hydrogen, nitrogen, and oxygen) samples were collected for chemical and radiochemical analyses. Groundwater samples from the Cerros del Rio lavas were analyzed as both filtered (Table 11.2-1a) and nonfiltered (Table 11.2-1b) samples. Only nonfiltered groundwater samples from the Puye Formation were analyzed. Aliquots of the samples selected for filtering were passed through a 0.45- μm Gelman filter. Samples were acidified with analytical-grade HNO_3 to a pH of 2.0 or less for metal and major ion analyses. All groundwater samples collected in the field were stored at 4°C until they were analyzed. Alkalinity was determined in the laboratory using standard titration techniques, which may approximate field conditions due to sample degassing. Water samples were also preserved with non-filtered HNO_3 prior to radiometric/radiochemical analyses.

Groundwater samples were analyzed using techniques specified in the U.S. Environmental Protection Agency (EPA) SW-846 manual including ion chromatography for bromide, chloride, fluoride, nitrate plus nitrite, phosphate, and sulfate; colorimetry for total cyanide; ion selective electrode for ammonium; cold vapor atomic absorption for mercury; and inductively coupled (argon) plasma emission spectroscopy (ICPES) for aluminum, antimony, arsenic, barium, beryllium, cadmium, calcium, chromium, cobalt, copper, iron, lead, magnesium, manganese, nickel, potassium, selenium, silver, sodium, thallium, vanadium, and zinc. Uranium (non-isotopic) was analyzed by laser-induced kinetic phosphorimetric analysis. A contract laboratory, Paragon Analytics, Inc., performed this work.

Radionuclide activity in groundwater was determined by electrolytic enrichment for low-level tritium; alpha spectrometry for americium, plutonium, and uranium isotopes; and gamma spectrometry for cesium-137 and other gamma-emitting isotopes. Contract laboratories performing this work were Paragon Analytics, Inc., (radionuclides) and the University of Miami (low-level tritium).

HE compounds and associated degradation products such as 2,4,6-trinitrotoluene were analyzed by high-pressure liquid chromatography at Paragon Analytics, Inc. None of these HE compounds or degradation products were detected in the water samples from R-31.

Stable isotopes of oxygen ($\delta^{18}\text{O}$), hydrogen (δD), and nitrogen (nitrogen-15/nitrogen-14 ratio, or $\delta^{15}\text{N}$) were analyzed by Geochron Laboratories (Cambridge, Massachusetts) and Coastal Science Laboratories, Inc., (Austin, Texas), respectively, using isotope ratio mass spectrometry.

Laboratory blanks were collected and analyzed in accordance with EPA and Laboratory procedures. The precision limits (analytical error) for major ion and trace element analyses were generally $\pm 10\%$.

Samples of core and cuttings were not collected from R-31 to be analyzed for contaminants of concern because HE compounds were not detected in groundwater and because these contaminants would not adsorb onto Bandelier Tuff, Cerros del Rio lavas, and Puye Formation sediments due to the low amounts of solid organic carbon present in these formations.

Due to the presence of EZ-MUD® and other drilling fluids, the borehole water samples were not representative of purely native groundwater. Consequently, these water analysis data were only used to assist drilling decisions. Groundwater samples will be collected and analyzed for major ions, trace metals, stable isotopes, organic compounds, selected radionuclides, and other chemicals during characterization sampling using the Westbay™ MP55 system, and the data will be presented in future groundwater geochemistry reports.

Table 11.2-1a
Anion and Cation Hydrochemistry of Regional Aquifer Samples from R-31
(Filtered and Nonfiltered Samples)

| Depth (ft) | 545 | 625 | 1087 |
|--|----------------|----------------|----------------|
| Preparation | Filtered | Filtered | Nonfiltered |
| Geologic Unit | Cerros del Rio | Cerros del Rio | Puye Formation |
| Date Sampled | 01/22/00 | 01/23/00 | 02/07/00 |
| Alkalinity (mg CaCO ₃ /L) | 98 | 95 | — |
| Al (mg/L) | <0.068, U | <0.058, U | 13.0 |
| NH ₄ (as N) (mg/L) | — | — | <0.50, U |
| Sb (mg/L) | <0.0028, U | <0.0028, U | <0.000683, U |
| As (mg/L) | 0.0027 | 0.0043 | 0.0031 |
| Ba (mg/L) | 0.020 | 0.024 | 0.250 |
| Be (mg/L) | <0.00013, U | <0.00013, U | 0.000159 |
| Br (mg/L) | <0.20, U | <0.20, U | <0.20, U |
| Cd (mg/L) | <0.0002, U | <0.0002, U | <0.00013, U |
| Ca (mg/L) | 16.00 | 16.00 | 13.00 |
| Cl (mg/L) | 4.30 | 5.2 | 2.0 |
| Cr (mg/L) | 0.0026 | 0.00059 | 0.051 |
| Co (mg/L) | <0.00062, U | <0.0018, U | 0.010 |
| Cu (mg/L) | <0.00042, U | <0.00042, U | 0.018 |
| F (mg/L) | 0.72 | 0.40 | 0.26 |
| Fe (mg/L) | <0.071, U | <0.055, U | 36.00 |
| Pb (mg/L) | <0.002, U | <0.002, U | 0.00116 |
| Mg(mg/L) | 4.70 | 4.90 | 6.10 |
| Mn (mg/L) | 0.041 | 0.074 | 0.650 |
| Hg (mg/L) | <0.000011, U | <0.000011, U | 0.000013 |
| Ni (mg/L) | <0.0029, U | 0.0033 | 0.028 |
| NO ₃ + NO ₂ (mg/L) | <0.10, U | 0.24 | 0.19 |
| P (mg/L) | — | — | 0.17 |
| K (mg/L) | 3.3 | 2.5 | 5.8 |
| Se (mg/L) | <0.0038, U | <0.0038, U | 0.0048 |
| Ag (mg/L) | 0.00068 | <0.00064, U | <0.00064, U |
| Na (mg/L) | 18.00 | 15.00 | 13.00 |
| SO ₄ (mg/L) | 3.20 | 3.8 | 1.50 |
| Tl (mg/L) | <0.0032, U | <0.0032,U | 0.000744 |
| U (mg/L) | 0.00225 | 0.00208 | 0.000375 |
| V (mg/L) | 0.0061 | 0.0038 | 0.028 |
| Zn (mg/L) | <0.0013, U | <0.009, U | 0.050 |

Note: U means not detected, and the value listed is the instrument detection limit (DL); a dash means not analyzed.

Table 11.2-1b
Radionuclide, Cyanide, Total Organic Carbon, and
Stable Isotope Hydrochemistry of Regional Aquifer Samples from R-31
(Nonfiltered Samples)

| Depth (ft) | 545 | 625 | 1087 |
|------------------------|----------------|----------------|----------------|
| Geologic Unit | Cerros del Rio | Cerros del Rio | Puye Formation |
| Date Sampled | 01/22/00 | 01/23/00 | 02/07/00 |
| Tritium (pCi/L) | 0.57 | 0.32 | <0.27, U |
| Am-241 (pCi/L) | — | — | <0.006, U |
| Cs-137 (pCi/L) | — | — | <0.7, U |
| Co-60 (pCi/L) | — | — | <1.5, U |
| Eu-152 (pCi/L) | — | — | 8.7 |
| Gross α (pCi/L) | — | — | 5.2 |
| Gross β (pCi/L) | — | — | 14.1 |
| Gross γ (pCi/L) | — | — | 147 |
| Pu-238 (pCi/L) | — | — | <0.014, U |
| Pu-239,240 (pCi/L) | — | — | <0.005, U |
| U-234 (pCi/L) | — | — | 0.198 |
| U-235 (pCi/L) | — | — | <0.008, U |
| U-238 (pCi/L) | — | — | 0.125 |
| Cyanide total (mg/L) | — | — | <0.010, U |
| TOC (mg/L) | — | — | 11.00 |
| δD (‰) | — | — | -74 |
| $\delta^{15}N$ (‰) | — | — | +1.9 |
| $\delta^{18}O$ (‰) | — | — | -11.1 |

Note: U means not detected, and the value listed is the DL; a dash means not analyzed.

11.2.2 Results of Geochemical Analysis of Regional Aquifer Samples from the Cerros del Rio Lavas in R-31

Activities of tritium in regional aquifer samples from the Cerros del Rio lavas at 545 and 625 ft are 0.57 and 0.32 pCi/L, respectively (Table 11.2-1b). These findings suggest that recharge to this part of the aquifer has not occurred since the 1940s. The dominant potential sources of tritium are from Laboratory discharges and atmospheric (worldwide) fallout from weapons testing. Activities of other radionuclides were not measured in these samples because of limited sample volumes and low activities of tritium suggesting that radionuclide contamination is absent at R-31. The isotope Eu-152 was detected, however, at an activity of 8.7 pCi/L in the deeper aquifer sample (1087-ft depth) using gamma spectroscopy.

Filtered borehole water samples collected from within the Cerros del Rio lavas in R-31 are characterized by a calcium-sodium-bicarbonate ionic composition (Table 11.2-1a). Concentrations of sulfate and chloride are less than 6 mg/L, and concentrations of nitrate plus nitrite (as nitrogen) are less than 0.3 mg/L. Concentrations of dissolved iron are generally less than DLs, suggesting overall oxidizing conditions with respect to these two solutes. Under relatively oxidizing conditions, iron and manganese

precipitate from solution, forming moderately insoluble phases. Concentrations of uranium are 0.00225 and 0.00208 mg/L within the perched saturated zones (Table 11.2-1a).

Concentrations of aluminum, antimony, beryllium, bromide, cadmium, cobalt, copper, lead, mercury, selenium, thallium, and zinc are less than DLs (ICPES) in the water samples collected from within the Cerros del Rio lavas in R-31. Silver was detected at 0.00068 mg/L, just above the DL of 0.00064 mg/L, in the groundwater sample collected at a depth of 545 ft (Table 11.2-1a).

HE compounds and associated degradation products were not detected in water samples collected from within the Cerros del Rio lavas during drilling of R-31.

Based on the above analytical results for the R-31 borehole water samples collected from within the Cerros del Rio lavas, it appears that contamination from Laboratory discharges is not present in the regional aquifer at this well site. Additional characterization sampling will be conducted at the R-31 site.

11.2.3 Results of Geochemical Analysis of Regional Aquifer Samples from Puye Formation River Gravels in R-31

The nonfiltered regional aquifer sample collected from the Puye Formation river gravels at the 1087-ft depth is characterized by a calcium-sodium-bicarbonate ionic composition (Table 11.2-1a). Concentrations of sulfate and chloride are 1.5 and 2 mg/L, respectively, whereas the concentration of nitrate plus nitrite (as nitrogen) is less than 0.2 mg/L. The concentration of ammonium is less than the DL (0.50 mg/L). Sulfate reduction may account for the low concentration of this solute due to the oxidation (biodegradation) of EZ-MUD®. Sulfate and other oxidized solutes are electron acceptors (oxidizing agents) whereas EZ-MUD® is an electron donor (reducing agent). Under such conditions, microbial (anaerobic) populations increase due to the presence of EZ-MUD®, which provides a food source, and the groundwater becomes reducing with respect to manganese, iron, and sulfur. Based on thermodynamics and energy yields, the order of reduction (most oxidizing to most reducing) is as follows: dissolved oxygen, followed by manganese, followed by iron, and, finally, sulfate (Langmuir 1997, 56037). This oxidation-reduction process has been observed in R-7, R-9i, R-12, CdV-R15-3, R-19, and R-22 where EZ-MUD® and other organic-based drilling fluids were used. The aqueous chemistry of the regional aquifer at R-31 will eventually return to predrilling conditions after the EZ-MUD® has oxidized to CO₂ and H₂O and aerobic conditions are re-established. Elevated concentrations of alkalinity, mainly as bicarbonate, however, occur as an oxidation product of EZ-MUD® as observed in other R-series wells including R-7, R-12, and R-22.

An elevated concentration of aluminum (13 mg/L) is observed in the nonfiltered Puye Formation groundwater sample, which may reflect the presence of particulates or colloids. At this concentration, solubilities of kaolinite, illite, and smectite are exceeded, and the groundwater is predicted to be oversaturated with respect to these minerals. It is also possible, however, that these clay minerals are unstable, in which case, aluminum forms complexes with the dissociated carboxylic acids and other organic anions present in the EZ-MUD® copolymer as it biodegrades.

Due to the presence of residual EZ-MUD® in R-31 during well completion and development, elevated concentrations of iron (36 mg/L) and manganese (0.650 mg/L) are prevalent. Reductive dissolution of ferric and manganese (oxy)hydroxides occurs under such strongly reducing conditions (Langmuir 1997, 56037). Alternatively, the occurrence of high iron and manganese concentrations in the Puye Formation aquifer zone may reflect actual formation chemistry or colloid-related chemistry. Further analysis of this problem is planned.

Concentrations of antimony, cadmium, bromide, and silver are less than DLs in the nonfiltered Puye Formation groundwater sample from R-31. Several analytes, however, were detected at low concentrations close to DLs using ICPEs. Mercury was detected at 0.000013 mg/L (DL of 0.000011 mg/L), and beryllium was detected at 0.000159 mg/L (DL of 0.00013 mg/L).

The concentration of TOC is 11.0 mg/L, suggesting the presence of residual drilling fluids at the time of sampling. The occurrence of EZ-MUD® and other drilling fluids in the borehole water contributes to TOC consisting of hydrophilic and hydrophobic organic compounds. Bis(2-ethylhexyl)phthalate was detected at 4.6 µg/L; it is a volatile organic compound that is frequently detected, possibly due to the extensive use of plastics worldwide.

As in the Cerros del Rio regional aquifer samples, the activity of tritium within the Puye Formation water sample is low (less than 0.27 pCi/L; Table 11.2-1b). This value suggests that no recharge has occurred to any part of the regional aquifer sampled at the R-31 site since the early 1940s. Activities of Am-241, Pu-238, Pu-239,240, Co-60, and Cs-137 are less than DLs. Activities of U-234 and U-238 are 0.198 and 0.125 pCi/L, respectively, which is within the natural distribution observed at the Laboratory. The activity of U-235 is less than 0.008 pCi/L (U qualified). Activities of gross alpha, gross beta, and gross gamma are 5.2, 14.1, and 147 pCi/L, respectively. Gamma activity is due to the presence of gamma-emitting isotopes within the U-238 and U-235 decay chains. These include Pa-234, Rn-222, Po-218, Bi-214, Po-214, Bi-210, and Po-210 for the U-238 decay series, and Pa-231, Th-227, Ra-223, Rn-219, Po-215, Tl-207, Po-214, Pb-207 for the U-235 decay series.

Values for δD and $\delta^{18}O$ are -74‰ and -11.1‰, respectively, suggesting that the borehole water in the regional aquifer is derived from a meteoric (atmospheric) source and that evaporation has not taken place to a significant extent. The equation for the Jemez Mountains meteoric line (JMML) (Blake et al. 1995, 49931) is given by the following expression:

$$\delta D = 8\delta^{18}O + 12. \qquad \text{Equation 11-1}$$

The measured values for δD and $\delta^{18}O$ plot slightly above the JMML with analytical errors for δD and $\delta^{18}O$ of ± 4 ‰ and 0.2‰, respectively. The value for $\delta^{15}N$ (NO_3) is 1.9‰, suggesting that nitrate plus nitrite is derived from an abiotic source (volcanic sediments, Clark and Fritz 1997, 59168). Denitrification is not occurring to a significant extent (Clark and Fritz 1997, 59168) at the R-31 site. Denitrification produces positive $\delta^{15}N$ values (3‰ to > 30‰) because ^{14}N is consumed by catabolic organisms, resulting in enriched ^{15}N in solid waste (manure) (Clark and Fritz 1997, 59168).

Analyses of the borehole water sample collected at 1087 ft did not detect any HE compounds or associated degradation products.

12.0 SUMMARY OF HYDROGEOLOGIC FEATURES AT SCREENED INTERVALS

The five screened intervals in R-31 include three zones in basalt and two in Puye Formation "Totavi"-like river gravels. Screen #1 is the only screen located above the regional water table; this screen spans the sediment between flow series E and F in the Cerros del Rio lavas. Screen #2 spans the regional water table, which occurs near the contact between the upper Cerros del Rio alkalic-to-tholeiitic lavas and the Cerros del Rio basaltic andesites (mugearites). Open-hole video logging and a lack of clay returns in cuttings indicate that there are open fractures at screen #3, which is within the lowest basaltic unit in R-31, the Cerros del Rio low-Ni,Cr alkalic basalts. Screens #4 and #5 are both within river gravels that produced large volumes of water during drilling.

Screen #1 is located at a depth where evidence from the borehole video indicated water flowing into the borehole. The video indicates water first flowing into the borehole in basaltic-breccia sediments at the ~440-ft depth, with sheet flow along the borehole wall below this depth. At a screened depth of 439.1 to 454.4 ft, screen #1 includes the full sequence of sediments between Cerros del Rio flow series E and F (444- to 450-ft depth). The top of the screen has access to the breccia zone at the base of flow series F; the bottom of the screen is within the breccia zone at the top of flow series E. Most of the screened interval is within the clay-rich sediments between these flow series. As described in Section 8.4.1, these sediments provide the most abundant clay content of any bulk samples from R-31 (36% smectite and 1% kaolinite). The sediments also contain a small but significant amount of the zeolite clinoptilolite (~3%). Although intercalated within the upper alkalic to tholeiitic flow series in R-31, these sediments are dominated by detritus that is not derived from the basalts (quartz, biotite, hornblende), indicating distant source areas and an aggrading stream system active during a hiatus in volcanic activity. The high clay content within the sediments, as well as within the adjacent flow breccias, makes this a relatively low-productivity perching horizon; to date, no water has been collected from this screen, but water may be collected in the future.

Screen #2 is positioned to include the top of the zone of regional saturation. DTW measurements throughout the drilling of R-31 fluctuated between 521 and 537 ft; DTW was measured at 522 ft following well completion but before insertion of the Westbay™ MP55 system. This depth is within the clay-altered zone between two major flow series of the Cerros del Rio—the upper alkalic-to-tholeiitic series (flow series C to F) and the basaltic andesite (mugearite; flow series B). Despite the clay associated with this zone, the breccias and clastic detritus produced a considerable amount of water during development (Table 4.3-1).

Screen #3 is within the Cerros del Rio low-Ni,Cr alkalic basalt, which provided a borehole with exceptionally smooth walls but abundant columnar fractures. Borehole video of the interval from 630 to 693 ft indicated abundant fractures with little evidence of fracture filling. Screen #3, at 666.3 to 676.3 ft, is centered in this fracture zone and thus provides information on characteristics of a representative fracture system in massive basalt. Slug injection testing at this screen indicates a hydraulic conductivity of ~4–7 ft/day (Table 10.2-1 and Section 10.2).

Screen #4 (826.6- to 836.6-ft depth) is centered within a thick sequence of quartzite-bearing river gravels that produced large amounts of water during drilling. Sediments representative of this screened interval have an abundance of quartzite and represent stream-worn gravels from distant sources. As the interval from 827 to 847 ft was being drilled, the debris-laden flux circulated out of the hole was so high that the jetted sand and gravel wore a hole in the cyclone. This observation fits well with the concept of high water content and ready water transmission in these gravels. However, initial injection testing at this screen produced an apparently low transmissivity (~0.7–0.9 ft²/day; Table 10.2-1 and Section 10.2). In a second round of testing, however, these values rose to ~6 ft²/day.

Screen #5 is located at greater depth within river gravels similar to those at screen #4 to provide two sampling ports within this important hydrogeologic unit. These sediments also produced large amounts of water during drilling. The sediments at screen #5 are not quite as quartzite-rich as those at screen #4 but are equally representative of riverine gravel deposits. Hydraulic testing at this screen indicated a high hydraulic conductivity, ~23 ft/day (Table 10.2-1 and Section 10.2). Although not directly comparable with conductivity, the low transmissivity at screen #4 (~6 ft²/d) indicates that hydraulic conductivity there is significantly lower than at screen #5. The causes of the discrepancy in water production at screens #4 and #5 are not certain and will be a subject of further analysis.

13.0 IMPLICATIONS OF R-31 FOR CONCEPTUAL MODELS OF GEOLOGY, HYDROLOGY, AND GEOCHEMISTRY

The conceptual geologic model for the Laboratory has been considerably modified following the completion of R-31. Inaccuracies in the model as it existed prior to drilling, compared with the as-drilled stratigraphy, are illustrated in Figure 8.0-1a. Although the underestimated thickness of the Bandelier Tuff at this site is one of the major differences between the predicted and actual stratigraphy, the more significant impacts with regard to the hydrogeology are (1) the occurrence of the regional water table within Cerros del Rio lavas rather than within Puye Formation fanglomerates and (2) the unexpected thickness of the river-gravel ("Totavi") unit of the Puye Formation. The occurrence of regional saturation within basaltic lavas rather than fanglomerates indicates a system in which flow is fracture-controlled rather than porous. Less access to reactive glass but more access to ferrous iron are both consequences of this location. At greater depth, the more extensive occurrence of coarse river gravels with well-rounded clasts and little fine matrix provides access to large amounts of highly transmissive material. Extension of this transmissive unit to depths below the present Rio Grande (Figures 8.0-3 and 8.0-4) may influence the geometry of flow paths toward the river.

The conceptual hydrologic model has been strengthened by new data regarding the saturated hydraulic conductivity of the basaltic lava and river-gravel lithologies beneath the Laboratory. Data from the lavas, compared with previous data (Broxton et al. 2001, 66599), indicate a wide range of hydraulic conductivities depending largely on fracture conditions, lava-flow integrity, and clay distribution. The two data points for river gravels at the R-31 site provide a new view of this hydrogeologic unit. The discrepancy between hydraulic test results for screens #4 and #5 (Table 10.2-1) will require further analysis.

The absence of contamination at the R-31 site has little impact on the conceptual model of geochemistry for the Laboratory, but this absence serves as a benchmark against which the results of future characterization water samples from R-31 can be evaluated. Differences in groundwater geochemistry between samples from the Cerros del Rio lavas and from the Puye Formation river gravels, particularly those that will be collected after the well has stabilized, will provide information on baseline variability in the regional aquifer beneath the Laboratory.

14.0 ACKNOWLEDGMENTS AND CONTRIBUTIONS

Management guidance and support for the drilling of R-31 was provided through Julie Canepa, ER Project manager, and Charlie Nylander, Monitoring Well Installation Program manager. Allyn Pratt provided project leadership, and David Broxton was the team leader for R-31 activities.

SBDC provided Phase I drilling services. Dynatec Drilling Company provided Phase II drilling services under the direction of John Eddy, the drilling supervisor.

Joe Skalski of the FSF provided the Laboratory yard support necessary for R-31 operations. Steve Bolivar supervised FSF sample operations.

Doug Barney was the site safety officer. Site access and integration with TA-39 facility operations was provided through Michelle Cash, Jim King, and Jerry Vasilk.

Jon Marin, Rich Koch, and Michelle Benak of SAIC provided geologic field support at the R-31 site. Rich Koch also supported hydrologic testing. Bob Hull was the drilling consultant.

15.0 REFERENCES

- Blake, W. D., F. Goff, A. I. Adams, and D. Counce, May 1995. "Environmental Geochemistry for Surface and Subsurface Waters in the Pajarito Plateau and Outlying Areas, New Mexico," Los Alamos National Laboratory report LA-12912-MS, Los Alamos, New Mexico. (Blake et al. 1995, 49931)
- Bouwer, H. and R. C. Rice, 1976. "A Slug Test for Determining Hydraulic Conductivity of Unconfined Aquifers with Completely or Partially Penetrating Wells," *Water Resources Research*, Vol. 12, pp. 423–428. (Bouwer and Rice 1976, 64056)
- Broxton, D., personal communication from F.W. McDowell on K-Ar ages, May 22, 1987. (Broxton 1987, 71428)
- Broxton, D., personal communication from G. WoldeGabriel on age determinations, March 11, 1999. (Broxton 1999, 71429)
- Broxton D., R. Gilkeson, P. Longmire, J. Marin, R. Warren, D. Vaniman, A. Crowder, B. Newman, B. Lowry, D. Rogers, W. Stone, S. McLin, G. WoldeGabriel, D. Daymon, and D. Wyckoff, May 2001. "Characterization Well R-9 Completion Report." Los Alamos National Laboratory report LA-13742-MS, Los Alamos, New Mexico. (Broxton et al. 2001, 66599)
- Clark I. D. and P. Fritz, 1997. *Environmental Isotopes in Hydrogeology*, Lewis Publishers, New York, New York. (Clark and Fritz 1997, 59168)
- Dethier, D. P., 1997. "Geology of White Rock Quadrangle, Los Alamos and Santa Fe Counties, New Mexico," Geologic Map 73, New Mexico Bureau of Mines and Mineral Resources, Socorro, New Mexico, scale 1:24,000. (Dethier 1997, 49843)
- Gee, G. W., M. D. Campbell, G. S. Campbell, and J. H. Campbell, 1992. "Rapid Measurement of Low Soil Water Potentials Using a Water Activity Meter." *Soil Science Society of America Journal*, Vol. 56, pp. 1068–1070. (Gee et al. 1992, 58717)
- Hantush, M. S., and C. E. Jacob, 1955. "Non-Steady Radial Flow in an Infinite Leaky Aquifer," *American Geophysical Union Transactions*, Vol. 36, pp. 95–100. (Hantush and Jacob 1955, 70091)
- Kendall, C., and T. B. Coplen, 1985. "Multisample Conversion of Water to Hydrogen by Zinc for Stable Isotope Determination," *Analytical Chemistry*, Vol. 57, pp. 1437–1446. (Kendall and Coplen 1985, 64061)
- Langmuir, D., 1997. *Aqueous Environmental Geochemistry*, Prentice-Hall, Inc., Upper Saddle River, New Jersey. (Langmuir 1997, 56037)
- LANL (Los Alamos National Laboratory), June 1993. "RFI Work Plan for Operable Unit 1132," Los Alamos, New Mexico. (LANL 1993, 15316)
- LANL (Los Alamos National Laboratory), January 31, 1996. "Groundwater Protection Management Program Plan," rev. 2.0, Los Alamos, New Mexico. (LANL 1996, 70215)
- LANL (Los Alamos National Laboratory), May 1998. "Hydrogeologic Workplan," Los Alamos, New Mexico. (LANL 1998, 59599)
- Purtymun, W. D., January 1984. "Hydrologic Characteristics of the Main Aquifer in the Los Alamos Area: Development of Ground Water Supplies," Los Alamos National Laboratory report LA-9957-MS, Los Alamos, New Mexico. (Purtymun 1984, 6513)

Shurbaji, A.-R. M. and A. R. Campbell, 1997. "Study of Evaporation and Recharge in Desert Soil Using Environmental Tracers, New Mexico, USA." *Environmental Geology*, Vol. 29. pp. 147–151. (Shurbaji and Campbell 1997, 64063)

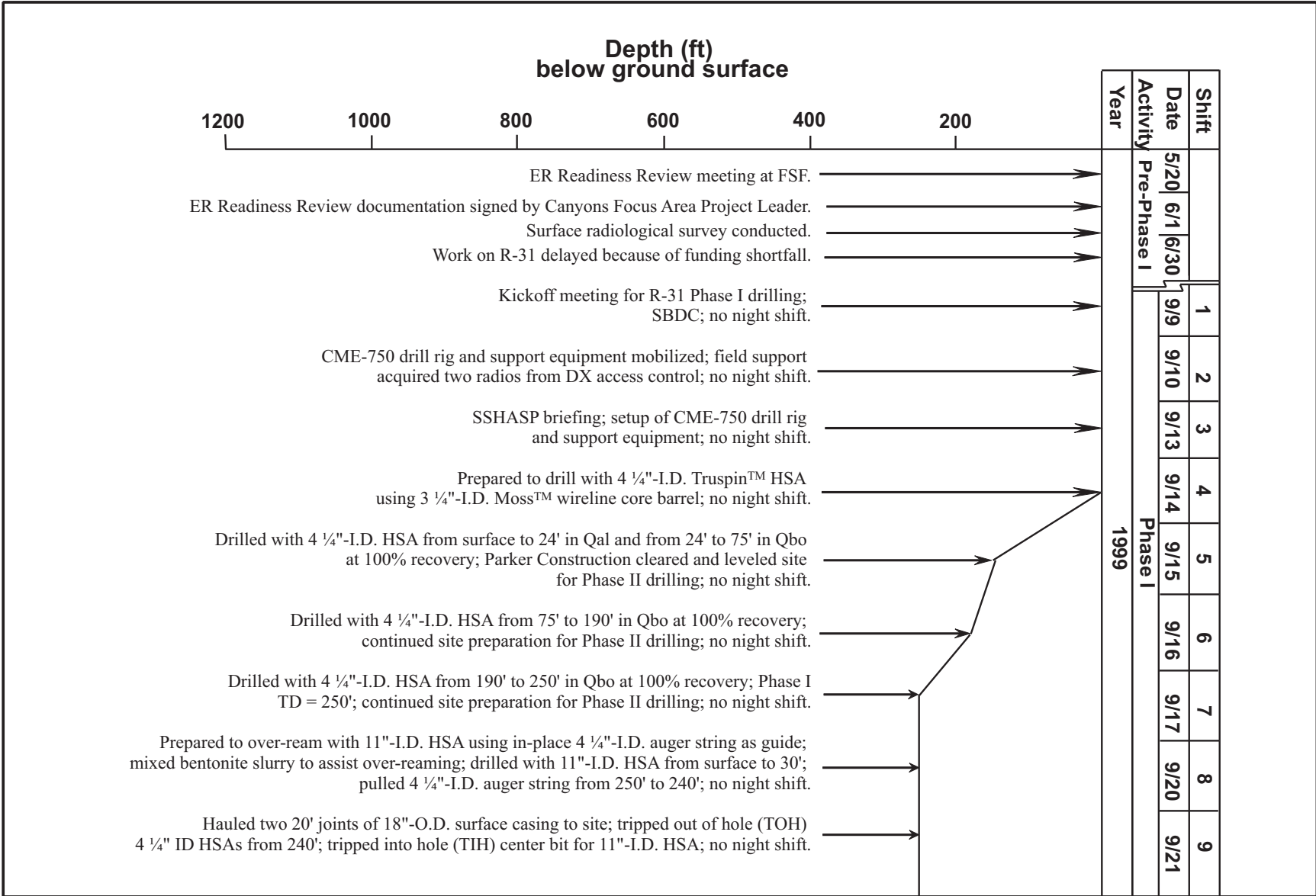
Socki, R. A., H. R. Karlsson, and E. K. Gibson, 1992. "Extraction Technique for Determination of Oxygen-18 in Water Using Preevacuated Glass Vials," *Analytical Chemistry*, Vol. 64, pp. 829–831. (Socki et al. 1992, 64064)

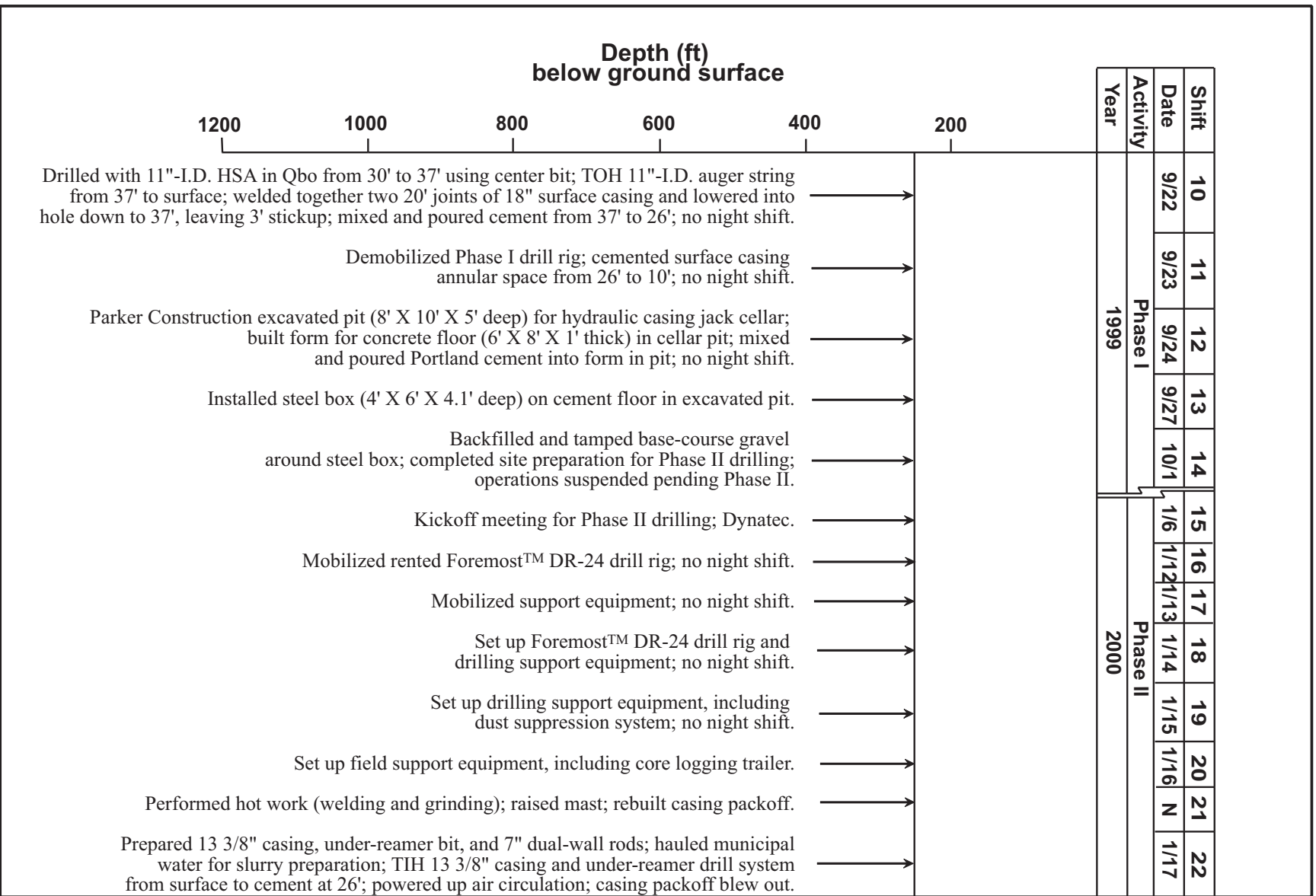
Stone, W., S. McLin, and D. Vaniman, 2001. "Hydraulic Conductivity vs. Geology in New Los Alamos Wells" (abstract), New Mexico Geological Society Spring Meeting, Socorro, Abstracts, p. 32. (Stone et al. 2001, 70090)

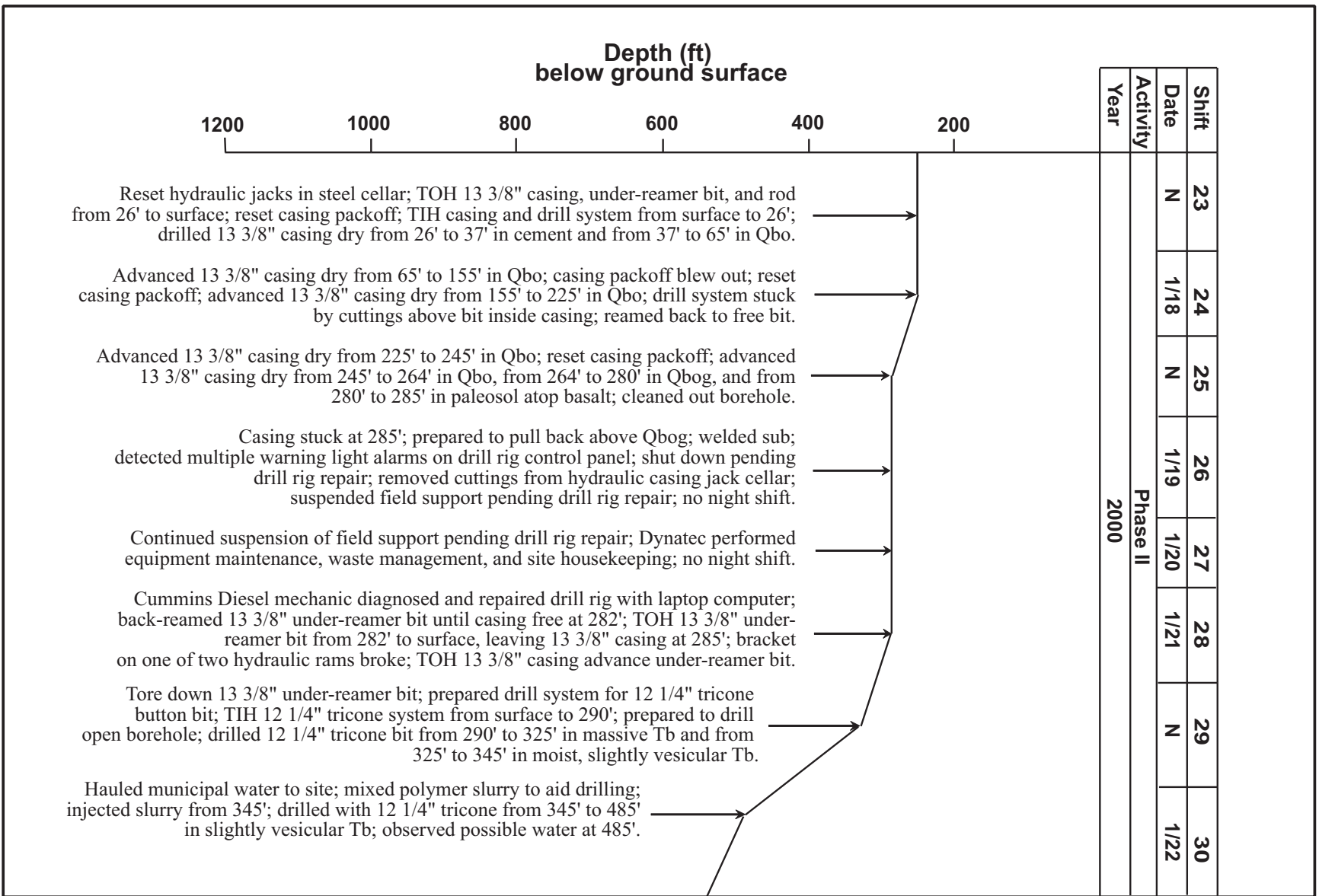
WoldeGabriel, G., A. W. Laughlin, D. P. Dethier, and M. Heizler, 1996. "Temporal and Geochemical Trends of Lavas in White Rock Canyon and the Pajarito Plateau, Jemez Volcanic Field, New Mexico, USA," in *New Mexico Geological Society Guidebook, 47th Field Conference*, pp. 251–261. (WoldeGabriel et al. 1996, 54427)

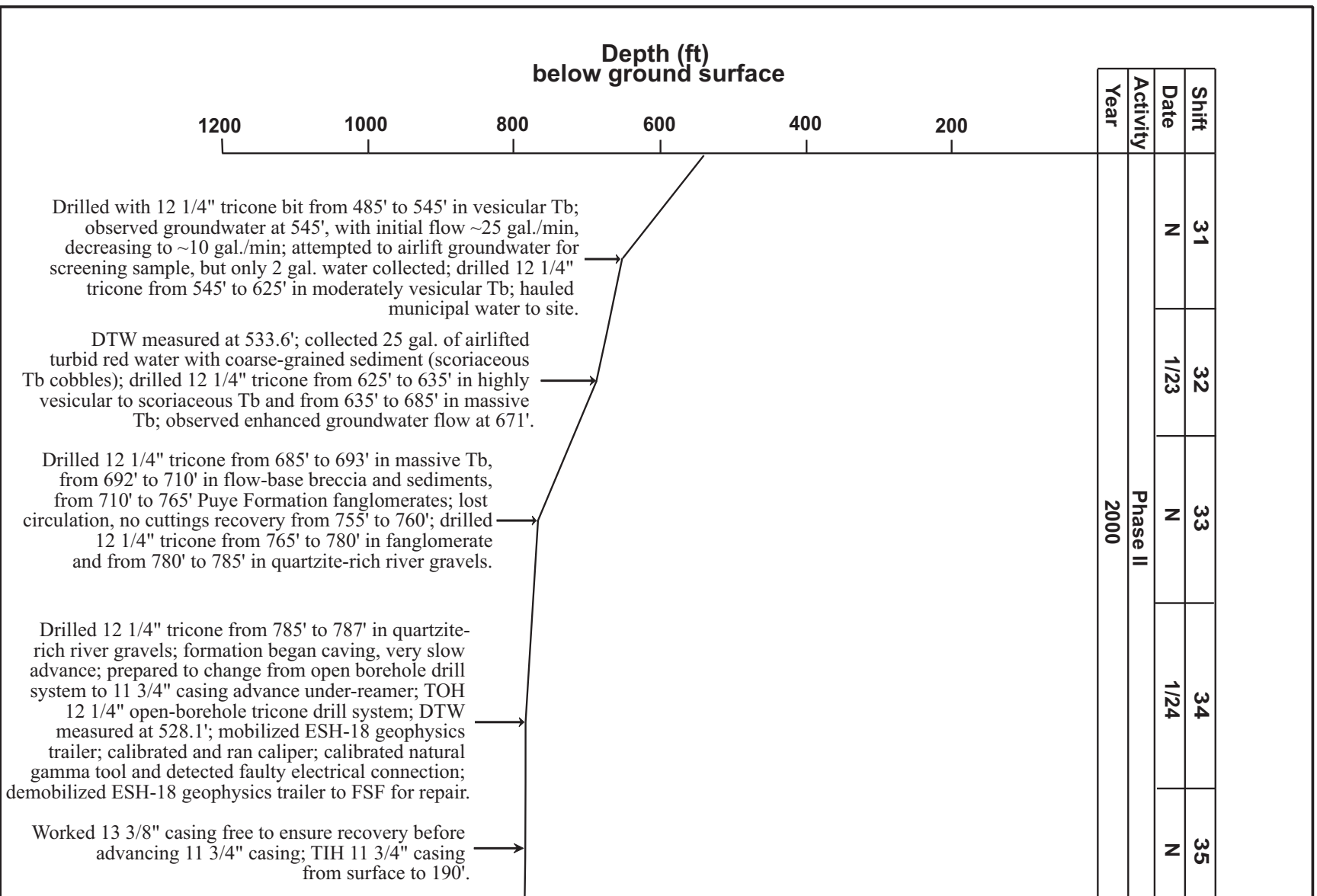
Appendix A

Diagram of Site Activities Related to Progress





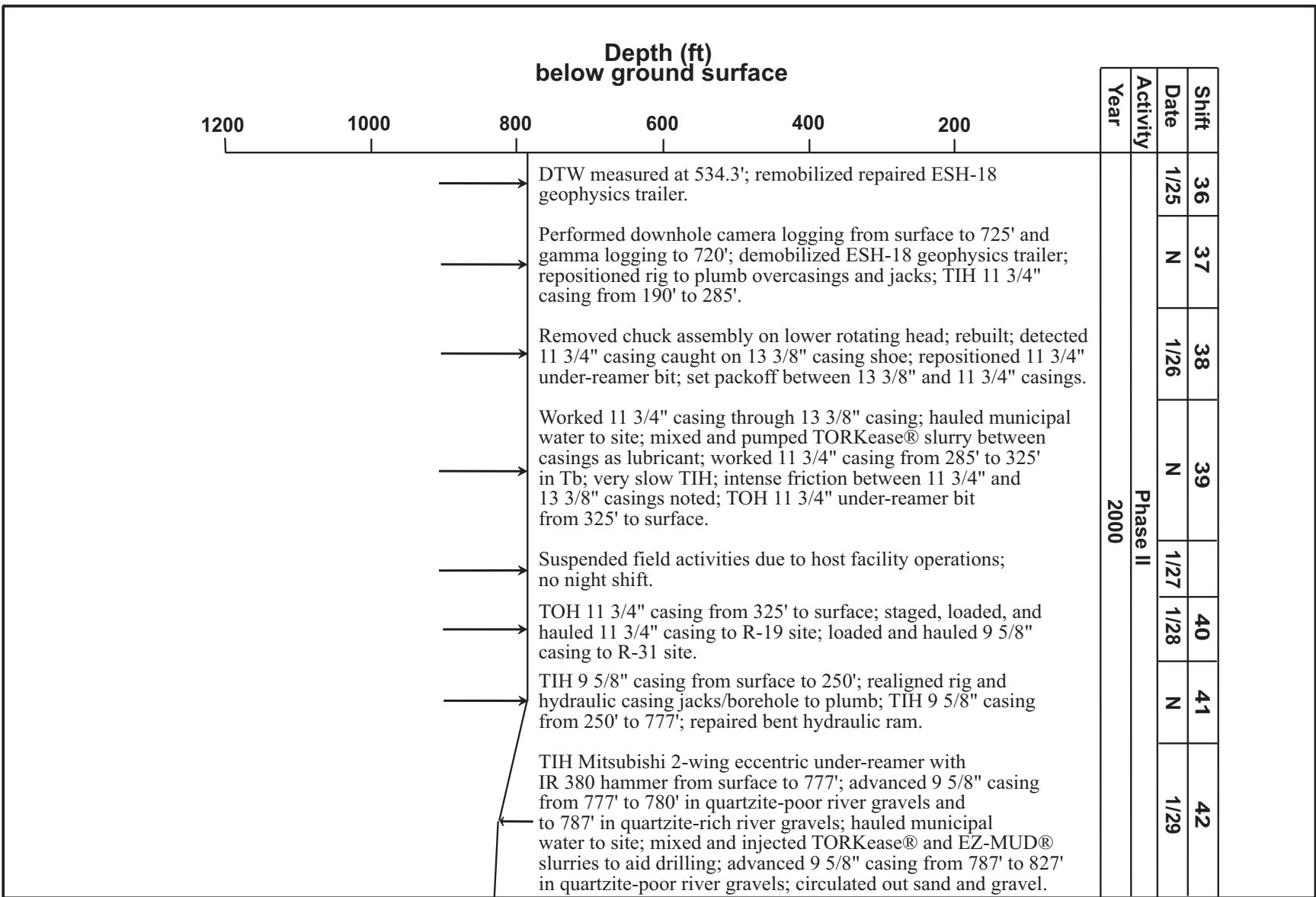


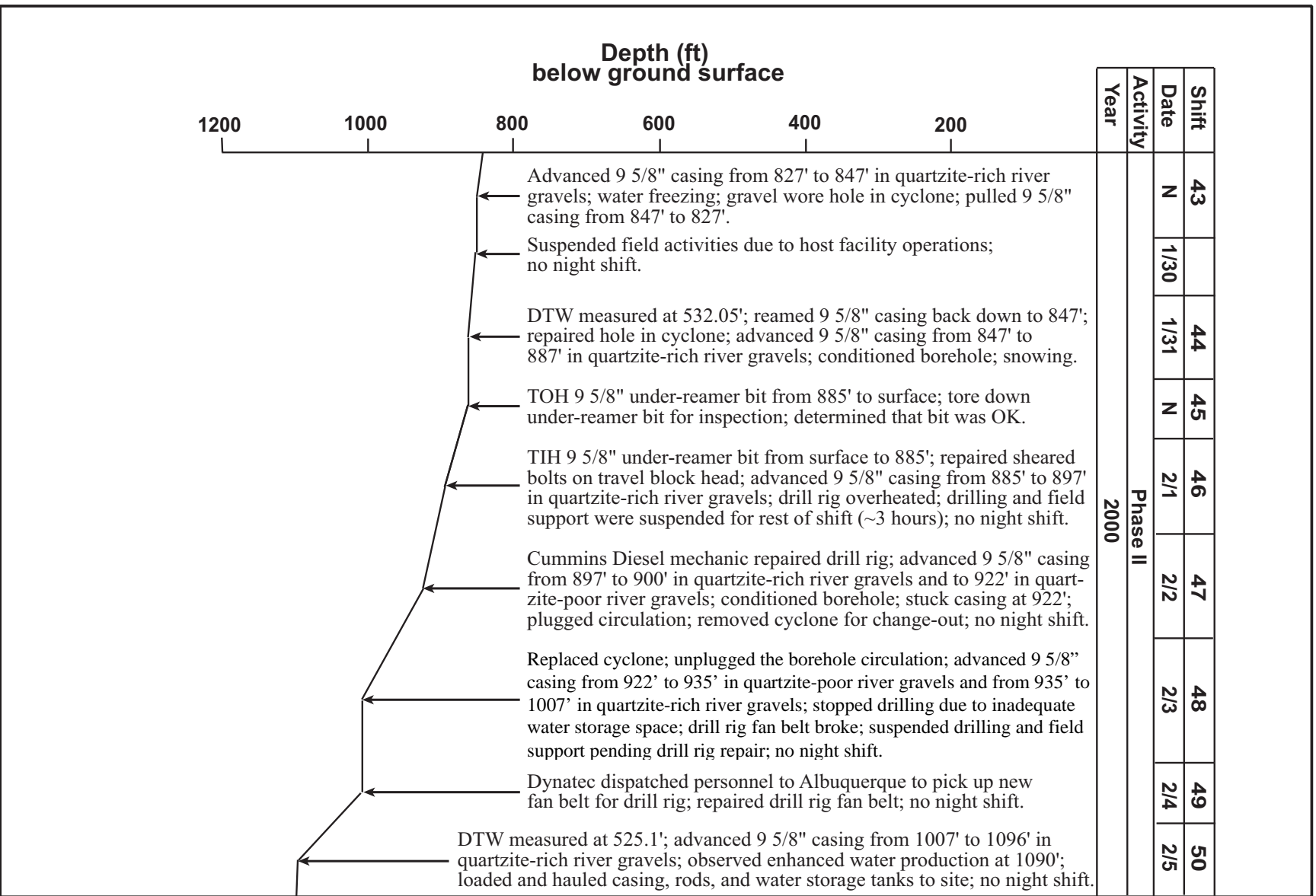


March 2002

A-4

ER2001-0704

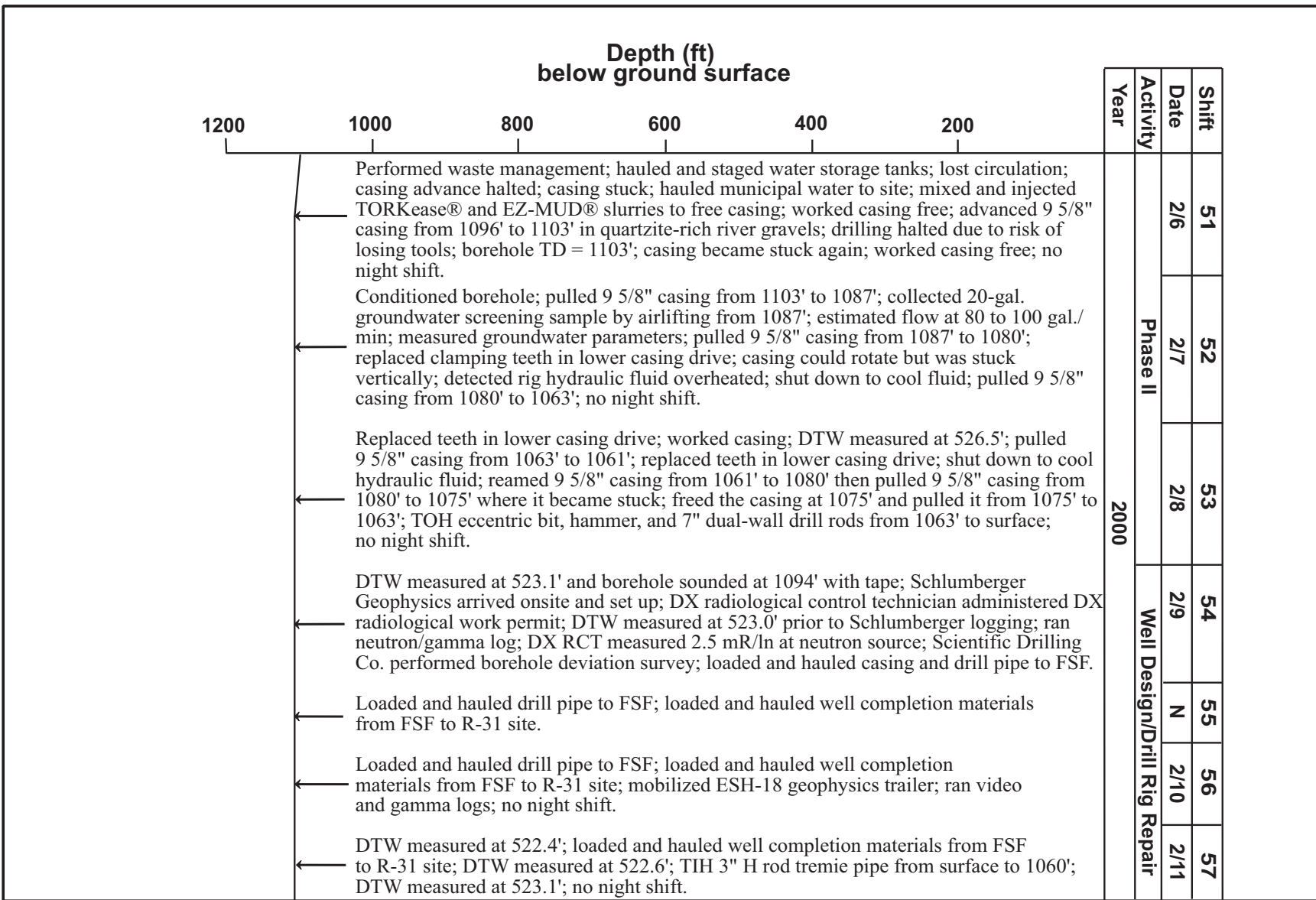


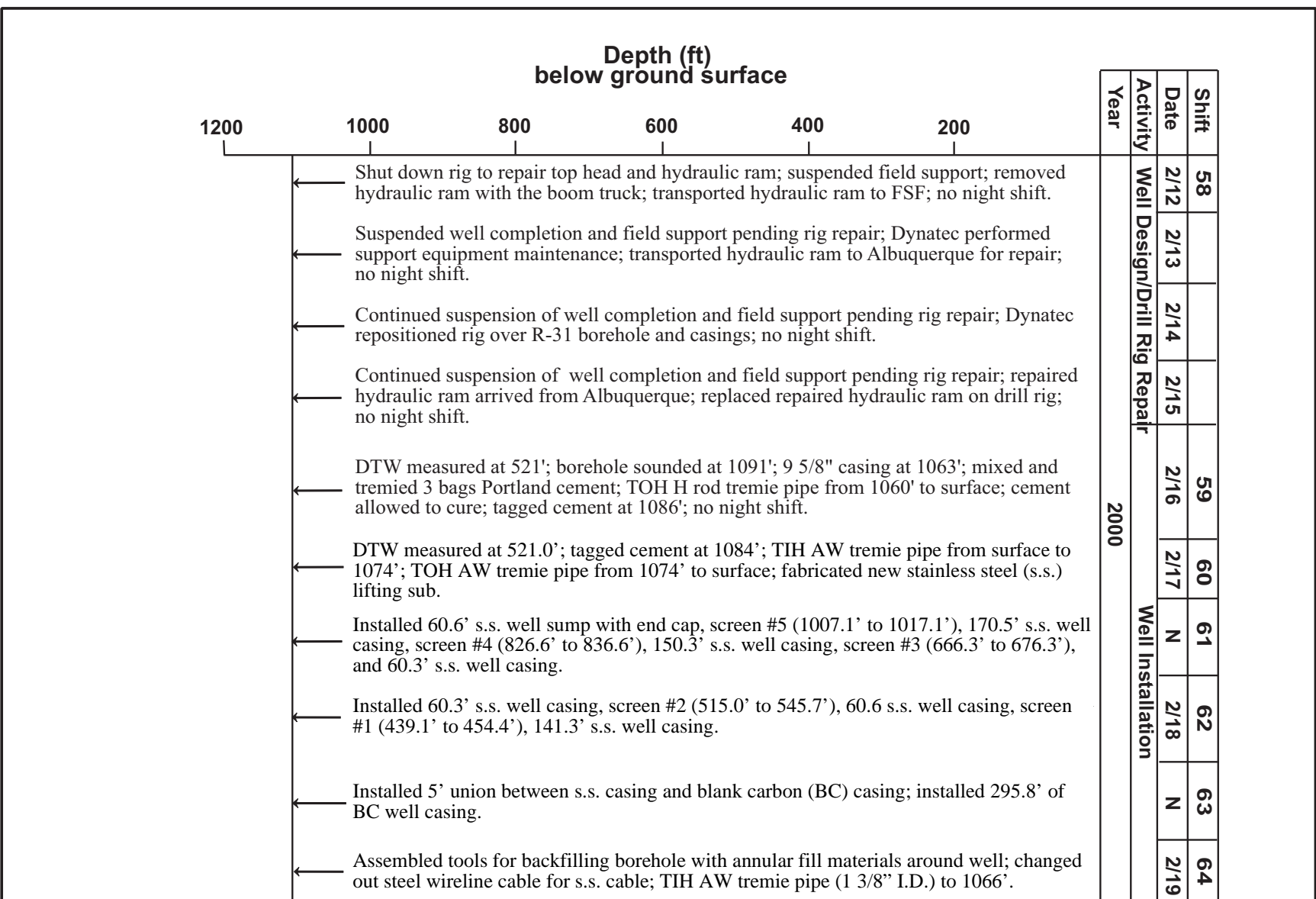


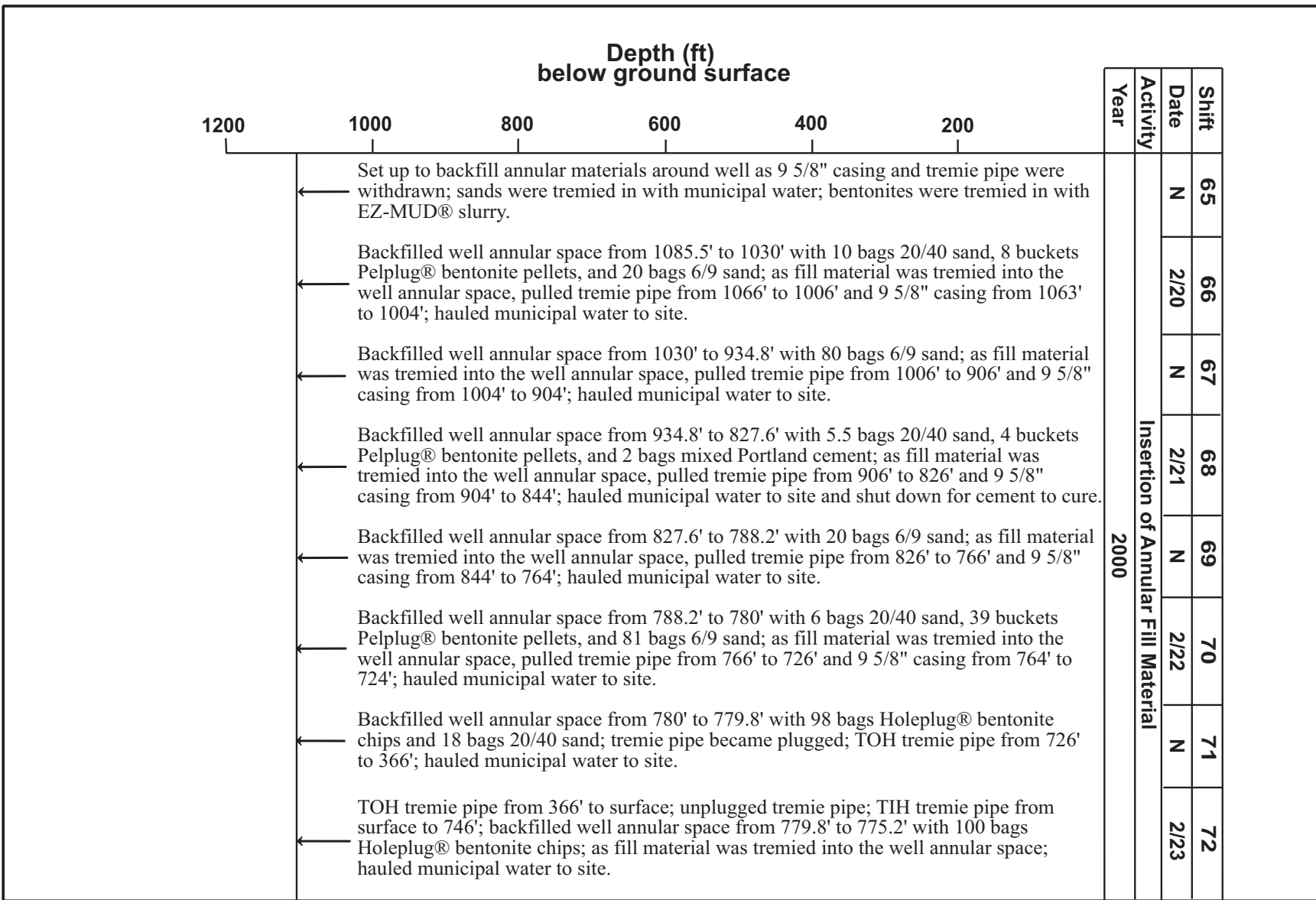
March 2002

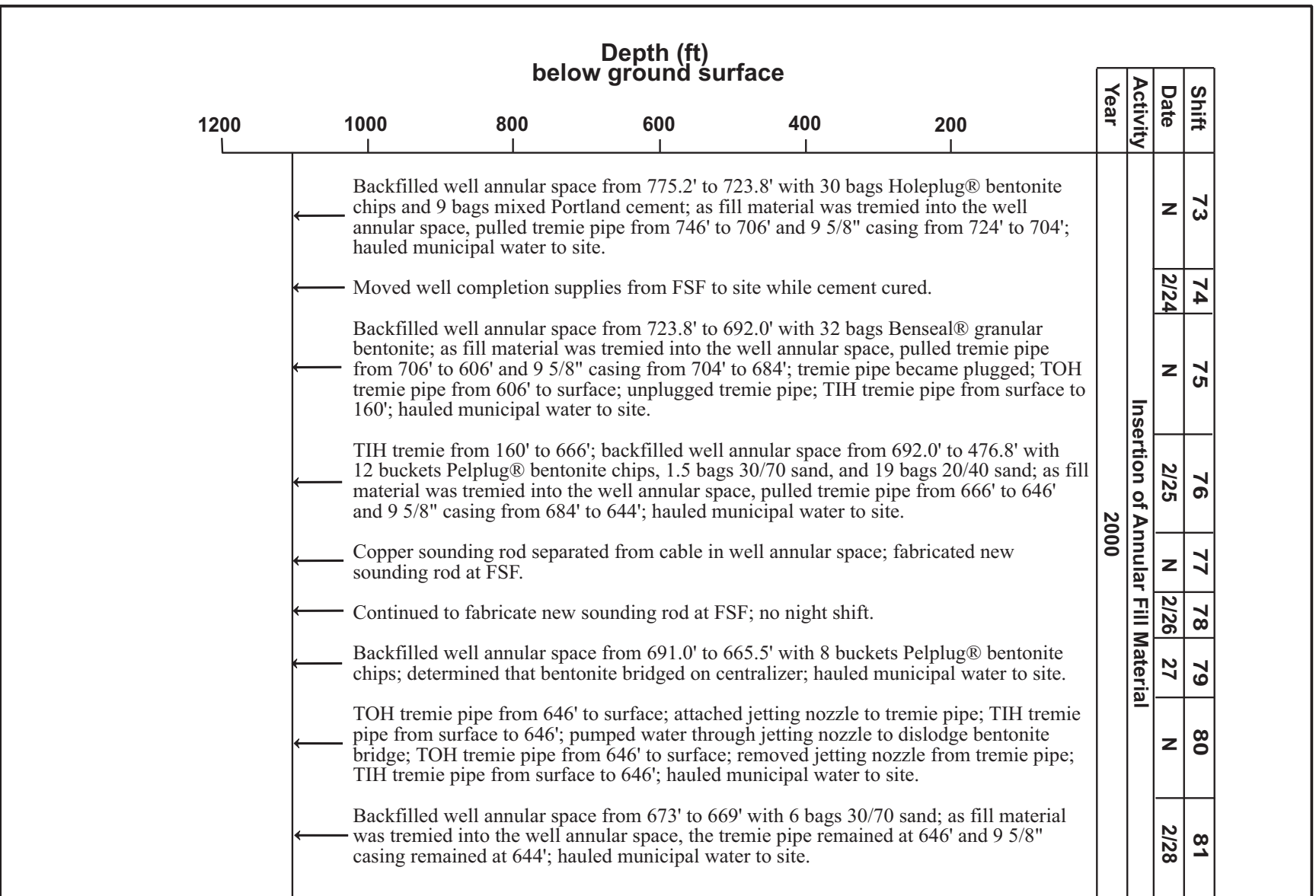
A-6

ER2001-0704





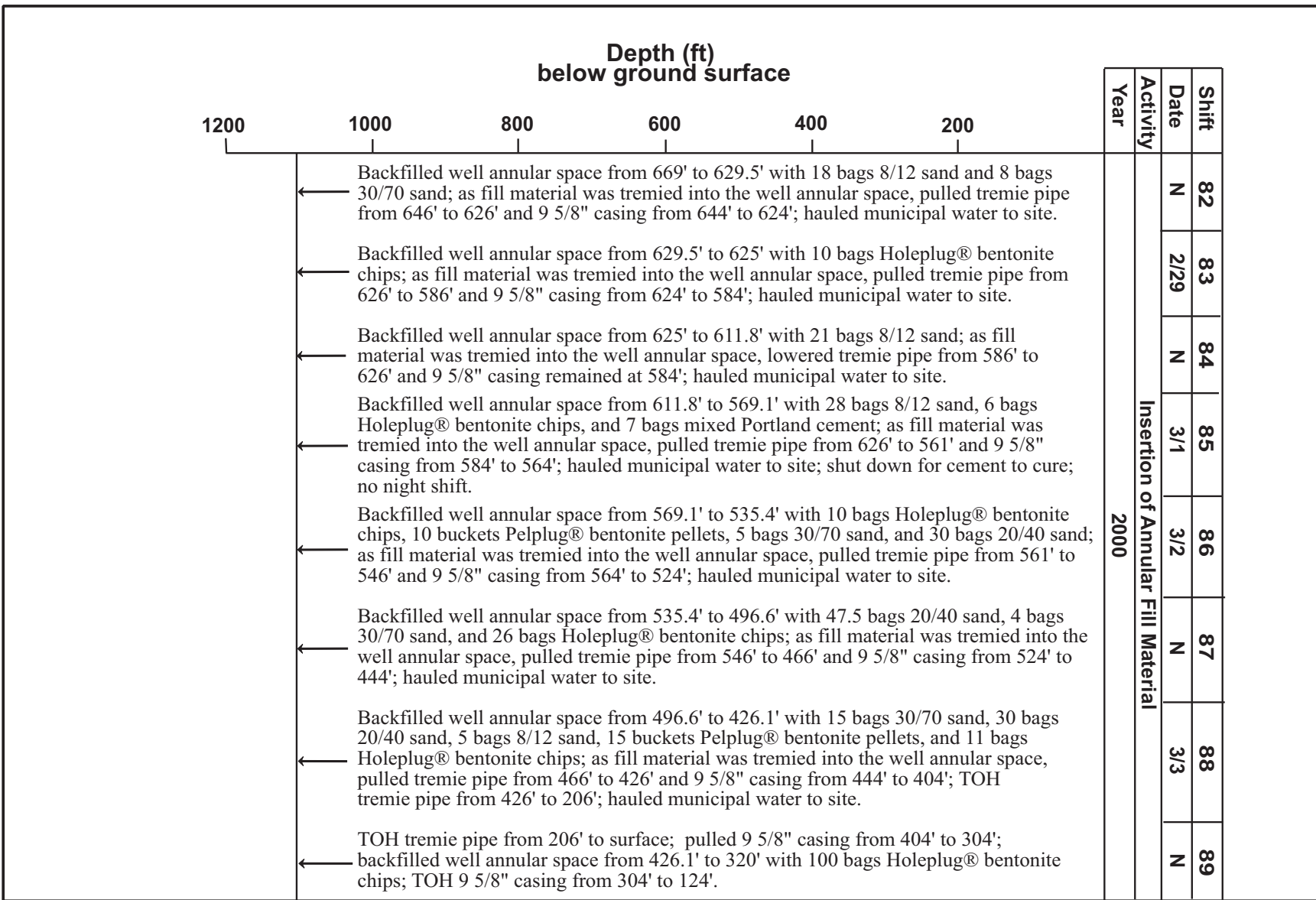


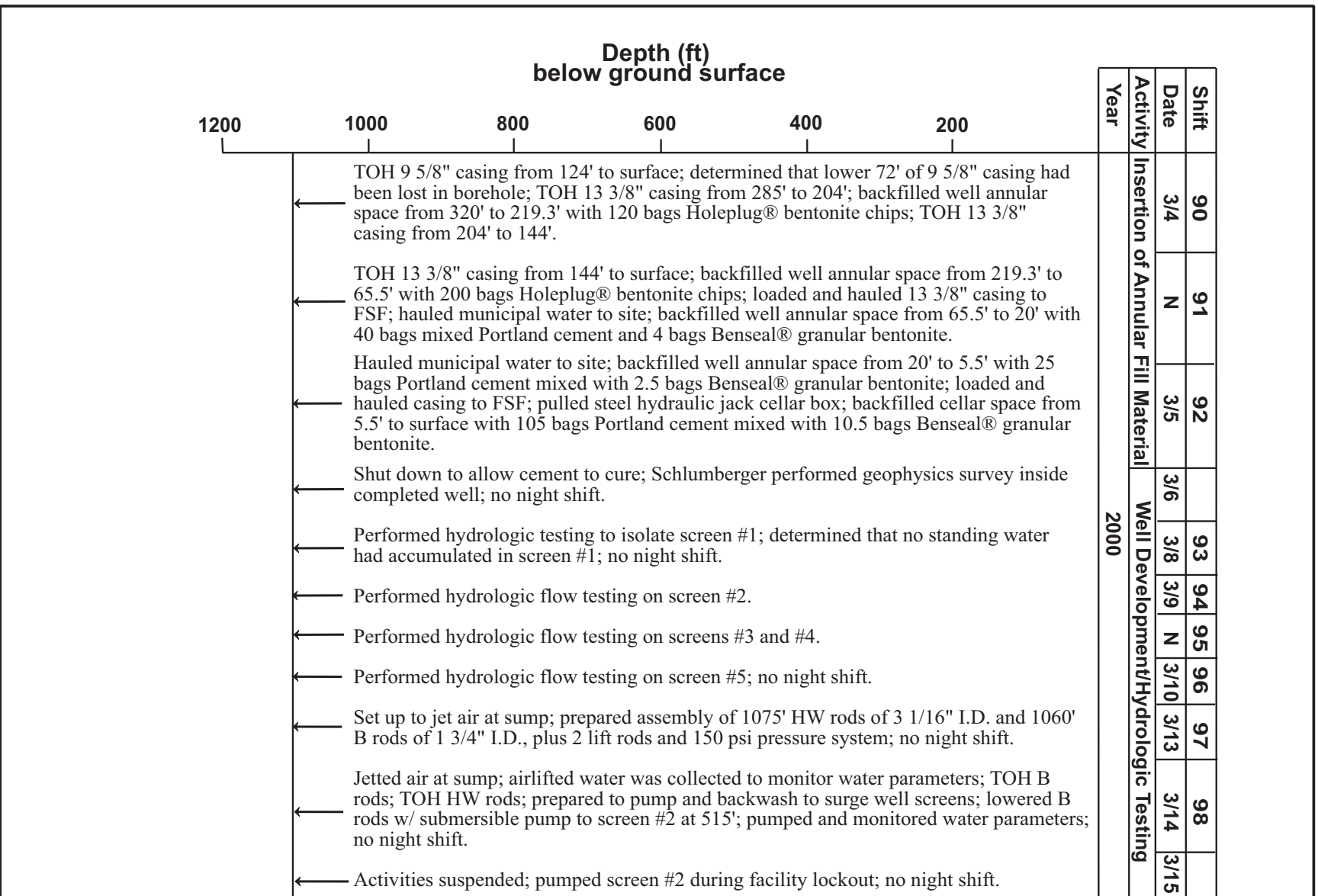


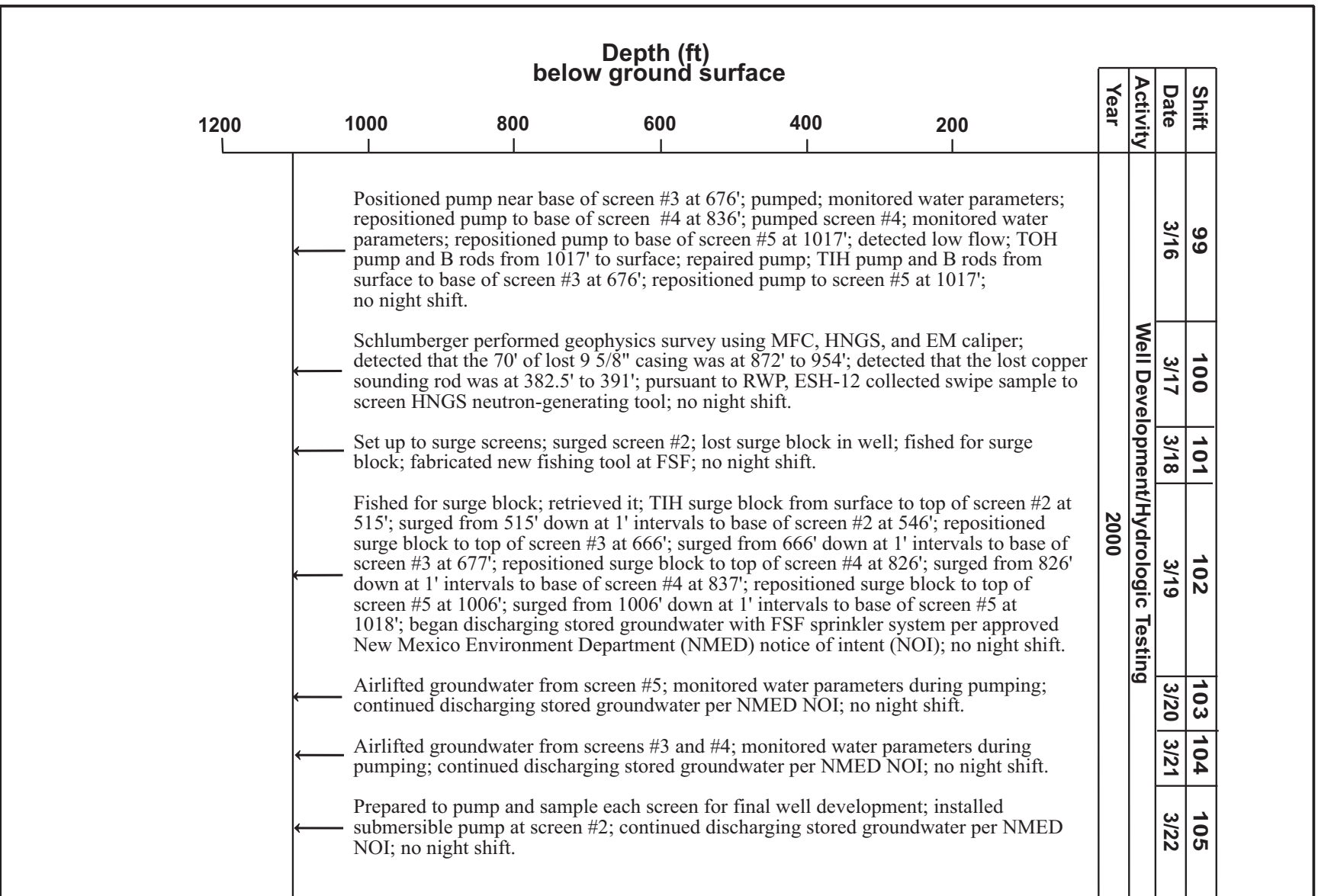
March 2002

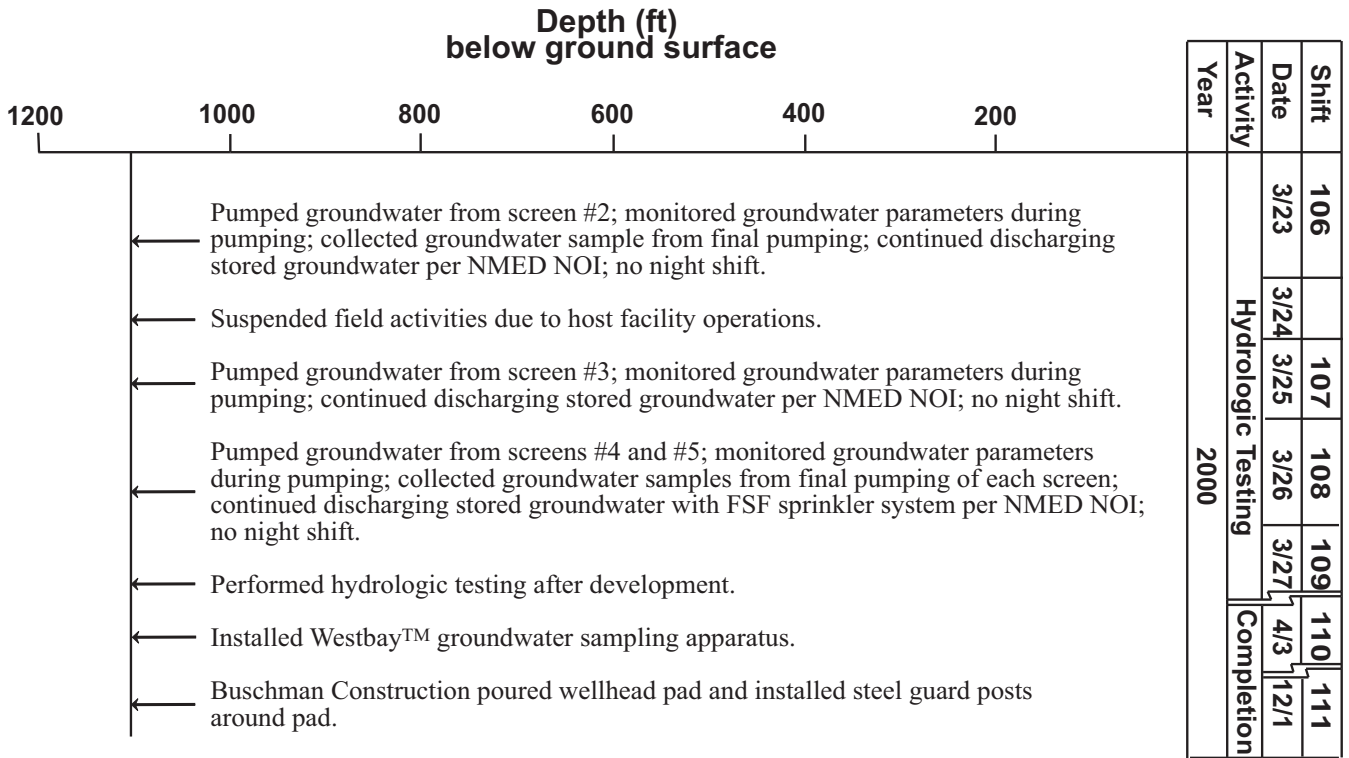
A-10

ER2001-0704









Note: "N" in date header indicates night shift. Geologic unit symbols (Qbo, Qbog, Tb) correspond to Appendix C.

Appendix B

Modifications to Work Plans

This appendix compares the actual characterization activities at the R-31 site with the activities planned in the "Hydrogeologic Workplan" (LANL 1998, 59599) and in the FIP for R-31.

The final depth of R-31 was within 3 ft of the depth called for in the FIP. Although casing advance was recommended in the FIP, it proved possible to drill open hole through the Cerros del Rio lavas, providing excellent borehole video data. This close approach to the planned completion depth was in part fortuitous, because the unexpectedly thick sequence of hydraulically transmissive river gravels ("Totavi") encountered during drilling was considered important enough to justify attempts to drill through this unit and determine its thickness. However, at the 1103-ft depth, the casing-advance system required for maintaining hole stability became stuck, and great difficulty in freeing the system led to a decision to terminate drilling at that depth. Core was not collected during Phase II drilling because core hydrologic data for basalts would not have represented large-scale permeability. The final completion design for R-31 was based on ongoing evaluations of hydrogeologic data, particularly on the evidence of perched water at the sediment between flow series E and F in the Cerros del Rio lavas (screen #1), monitoring of depth to the regional water level (screen #2), evidence from open-hole video logging of open fractures within the lowermost Cerros del Rio basalts (screen #3), and evidence of very high water production rates within the river gravels (screens #4 and #5).

The well design as outlined in the FIP called for silica sand filter materials as annular fill at each screen. This specification was realized at screens #1, #2, and #3 but was complicated by borehole wall instability at screens within the river gravels (screens #4 and #5). At these deeper screens, some coarse sand was inserted, but the bulk of the annular fill is composed of native sands and gravels that flowed into the annulus around the well as the drill casing was retracted.

The absence of evidence of any significant contamination in water samples, either from the vadose zone or the regional aquifer, led to a simplification of the contaminant survey in both water and core samples.

**Table B-1
Activities Planned for R-31 Compared with Actual Work Performed**

| | Hydrogeologic Workplan (Type 2 Well) | R-31 Field Implementation Plan | R-31 Actual Work |
|---------------------------|--|--|---|
| Planned Depth (ft) | 100 to 500 ft into top of regional aquifer | 1100 ft | 1103 ft |
| Drilling Method | Methods may include, but are not limited to, HSA, air rotary/Odex/Stratex, air-rotary/Barber rig, mud-rotary | HSA to refusal (Phase I); casing-advance air-rotary to TD (Phase II) with selected coring | HSA to 250-ft depth (Phase I); open-hole 12 1/4-in. tricone to 787-ft depth and casing advance with under-reamer from 787 ft to TD (Phase II) |
| Amount of Core | ~10% cored (core at perched zones, stratigraphic contacts, and top of regional aquifer) | Continuous core with HSA to depth of refusal (Phase I); core as necessary during Phase II for lithologic, hydraulic property, and contamination characterization | Continuous core with HSA to 250-ft depth (Phase I); no core collected during Phase II |

Table B-1 (continued)

| | Hydrogeologic Workplan (Type 2 Well) | R-31 Field Implementation Plan | R-31 Actual Work |
|---|---|--|--|
| Lithologic Log | Based on core, cuttings, and drilling performance | Based on core, cuttings, geophysical and video logs, and drilling performance | Based on core, cuttings, geophysical and video logs, and drilling performance |
| Number of Water Samples Collected for Contaminant Analysis | A water sample may be collected from each saturated zone; number of sampling events after well completion unspecified | Water samples to be collected from each saturated zone providing at least 5 ft of standing water in the borehole during Phase II (up to seven sampling events) | No perched waters were present in amounts sufficient to be sampled; three samples collected and analyzed from the regional aquifer |
| Water Sample Analytes | Radiochemistry I, II, and III analytes; tritium, gamma spectroscopy scan, general inorganic chemicals, metals, volatile organic compounds (VOCs), isotopes | Dissolved metals and anions, total metals and anions, VOCs, polycyclic aromatic hydrocarbons, pesticides, polychlorinated biphenyls, HE, dissolved and total Am-241 – Cs-137 – Pu-238,239,240 – U-234,235,236,238 – Sr-90, stable isotopes (O, N, D/H), tritium, gross α - β - γ , cyanide, humic acid, TOC, TUICPMS, TUKPA, NH ₄ , NO ₃ , NO ₂ | For samples from 525 and 625 ft: dissolved metals and anions, total HE, tritium; for sample from 1047 ft: dissolved metals and anions, total HE, total Am-241 – Cs-137 – Pu-238,239,240 – U-234,235,236,238, stable isotopes ($\delta^{18}\text{O}$, $\delta^{15}\text{N}$, δD), tritium, gross α - β - γ , cyanide, TOC, TUKPA, NH ₄ , NO ₃ , NO ₂ |
| Water Sample Field Measurements | Alkalinity, pH, specific conductance, temperature, turbidity | Specific conductance, pH, temperature, turbidity | Specific conductance, pH, temperature, and turbidity during development |
| Number of Core/Cuttings Samples Collected for Contaminant Analysis | Twenty samples of core or cuttings to be analyzed for contaminants | Up to 31 samples to be collected during Phase II drilling | No samples collected for contaminant analyses, based on absence of any contamination in groundwaters |
| Core Sample Analytes (Contaminants) | Uppermost sample to be analyzed for full suite of potential contaminants; deeper samples to be analyzed for radiochemistry I, II, and III analytes, tritium, and metals; four samples to be analyzed for VOCs | Solid organic carbon, tritium, gamma spectroscopy, gross α - β - γ , Am-241 – Cs-137 – Pu-238,239,240 – U-234,235,238 – Sr-90, anions, metals and trace elements; if VOCs are detected during field screening, analyze for VOC and semivolatile organic compounds | Anion leaching performed on 50 core and 20 cuttings samples; no other analyses performed on core because of absence of contamination in groundwaters |
| Laboratory Hydraulic Property Tests | Physical properties to be determined for five samples, typically including moisture content, porosity, particle density, bulk density, saturated hydraulic conductivity, and water retention | Phase I: moisture content, matric potential, and hydraulic properties for 86 core samples; Phase II: moisture content and matric potential to be determined for 181 cuttings samples and hydraulic properties for 53 core samples | Phase I: moisture content, matric potential, and hydraulic properties determined for 50 core samples; Phase II: moisture content, and matric potential determined for 20 cuttings samples; no hydraulic properties determined for core samples |

Table B-1 (continued)

| | Hydrogeologic Workplan (Type 2 Well) | R-31 Field Implementation Plan | R-31 Actual Work |
|---------------------------------------|--|--|---|
| Geology | Approximately 10 samples to be collected for mineralogy, petrography, and rock chemistry | Number of samples to be determined from cuttings and core examined during drilling; core to be collected from lower Puye Formation if tuffaceous and from Santa Fe Group sediments at TD | Geologic characterization based on mineralogic analyses (10 samples), petrographic analyses (25 samples), and rock chemistry analyses (18 samples) of cuttings |
| Geophysics | For open borehole, general analyses to include caliper, electromagnetic induction, natural gamma, magnetic susceptibility, color video, fluid temperature (saturated), fluid resistivity (saturated), single-point resistivity (saturated), and spontaneous potential (saturated); for cased borehole, general analyses to include gamma-gamma density, natural gamma, and thermal neutron | No geophysical logging during Phase I; natural gamma whenever there is a change in casing size, and video logging of open borehole during Phase II | No geophysical logging during Phase I; natural gamma and caliper logging of open borehole, natural gamma logging of cased borehole, and video logging of open borehole during Phase II; Schlumberger caliper, gamma, neutron, and electromagnetic logging of installed well |
| Water-Level Measurements | | Water levels to be determined for each saturated zone by water-level meter or by pressure transducer; additional water-level readings to be made at as many depths as possible for vertical gradient determination | Water levels measured at borehole depths ranging from 485 to 1094 ft; however, in all but one case, there was a considerable length of open borehole and values obtained permit calculation of only composite heads |
| Field Hydraulic-Property Tests | | Slug or pumping tests may be conducted in saturated intervals once the well is completed | Straddle-packer/slug-injection tests conducted for all saturated intervals. |
| Surface Casing | ~20-in.-O.D. to extend from ground surface to 10-ft depth in underlying competent layer and grouted in place | 18-in. or 16-in.-O.D. low-carbon steel from 37 ft below ground level to 3 ft above ground surface | 18-in.-O.D. low-carbon steel from 37 ft below ground level to 3 ft above ground surface |
| Minimum Well Casing Size | 6-5/8-in.-O.D. | 5 9/16-in.-O.D. | 5 1/4-in.-O.D. |
| Well Screen | Machine-slotted (0.01-in.) stainless steel screens with flush-jointed threads; typically single screen although multiple screen may be considered | Wire-wrapped 0.01-in. screens; two 10-ft screens in perched zones and one 25-ft and two 10-ft screens in the regional zone of saturation | Wire-wrapped 0.01-in. screens; one 15-ft screen in a perched zone, one 30-ft screen at the regional level of saturation, and three 10-ft screens within the regional zone of saturation |

Table B-1 (continued)

| | Hydrogeologic Workplan (Type 2 Well) | R-31 Field Implementation Plan | R-31 Actual Work |
|-------------------------------|--|--|--|
| Filter Material | >90% silica sand, properly sized for 0.01-in. slotted screen; to extend 2 ft above and below the well screen | Primary filter packs of washed and resieved silica sand to 10 ft above and below each screen; secondary filter packs of finer (30/70) sand 3 ft below and 5 ft above primary filter packs | At screen #1, 8/12 and 20/40 sand were used across the screened interval with 30/70 sand above and below; at screens #2 and #3, 20/40 sand was used across the screened intervals with 30/70 sand above and below; at the lower two screens, 6/9 sand was used with natural fill |
| Conductor Casing | Carbon-steel casing from land surface to top of stainless steel casing | Carbon-steel 5 9/16-in.-O.D. casing from land surface to transition to stainless steel casing of same O.D. above highest zone of saturation | Carbon-steel 5 1/4-in.-O.D. casing with transition to stainless steel casing of same O.D. at 297.8-ft depth |
| Annular Fill Materials | Uncontaminated drill cuttings below sump and bentonite above sump | Interval from TD to 5 ft below lowest screen and all annular space between filter packs to be sealed with bentonite grout; annular space from land surface to 50-ft depth to be filled with cement grout | Portland cement below end cap, sand plus bentonite from this cement base to 1072.6-ft depth, natural fill (flowing sand and gravel) plus very coarse sand (1072.6 to 873.7 ft), bentonite plus sand (873.7 to 857.2 ft), Portland cement (857.2 to 842 ft), natural fill plus very coarse sand (842 to 780.5 ft), bentonite (780.5 to 753.5 ft), Portland cement (753.5 to 748.1 ft), bentonite (748.1 to 677.0), sand pack (677.0 to 659.0), bentonite (659.0 to 584.7), Portland cement (584.7 to 574.0), bentonite (574.0 to 551.3), sand pack (551.3 to 496.3), bentonite (496.3 to 460.6), sand pack (460.6 to 432.8), bentonite (432.8 to 65.5), cement grout from 65.5 to surface |
| Sump | Stainless steel casing with end cap | 30-ft section of stainless steel casing with end cap | 60.6 ft of stainless-steel casing with end cap |
| Bottom Seal | Bentonite | Bentonite | Bentonite plus sand above Portland cement |

Appendix C

Borehole Log

LOS ALAMOS NATIONAL LABORATORY
 REGIONAL HYDROGEOLOGIC CHARACTERIZATION PROJECT
 ENVIRONMENTAL RESTORATION, CANYONS FOCUS AREA
 BOREHOLE LOG

| BOREHOLE ID: R-31 | | TA/OU: TA-39 | | Page 1 of 5 | | | | | |
|--|----------------|--|----------|--|---|-------------------------------------|--|-------------|-------------------|
| PHASE 1: 9/9/99 - 10/1/99 | | Stewart Brothers Drilling Co. | | EQUIPMENT/METHOD: CME-750/HSA/wireline core | | | | | |
| PHASE 2: 1/6/00 - 2/8/00 | | Dynatec Drilling Co. | | EQUIPMENT/METHOD: Foremost™ DR-24/air rotary | | | | | |
| DRILLERS: Johnson, Thoren, Woodward, Wilson, Brown | | | | GROUND ELEVATION: 6361.5' above sea level | | | | | |
| GEOLOGY P.I.: D. Vaniman | | | | TOTAL DEPTH = 1103' bgs | | | | | |
| | | | | SITE GEOLOGISTS: J. Marin/M. Benak/R. Koch | | | | | |
| Depth (ft) | Elevation (ft) | Core Run # (amt. - recov./amt. attempt.) | Core Run | Cuttings Collected | Hydrologic Property (Physprop) and Geochemical (Geochem) Samples (CAAN-00-xxxx) | Moisture/Matric Pot. R31-depth (ft) | Lithology | Graphic Log | Lithologic Symbol |
| 0 | 6360 | 12.5/2.5 | | | | | ALLUVIUM: (0-24 ft) Very dry, light to dark brown, organic, silt and sand, soft, rounded sanidine and quartz grains. | | Qal |
| 5 | 6355 | 22.5/2.5 | | | Moisture-Protected HSA Core (3.5-4.0') | R-31-5.0 R-31-7.5 | OTOWI MEMBER OF THE BANDELIER TUFF: (24-264 ft) Ash flow tuff, moderate reddish brown (10 R 6/6), pumice lapilli up to 8 cm (2%), intermediate composition volcanic rock lithics to 5%. | | Qbo |
| 10 | 6350 | 32.5/2.5 | | | Moisture-Protected HSA Core (9.5-10.0') | R-31-12.5 | | | |
| 15 | 6345 | 42.5/2.5 | | | Moisture-Protected HSA Core (14.5-15.0') | R-31-17.5 | | | |
| 20 | 6340 | 52.5/2.5 | | | Moisture-Protected HSA Core (19.5-20.0') | R-31-22.5 | | | |
| 25 | 6335 | 62.5/2.5 | | | Moisture-Protected HSA Core (24.4-25.0') | R-31-27.5 | | | |
| 30 | 6330 | 72.5/2.5 | | | Moisture-Protected HSA Core (29.5-30.0') | R-31-32.5 | | | |
| 35 | 6325 | 82.5/2.5 | | | Moisture-Protected HSA Core (34.5-35.0') | R-31-37.5 | | | |
| 40 | 6320 | 92.5/2.5 | | | Moisture-Protected HSA Core (39.5-40.0') | R-31-42.5 | | | |
| 45 | 6315 | 102.5/2.5 | | | Moisture-Protected HSA Core (44.5-45.0') | R-31-47.5 | | | |
| 50 | 6310 | 112.5/2.5 | | | Moisture-Protected HSA Core (49.5-50.0') | R-31-52.5 | | | |
| 55 | 6305 | 122.5/2.5 | | | Moisture-Protected HSA Core (54.5-55.0') | R-31-57.5 | | | |
| 60 | 6300 | 132.5/2.5 | | | Moisture-Protected HSA Core (59.5-60.0') | R-31-62.5 | | | |
| 65 | 6295 | 142.5/2.5 | | | Moisture-Protected HSA Core (64.5-65.0') | R-31-67.5 | | | |
| 70 | 6290 | 152.5/2.5 | | | Moisture-Protected HSA Core (69.5-70.0') | R-31-72.5 | | | |
| 75 | 6285 | 162.5/2.5 | | | Moisture-Protected HSA Core (74.5-75.0') | R-31-77.5 | | | |
| 80 | 6280 | 172.5/2.5 | | | Moisture-Protected HSA Core (79.5-80.0') | R-31-82.5 | | | |
| 85 | 6275 | 182.5/2.5 | | | Moisture-Protected HSA Core (84.5-85.0') | R-31-87.5 | | | |
| 90 | 6270 | 192.5/2.5 | | | Moisture-Protected HSA Core (89.5-90.0') | R-31-92.5 | | | |
| 95 | 6265 | 202.5/2.5 | | | Moisture-Protected HSA Core (94.5-95.0') | R-31-97.5 | | | |
| 100 | 6260 | 212.5/2.5 | | | Moisture-Protected HSA Core (99.5-100.0') | R-31-102.5 | | | |
| 105 | 6255 | 222.5/2.5 | | | Moisture-Protected HSA Core (104.5-105.0') | R-31-107.5 | | | |
| 110 | 6250 | 232.5/2.5 | | | Moisture-Protected HSA Core (109.5-110.0') | R-31-112.5 | | | |
| 115 | 6245 | 242.5/2.5 | | | Moisture-Protected HSA Core (114.5-115.0') | R-31-117.5 | | | |
| 120 | 6240 | 252.5/2.5 | | | Moisture-Protected HSA Core (119.5-120.0') | R-31-122.5 | | | |
| 125 | 6235 | 262.5/2.5 | | | Moisture-Protected HSA Core (124.5-125.0') | R-31-127.5 | | | |
| 130 | 6230 | 272.5/2.5 | | | Moisture-Protected HSA Core (129.5-130.0') | R-31-132.5 | | | |
| 135 | 6225 | 282.5/2.5 | | | Moisture-Protected HSA Core (134.5-135.0') | R-31-137.5 | | | |
| 140 | 6220 | 292.5/2.5 | | | Moisture-Protected HSA Core (139.5-140.0') | R-31-142.5 | | | |
| 145 | 6215 | 302.5/2.5 | | | Moisture-Protected HSA Core (144.5-145.0') | R-31-147.5 | | | |
| 150 | 6210 | 312.5/2.5 | | | Moisture-Protected HSA Core (149.5-150.0') | R-31-152.5 | | | |
| 155 | 6205 | 322.5/2.5 | | | Moisture-Protected HSA Core (154.5-155.0') | R-31-157.5 | | | |
| 160 | 6200 | 332.5/2.5 | | | Moisture-Protected HSA Core (159.5-160.0') | R-31-162.5 | | | |
| 165 | 6195 | 342.5/2.5 | | | Moisture-Protected HSA Core (164.5-165.0') | R-31-167.5 | | | |
| 170 | 6190 | 352.5/2.5 | | | Moisture-Protected HSA Core (169.5-170.0') | R-31-172.5 | | | |
| 175 | 6185 | 362.5/2.5 | | | Moisture-Protected HSA Core (174.5-175.0') | R-31-177.5 | | | |
| 180 | 6180 | 372.5/2.5 | | | Moisture-Protected HSA Core (179.5-180.0') | R-31-182.5 | | | |
| 185 | 6175 | 382.5/2.5 | | | Moisture-Protected HSA Core (184.5-185.0') | R-31-187.5 | | | |
| 190 | 6170 | 392.5/2.5 | | | Moisture-Protected HSA Core (189.5-190.0') | R-31-192.5 | | | |
| 195 | 6165 | 402.5/2.5 | | | Moisture-Protected HSA Core (194.5-195.0') | R-31-197.5 | | | |
| 200 | 6160 | 412.5/2.5 | | | Moisture-Protected HSA Core (199.5-200.0') | R-31-202.5 | | | |
| 205 | 6155 | 422.5/2.5 | | | Moisture-Protected HSA Core (204.5-205.0') | R-31-207.5 | | | |
| 210 | 6150 | 432.5/2.5 | | | Moisture-Protected HSA Core (209.5-210.0') | R-31-212.5 | | | |
| 215 | 6145 | 442.5/2.5 | | | Moisture-Protected HSA Core (214.5-215.0') | R-31-217.5 | | | |
| 220 | 6140 | 452.5/2.5 | | | Moisture-Protected HSA Core (219.5-220.0') | R-31-222.5 | | | |
| 225 | 6135 | 462.5/2.5 | | | Moisture-Protected HSA Core (224.5-225.0') | R-31-227.5 | | | |
| 230 | | | | | | | | | |

LOS ALAMOS NATIONAL LABORATORY
 REGIONAL HYDROGEOLOGIC CHARACTERIZATION PROJECT
 ENVIRONMENTAL RESTORATION, CANYONS FOCUS AREA
 BOREHOLE LOG

| BOREHOLE ID: R-31 | | TA/OU: TA-39 | | Page 2 of 5 | | | | | |
|--|----------------|---------------------------------------|----------|--|---|-------------------------------------|--|-------------|-------------------|
| PHASE 1: 9/9/99 - 10/1/99 | | Stewart Brothers Drilling Co. | | EQUIPMENT/METHOD: CME-750/HSA/wireline core | | | | | |
| PHASE 2: 1/6/00 - 2/8/00 | | Dynatec Drilling Co. | | EQUIPMENT/METHOD: Foremost™ DR-24/air rotary | | | | | |
| DRILLERS: Johnson, Thoren, Woodward, Wilson, Brown | | | | GROUND ELEVATION: 6361.5' above sea level | | | | | |
| GEOLOGY P.I.: D. Vaniman | | | | TOTAL DEPTH = 1103' bgs | | | | | |
| | | | | SITE GEOLOGISTS: J. Marin/M. Benak/R. Koch | | | | | |
| Depth (ft) | Elevation (ft) | Core Run # (amt.-recov./amt. attemp.) | Core Run | Cuttings Collected | Hydrologic Property (Physprop) and Geochemical (Geochem) Samples (CAAN-00-xxxx) | Moisture/Matric Pot. R31-depth (ft) | Lithology | Graphic Log | Lithologic Symbol |
| 230 | 6130 | 91(2.5/2.5) | | | Moisture-Protected HSA Core (229.5-230.0') | R-31-232.5 | | | |
| 235 | 6125 | 92(2.5/2.5) | | | Moisture-Protected HSA Core (234.5-235.0') | R-31-237.5 | | | |
| 240 | 6120 | 93(2.5/2.5) | | | Moisture-Protected HSA Core (239.5-240.0') | R-31-242.5 | | | |
| 245 | 6115 | 94(2.5/2.5) | | | Moisture-Protected HSA Core (244.5-245.0') | R-31-247.5 | | | Qbo |
| 250 | 6110 | 95(2.5/2.5) | | | Moisture-Protected HSA Core (249.5-250.0') | R-31-255.0 | | | |
| 255 | 6105 | 96(2.5/2.5) | | | | R-31-260.0 | | | |
| 260 | 6100 | | | | | R-31-265.0 | | | |
| 265 | 6095 | | | | | R-31-269.5 | GUAJE PUMICE BED: (264-280 ft) Light tannish white to very pale orange (10 YR 8/2) vitric pumice lapilli aggregate. | | Qbog |
| 270 | 6090 | | | | | R-31-275.0 | | | |
| 275 | 6085 | | | | | R-31-280.0 | | | |
| 280 | 6080 | | | | | R-31-285.0 | SEDIMENT: (280-285 ft) Clay- and silt-rich sand with weathered basalt fragments. | | n/a |
| 285 | 6075 | | | | | R-31-294.5 | BASALT OF THE CERROS DEL RIO VOLCANIC FIELD, UNDIVIDED: (285-444 ft) Massive to slightly vesicular basalt, olivine-porphyrific. Prominent breccia zones observed in borehole video at 285 to ~294 ft, 305-312 ft, 340-365 ft, and 416-444 ft. Abundant clay returns in cuttings at 345-255 ft, 375-385 ft, and 420-425 ft. | | |
| 290 | 6070 | | | Moisture-Protected Cuttings (289.5-290.0') | | R-31-300.0 | | | |
| 295 | 6065 | | | Moisture-Protected Cuttings (294.5-295.0') | | R-31-305.0 | | | |
| 300 | 6060 | | | | | R-31-310.0 | | | |
| 305 | 6055 | | | | | R-31-314.5 | | | |
| 310 | 6050 | | | | | R-31-320.0 | | | |
| 315 | 6045 | | | Moisture-Protected Cuttings (314.5-315.0') | | R-31-325.0 | | | |
| 320 | 6040 | | | | | R-31-330.0 | | | |
| 325 | 6035 | | | | | R-31-334.5 | | | |
| 330 | 6030 | | | | | R-31-340.0 | | | |
| 335 | 6025 | | | Moisture-Protected Cuttings (334.5-335.0') | | R-31-345.0 | | | |
| 340 | 6020 | | | | | R-31-350.0 | | | |
| 345 | 6015 | | | | | R-31-355.0 | | | |
| 350 | 6010 | | | | | | | | |
| 355 | 6005 | | | | | | | | |
| 360 | 6000 | | | | | | | | |
| 365 | 5995 | | | | | | | | |
| 370 | 5990 | | | | | | | | |
| 375 | 5985 | | | | | | | | |
| 380 | 5980 | | | | | | | | |
| 385 | 5975 | | | | | | | | |
| 390 | 5970 | | | | | | | | |
| 395 | 5965 | | | | | | | | |
| 400 | 5960 | | | | | | | | |
| 405 | 5955 | | | | | | | | |
| 410 | 5950 | | | | | | | | |
| 415 | 5945 | | | | | | | | |
| 420 | 5940 | | | | | | | | |
| 425 | 5935 | | | | | | | | |
| 430 | 5930 | | | | | | | | |
| 435 | 5925 | | | | | | | | |
| 440 | 5920 | | | | | | | | |
| 445 | 5915 | | | | | | | | |
| 450 | 5910 | | | | | | | | |
| 455 | 5905 | | | | | | | | |
| 460 | 5900 | | | | | | SEDIMENT: (444-450 ft) Clay- and silt-rich sediment with weathered basalt fragments | | n/a |
| | | | | | | | BASALT OF THE CERROS DEL RIO VOLCANIC FIELD, UNDIVIDED: (450-473 ft) Massive to slightly vesicular basalt, olivine - porphyritic. Prominent breccia zones observed in borehole video at 450-455 ft and 471-473 ft. | | Tb |

LOS ALAMOS NATIONAL LABORATORY
 REGIONAL HYDROGEOLOGIC CHARACTERIZATION PROJECT
 ENVIRONMENTAL RESTORATION, CANYONS FOCUS AREA
 BOREHOLE LOG

| BOREHOLE ID: R-31 | | TA/OU: TA-39 | | Page 3 of 5 | | | | | |
|--|----------------|---------------------------------------|----------|--|---|-------------------------------------|--|-------------|-------------------|
| PHASE 1: 9/9/99 - 10/1/99 | | Stewart Brothers Drilling Co. | | EQUIPMENT/METHOD: CME-750/HSA/wireline core | | | | | |
| PHASE 2: 1/6/00 - 2/8/00 | | Dynatec Drilling Co. | | EQUIPMENT/METHOD: Foremost™ DR-24/air rotary | | | | | |
| DRILLERS: Johnson, Thoren, Woodward, Wilson, Brown | | | | GROUND ELEVATION: 6361.5' above sea level | | | | | |
| GEOLOGY P.I.: D. Vaniman | | | | TOTAL DEPTH = 1103' bgs | | | | | |
| | | | | SITE GEOLOGISTS: J. Marin/M. Benak/R. Koch | | | | | |
| Depth (ft) | Elevation (ft) | Core Run # (amt.-recov./amt. attemp.) | Core Run | Cuttings Collected | Hydrologic Property (Physprop) and Geochemical (Geochem) Samples (CAAN-00-xxxx) | Moisture/Matric Pot. R31-depth (ft) | Lithology | Graphic Log | Lithologic Symbol |
| 460 | 5900 | | | | | | | | |
| 465 | 5895 | | | | | | | | |
| 470 | 5890 | | | | | | | | |
| 475 | 5885 | | | | | | | | |
| 480 | 5880 | | | | | | BASALT OF THE CERROS DEL RIO VOLCANIC FIELD, UNDIVIDED: (473-534 ft) Massive to slightly vesicular basalt. Clay-rich cuttings from 530-534 ft. Prominent breccia zones observed in borehole video from 473-485 ft, 511-515 ft, and 530-534 ft. | | |
| 485 | 5875 | | | | | | | | |
| 490 | 5870 | | | | | | | | |
| 495 | 5865 | | | | | | | | |
| 500 | 5860 | | | | | | | | |
| 505 | 5855 | | | | | | | | |
| 510 | 5850 | | | | | | | | |
| 515 | 5845 | | | | | | | | |
| 520 | 5840 | | | | | | | | |
| 525 | 5835 | | | | | | | | |
| 530 | 5830 | | | | | | | | |
| 535 | 5825 | | | | | | | | |
| 540 | 5820 | | | | | | BASALT OF THE CERROS DEL RIO VOLCANIC FIELD, UNDIVIDED: (534-596 ft) Moderately vesicular basaltic andesite, olivine - porphyritic. Local occurrences of quartz xenocrysts and sieved plagioclase phenocrysts. Clay-rich cuttings from 534-545 ft and 585-596 ft. Prominent breccia zones observed in borehole video from 534-548 ft and 589-596 ft. | | |
| 545 | 5815 | | | | | | | | |
| 550 | 5810 | | | | | | | | |
| 555 | 5805 | | | | | | | | |
| 560 | 5800 | | | | | | | | |
| 565 | 5795 | | | | | | | | |
| 570 | 5790 | | | | | | | | |
| 575 | 5785 | | | | | | | | |
| 580 | 5780 | | | | | | | | |
| 585 | 5775 | | | | | | | | |
| 590 | 5770 | | | | | | | | |
| 595 | 5765 | | | | | | | | |
| 600 | 5760 | | | | | | BASALT OF THE CERROS DEL RIO VOLCANIC FIELD, UNDIVIDED: (596-625 ft) Moderately vesicular basaltic alluvial scoria, rounded. | | |
| 605 | 5755 | | | | | | | | |
| 610 | 5750 | | | | | | | | |
| 615 | 5745 | | | | | | | | |
| 620 | 5740 | | | | | | | | |
| 625 | 5735 | | | | | | | | |
| 630 | 5730 | | | | | | | | |
| 635 | 5725 | | | | | | BASALT OF THE CERROS DEL RIO VOLCANIC FIELD, UNDIVIDED: (625-635 ft) Highly vesicular to scoriaceous basalt, olivine - porphyritic. | | |
| 640 | 5720 | | | | | | | | |
| 645 | 5715 | | | | | | | | |
| 650 | 5710 | | | | | | BASALT OF THE CERROS DEL RIO VOLCANIC FIELD, UNDIVIDED: (635-693 ft) Massive basalt, rare olivine phenocrysts. Clay-rich cuttings from 685-690 ft. | | |
| 655 | 5705 | | | | | | | | |
| 660 | 5700 | | | | | | | | |
| 665 | 5695 | | | | | | | | |
| 670 | 5690 | | | | | | | | |
| 675 | 5685 | | | | | | | | |
| 680 | 5680 | | | | | | | | |
| 685 | 5675 | | | | | | | | |
| 690 | 5670 | | | | | | | | |

Tb

LOS ALAMOS NATIONAL LABORATORY
 REGIONAL HYDROGEOLOGIC CHARACTERIZATION PROJECT
 ENVIRONMENTAL RESTORATION, CANYONS FOCUS AREA
 BOREHOLE LOG

| BOREHOLE ID: R-31 | | TA/OU: TA-39 | | Page 4 of 5 | | | | | |
|---|----------------|---------------------------------------|--|--|---|-------------------------------------|--|---|-------------------|
| PHASE 1: 9/9/99 - 10/1/99 Stewart Brothers Drilling Co. | | | EQUIPMENT/METHOD: CME-750/HSA/wireline core | | | | | | |
| PHASE 2: 1/6/00 - 2/8/00 Dynatec Drilling Co. | | | EQUIPMENT/METHOD: Foremost™ DR-24/air rotary | | | | | | |
| DRILLERS: Johnson, Thoren, Woodward, Wilson, Brown | | | | GROUND ELEVATION: 6361.5' above sea level | | | | | |
| GEOLOGY P.I.: D. Vaniman | | | | TOTAL DEPTH = 1103' bgs | | | | | |
| | | | | SITE GEOLOGISTS: J. Marin/M. Benak/R. Koch | | | | | |
| Depth (ft) | Elevation (ft) | Core Run # (amt.-recov./amt. attemp.) | Core Run | Cuttings Collected | Hydrologic Property (Physprop) and Geochemical (Geochem) Samples (CAAN-00-xxxx) | Moisture/Matric Pot. R31-depth (ft) | Lithology | Graphic Log | Lithologic Symbol |
| 690 | 5670 | | | | | | | | |
| 695 | 5665 | | | | | | FLOW-BASE BRECCIA: (693-703 ft) Clay-rich basalt breccia. |  | Tb |
| 700 | 5660 | | | | | | FLOW-BASE SEDIMENTS: (703-710 ft) Coarse sand and gravel. Clay-rich. |  | |
| 705 | 5655 | | | | | | PUYE FORMATION FANGLOMERATE FACIES: (710-745 ft) Gravel, heterogeneous lithologies consist of light to medium gray rhyolite/dacite plus reddish brown dacitic clasts. |  | Tpf |
| 710 | 5650 | | | | | | | | |
| 715 | 5645 | | | | | | PUYE FORMATION FANGLOMERATE FACIES: (745-780 ft) Coarse to very coarse sands and gravels, rhyodacitic to dacitic, including quartz-bearing dacitic lithologies. |  | Tpf |
| 720 | 5640 | | | | | | | | |
| 725 | 5635 | | | | | | PUYE FORMATION RIVER GRAVELS: (780-900 ft) Coarse to very coarse quartzite-rich sands and gravels, Totavi equivalents. Percentages of quartzite and of other Precambrian lithologies (estimated) are: 30% quartzite and 30% other at 780-790 ft; 50% quartzite and 0% other at 800-805 ft; 10% quartzite and 0% other at 840-850 ft; 40% quartzite and 10% other at 855-860 ft; 50% quartzite and 0% other at 860-865 ft; 20% quartzite and 20% other at 865-870 ft; 20% quartzite and 0% other at 870-880 ft; 10% quartzite and 0% other at 880-885 ft; 80% quartzite and 0% other at 885-890 ft. |  | Tpt |
| 730 | 5630 | | | | | | | | |
| 735 | 5625 | | | | | | | | |
| 740 | 5620 | | | | | | | | |
| 745 | 5615 | | | | | | | | |
| 750 | 5610 | | | | | | | | |
| 755 | 5605 | | | | | | | | |
| 760 | 5600 | | | | | | | | |
| 765 | 5595 | | | | | | | | |
| 770 | 5590 | | | | | | | | |
| 775 | 5585 | | | | | | | | |
| 780 | 5580 | | | | | | | | |
| 785 | 5575 | | | | | | | | |
| 790 | 5570 | | | | | | | | |
| 795 | 5565 | | | | | | | | |
| 800 | 5560 | | | | | | | | |
| 805 | 5555 | | | | | | | | |
| 810 | 5550 | | | | | | | | |
| 815 | 5545 | | | | | | | | |
| 820 | 5540 | | | | | | | | |
| 825 | 5535 | | | | | | | | |
| 830 | 5530 | | | | | | | | |
| 835 | 5525 | | | | | | | | |
| 840 | 5520 | | | | | | | | |
| 845 | 5515 | | | | | | | | |
| 850 | 5510 | | | | | | | | |
| 855 | 5505 | | | | | | | | |
| 860 | 5500 | | | | | | | | |
| 865 | 5495 | | | | | | | | |
| 870 | 5490 | | | | | | | | |
| 875 | 5485 | | | | | | | | |
| 880 | 5480 | | | | | | | | |
| 885 | 5475 | | | | | | | | |
| 890 | 5470 | | | | | | | | |
| 895 | 5465 | | | | | | | | |
| 900 | 5460 | | | | | | | | |
| 905 | 5455 | | | | | | | | |
| 910 | 5450 | | | | | | | | |
| 915 | 5445 | | | | | | | | |
| 920 | 5440 | | | | | | | | |
| | | | | | | | PUYE FORMATION FANGLOMERATE FACIES: (900-935 ft) Coarse to very coarse quartzite-poor sands and gravels. |  | Tpf |

LOS ALAMOS NATIONAL LABORATORY
 REGIONAL HYDROGEOLOGIC CHARACTERIZATION PROJECT
 ENVIRONMENTAL RESTORATION, CANYONS FOCUS AREA
 BOREHOLE LOG

| BOREHOLE ID: R-31 | | TA/OU: TA-39 | | Page 5 of 5 | | | | | |
|--|----------------|---------------------------------------|----------|--|---|-------------------------------------|-----------|-------------|-------------------|
| PHASE 1: 9/9/99 - 10/1/99 | | Stewart Brothers Drilling Co. | | EQUIPMENT/METHOD: CME-750/HSA/wireline core | | | | | |
| PHASE 2: 1/6/00 - 2/8/00 | | Dynatec Drilling Co. | | EQUIPMENT/METHOD: Foremost™ DR-24/air rotary | | | | | |
| DRILLERS: Johnson, Thoren, Woodward, Wilson, Brown | | | | GROUND ELEVATION: 6361.5' above sea level | | | | | |
| GEOLOGY P.I.: D. Vaniman | | | | TOTAL DEPTH = 1103' bgs | | | | | |
| | | | | SITE GEOLOGISTS: J. Marin/M. Benak/R. Koch | | | | | |
| Depth (ft) | Elevation (ft) | Core Run # (amt.-recov./amt. attemp.) | Core Run | Cuttings Collected | Hydrologic Property (Physprop) and Geochemical (Geochem) Samples (CAAN-00-xxxx) | Moisture/Matric Pot. R31-depth (ft) | Lithology | Graphic Log | Lithologic Symbol |
| 920 | 5440 | | | | | | | | |
| 925 | 5435 | | | | | | | | |
| 930 | 5430 | | | | | | | | Tpf |
| 935 | 5425 | | | | | | | | |
| 940 | 5420 | | | | | | | | |
| 945 | 5415 | | | | | | | | |
| 950 | 5410 | | | | | | | | |
| 955 | 5405 | | | | | | | | |
| 960 | 5400 | | | | | | | | |
| 965 | 5395 | | | | | | | | |
| 970 | 5390 | | | | | | | | |
| 975 | 5385 | | | | | | | | |
| 980 | 5380 | | | | | | | | |
| 985 | 5375 | | | | | | | | |
| 990 | 5370 | | | | | | | | |
| 995 | 5365 | | | | | | | | |
| 1000 | 5360 | | | | | | | | |
| 1005 | 5355 | | | | | | | | |
| 1010 | 5350 | | | | | | | | |
| 1015 | 5345 | | | | | | | | |
| 1020 | 5340 | | | | | | | | |
| 1025 | 5335 | | | | | | | | |
| 1030 | 5330 | | | | | | | | |
| 1035 | 5325 | | | | | | | | |
| 1040 | 5320 | | | | | | | | |
| 1045 | 5315 | | | | | | | | |
| 1050 | 5310 | | | | | | | | |
| 1055 | 5305 | | | | | | | | |
| 1060 | 5300 | | | | | | | | |
| 1065 | 5295 | | | | | | | | |
| 1070 | 5290 | | | | | | | | |
| 1075 | 5285 | | | | | | | | |
| 1080 | 5280 | | | | | | | | |
| 1085 | 5275 | | | | | | | | |
| 1090 | 5270 | | | | | | | | |
| 1095 | 5265 | | | | | | | | |
| 1100 | 5260 | | | | | | | | |

Appendix D

Descriptions of Geologic Samples

| | |
|--|--|
| R31-280/285 Hand-picked fragments | This polished thin section represents an immature basaltic sandstone. Sand grains within the sample include quartz, plagioclase, amphibole, clinopyroxene, olivine, magnetite, and glass. Lithic fragments of coarse-sand size are dominantly basaltic. |
| R31-285/290 Hand-picked fragments | This polished thin section represents 15 fragments of slightly vesicular medium- to coarse-grained hypocrySTALLINE subophitic basalt. Large voids (3.1%) include microvesicles (>0.03 mm) and vesicles. Minor amounts of original glass are preserved (2.3%), but most glass has devitrified to cryptocrystalline groundmass (3.1%). Plagioclase phenocrysts are scarce to rare (0.7%, median area 0.33 mm ² , strongly influenced by a single glomerocryst) and olivine phenocrysts, partly altered to iddingsite, are scarce (1.9%, 0.15 mm ²). Olivine in groundmass (5.8%, 0.0027 mm ²) is less strongly altered and partly ophitic. Ophitic groundmass clinopyroxene (11.6%, 0.0034 mm ²) ranges from deep brown to very pale brown in plane light and is entirely unaltered. Scarce to common Fe-Ti oxides in groundmass include skeletal and cruciform magnetite that is generally slightly altered to maghemite (1.5%, 0.0009 mm ²) and small, acicular unaltered ilmenite (0.4%, 0.0003 mm ²). Spinel, chromite, and Cr-rich magnetite, occur as numerous euhedral inclusions that constitute 0.15% of olivine phenocrysts. No accessories or lithics were observed. |
| R31-390/395 Hand-picked fragments | This polished thin section represents a single large fragment of slightly vesicular medium-grained pilotaxitic and partly cryptocrystalline pilotaxitic basalt. Large voids (6.0%) include microvesicles (>0.03 mm) and vesicles. Original glass has devitrified to cryptocrystalline groundmass (10%). Traces of smectite partly fill a few vesicles in geopetal fashion and are associated with areas surrounding large vesicles where original glass has been removed. Plagioclase phenocrysts are scarce to common (7.0%, median area 0.049 mm ²), mostly prismatic (57% of plagioclase), and olivine phenocrysts are scarce to rare (1.3%, 0.37 mm ²). Olivine in groundmass (9.0%, 0.0006 mm ²) and as phenocrysts is slightly altered to iddingsite, with phenocrysts altered only in thin rims; groundmass clinopyroxene (9.0%, 0.0002 mm ²) is entirely unaltered. Common magnetite (3.0%, 0.00006 mm ²) occurs as small, generally cruciform grains in groundmass, and spinel, chromite and Cr-rich magnetite occur as numerous euhedral inclusions that constitute 0.32% of olivine phenocrysts. No accessories or lithics were observed. |
| R31-435/440 Hand-picked fragments | This polished thin section represents a single large fragment of slightly vesicular medium-grained pilotaxitic basalt. Recognizable voids (4.0%) include microvesicles >0.03 mm and large vesicles. Total feldspar, including 39% in groundmass and 6% as phenocrysts, is lower than typical for holocrystalline basalt (>60%), suggesting that this basalt originally contained >15% glass that has been removed. However, smectite, usually associated with alteration of basaltic glass, was observed only in small amounts. Plagioclase phenocrysts are scarce to common (6.0%, median area 0.093 mm ²), mostly prismatic (57% of plagioclase), with some resorbed (7%). Abundant olivine phenocrysts (8.7%, 0.99 mm ²) invariably have a rim of iddingsite about 0.02 mm wide; thus iddingsite rims are very thin on large phenocrysts, but the smallest grains, particularly groundmass olivine (2.3%, 0.0005 mm ²), are nearly completely altered to iddingsite. Groundmass clinopyroxene (10.4%, 0.0002 mm ²) is entirely unaltered, and thus highly distinct from groundmass olivine. Scarce magnetite (1.9%, 0.00004 mm ²) occurs as small, generally cruciform groundmass grains entirely oxidized to maghemite; the texture and oxidation is characteristic of magnetite within hypocrySTALLINE basalt. Spinel, chromite, and Cr-rich magnetite occur as numerous euhedral inclusions that constitute 0.21% of olivine phenocrysts. No accessories or lithics were observed. |
| R31-450/455SS Hand-picked fragments (sediment above lava flow series E) | This polished thin section represents fragments of a siltstone matrix with clasts of basaltic pumice. The siltstone is fine-grained (20-30 μm) with common fragments of quartz, biotite, and muscovite plus clay matrix. The basaltic pumices consist of aphyric to clinopyroxene-porphyrific scoria. |

| | |
|---|--|
| <p>R31-450/455B Hand-picked fragments (representing the top of flow series E)</p> | <p>This polished thin section represents three fragments of slightly to moderately vesicular medium-grained pilotaxitic and hypocrystalline basalt. The largest fragment is orange vitric with cryptocrystalline groundmass bordering crystals, and the other two are opaque cryptocrystalline; all three, especially the vitric fragment, have lost glass or cryptocrystalline groundmass within portions of each fragment. A trace of smectite coats a portion of one vesicle. Prismatic plagioclase phenocrysts (7%) are common, and unaltered, often large olivine phenocrysts are abundant (6%). Rare unaltered magnetite (200 ppm of the sample by volume), absent within groundmass, occurs primarily as chromian magnetite and euhedral chromite within olivine phenocrysts.</p> |
| <p>R31-495/500 Hand-picked fragments</p> | <p>This polished thin section represents five fragments of moderately vesicular medium-grained pilotaxitic and moderately cryptocrystalline basalt; small portions of cryptocrystalline groundmass have been lost from most fragments. Prismatic plagioclase phenocrysts (2%) are scarce, and unaltered large phenocrysts of olivine and clinopyroxene are both common to abundant (each 4%); clinopyroxene is generally concentrically zoned and often forms glomerocrysts. Magnetite (2%) ranges among fragments from prevalent in one fragment to nearly absent in another; in all fragments, alteration ranges from unaltered to completely oxidized with exsolved maghemite. Inclusions of euhedral spinel, chromite, and chromian magnetite are sparse within olivine phenocrysts and rare within clinopyroxene phenocrysts. A few vesicles contain sandy argillite (1.5%) with 20% felsic phenocrysts, including quartz (60% of felsics), plagioclase (30%), and sanidine (10%), with a single grain of biotite also observed. Most quartz has wavy extinction and thus certainly represents a xenolithic source.</p> |
| <p>R31-515/520 Hand-picked fragments</p> | <p>This polished thin section represents nine fragments of slightly vesicular medium-grained pilotaxitic basalt, slightly to moderately cryptocrystalline in some fragments. Large voids (3.6%) include microvesicles (>0.03 mm) and vesicles. Minor smectite coats some vesicles. Phenocrysts include rare prismatic plagioclase (0.3%), common unaltered clinopyroxene (2.8%, median area 0.14 mm²), and scarce to common olivine altered to iddingsite in thin rims (1.9%, 0.20 mm²); clinopyroxene is generally concentrically zoned, often forms granular aggregates, and one is very strongly resorbed. In groundmass, clinopyroxene (11.9%, 0.0006 mm²) is unaltered, and olivine (3.0%, 0.0010 mm²) is slightly to completely altered to iddingsite. Common to abundant, generally unaltered fine-grained magnetite (3.9%, 0.00004 mm²) is equant in the groundmass of some fragments and cruciform in others. Inclusions of euhedral spinel, chromite, and chromian magnetite are sparse within olivine phenocrysts (0.19% of phenocrysts) and rarely occur within clinopyroxene phenocrysts.</p> |
| <p>R31-540/545 Hand-picked fragments</p> | <p>This polished thin section represents five fragments of slightly to moderately vesicular medium-grained pilotaxitic and somewhat cryptocrystalline mugearite. Scarce plagioclase phenocrysts (3%) are mostly prismatic, with a single moderately resorbed prism. One of three quartz phenocrysts (0.04%) present is haloed with a clinopyroxene reaction rim. Common olivine phenocrysts (3%) are slightly to entirely altered to iddingsite at rims. Rare clinopyroxene phenocrysts (0.1%) occur mostly as very strongly resorbed phenocrysts. Scarce to rare magnetite (0.7%) is fine-grained, equant, unaltered to slightly oxidized and exsolved to maghemite within groundmass, and occurs sparsely as coarser chromian magnetite and euhedral chromite within olivine phenocrysts. The three smallest fragments, which have the highest fraction of cryptocrystalline groundmass, have much lower magnetite contents than the other two and lack ilmenite, which occurs as tiny acicular unaltered groundmass (50 ppm of the sample by volume, median area <0.0001 mm²).</p> |
| <p>R31-585/590G1 Hand-picked fragments</p> | <p>The largest of four fragments within a polished thin section labeled R31-585/590G represents moderately vesicular medium-grained pilotaxitic and cryptocrystalline basalt. (The other three fragments, designated as sample R31-585/590G2, represent mugearite.) Recognizable voids (7.3%) include microvesicles (>0.03 mm) and large vesicles, and cryptocrystalline groundmass constitutes 21%. Plagioclase phenocrysts are scarce to rare (0.6%, median area 0.015 mm²), and mostly prismatic. Abundant olivine phenocrysts (7.9%, 0.83 mm²) are unaltered. Groundmass mafics are entirely unaltered olivine (6.7%, 0.0006 mm²) and cruciform clinopyroxene entirely within cryptocrystalline groundmass (4.3%, 0.0002 mm²). Scarce to rare magnetite (0.06%) occurs mostly as numerous euhedral inclusions of spinel, chromite, and chromian magnetite that constitute 0.65% of olivine phenocrysts. No accessories or lithics were observed.</p> |

March 2002

D-2

ER2001-0704

ER2001-0704

D-3

March 2002

| | |
|---|--|
| R31-585/590G2 Hand-picked fragments | The three smallest fragments within a polished thin section labeled R31-585/590G represent moderately vesicular medium-grained pilotaxitic and somewhat cryptocrystalline mugearite. (The other fragment, designated as sample R31-585/590G1, represents basalt.) Recognizable voids (6.4%) include microvesicles (>0.03 mm) and large vesicles, and cryptocrystalline groundmass constitutes 5.0%. Plagioclase phenocrysts are scarce to common (6.4%, median area 0.037 mm ²), mostly prismatic (56% of plagioclase), but include some very large, strongly resorbed phenocrysts (33%). Common olivine phenocrysts (3.5%, 0.049 mm ²) are generally moderately altered to iddingsite or moderately blackened at rims. Unaltered microphenocrysts of clinopyroxene are rare (0.2%, 0.027 mm ²). Groundmass mafics are olivine somewhat altered to iddingsite (3.5%, 0.0010 mm ²), unaltered clinopyroxene that frequently occurs as aggregates (11.3%, median area 0.0060 mm ² includes aggregates and single grains), and prismatic orthopyroxene (0.7%, 0.0016 mm ²). Scarce magnetite in groundmass (1%) is strongly to entirely oxidized to maghemite and also occurs as numerous euhedral inclusions of spinel, chromite, and chromian magnetite that constitute 0.38% of olivine phenocrysts. Unaltered ilmenite (0.05%) occurs as tiny acicular groundmass grains. No accessories or lithics were observed. |
| R31-585/590R Hand-picked fragments | This polished thin section represents three fragments of slightly vesicular medium-grained pilotaxitic mugearite, probably originally with cryptocrystalline groundmass that has been lost. Common plagioclase phenocrysts (10%) are mostly prismatic, but many are very large and strongly resorbed. Common olivine phenocrysts (4%) have iddingsite rims of a uniform thickness of 0.02 mm; thus the largest phenocryst, with an area of 2 mm ² , has a thin altered rim, but the smallest phenocrysts are mostly altered. Unaltered clinopyroxene occurs as rare microphenocrysts (0.3%) that are often granular (one is resorbed) and as groundmass also commonly in granular aggregates, one very coarse, probably representing a reaction rim with a reactive phase such as quartz that was not cut by the thin section. A single orthopyroxene phenocryst (0.02%) was observed. Rare magnetite (0.3%) occurs primarily as fine-grained equant groundmass, strongly oxidized to maghemite to unaltered, with much coarser chromian magnetite attached to rims of olivine phenocrysts and euhedral chromite within these phenocrysts. |
| R31-600/605 2- to 4-mm sieve fraction | This polished thin section represents 51 fragments, mostly opaque cryptocrystalline pilotaxitic and orange vitric slightly pilotaxitic scoria with 20-50% generally round to ovoid vesicles of 0.2 to 0.5 mm. These grade into slightly vesicular to massive pilotaxitic and cryptocrystalline mugearite that composes 20% of the fragments, with cryptocrystalline groundmass completely destroyed in many fragments. All of these volcanic fragments represent the same unit sampled as R31-585/590; they contain scarce to common plagioclase phenocrysts (5%), mostly prismatic but often very strongly resorbed. Scarce to common olivine phenocrysts (2%) range from entirely iddingsite-altered to unaltered: rare granular clinopyroxene microphenocrysts (0.3%) are unaltered. Groundmass Fe-Ti oxides are almost entirely fine-grained magnetite (1%) entirely oxidized to maghemite, but a single massive fragment bears medium grained magnetite entirely oxidized to maghemite and limonite, and tiny unaltered acicular ilmenite (0.005%, median area <0.0001 mm ²). A single fragment is silty argillite, which also partly fills some vesicles and coats some scoria. This highly micaceous silty argillite, 4% of the split, contains 5% felsic phenocrysts of quartz (50% of felsics) and plagioclase (50%); a single grain of muscovite was observed. This sediment probably represents infilling soil. |
| R31-665/670 Hand-picked fragments | This polished thin section represents four fragments of massive, medium-grained pilotaxitic basalt. Rare plagioclase microphenocrysts (0.7%, median area 0.019 mm ²) are generally prismatic. Scarce olivine microphenocrysts (1.6%, 0.020 mm ²), which are free of spinel inclusions, are generally unaltered in the smallest grains to almost entirely altered to iddingsite in the largest grains. In groundmass, clinopyroxene (9.5%, 0.0002 mm ²) and olivine (6.4%, 0.0008 mm ²) are entirely unaltered and thus poorly distinguishable from each other. Abundant magnetite in groundmass (5.1%, 0.0003 mm ²) is generally unaltered, with rims of some grains oxidized to maghemite. Groundmass includes apatite (0.7%, 0.00007 mm ²). No lithics were observed. |
| R31-680/685 Hand-picked fragments | This polished thin section represents seven fragments of slightly vesicular medium- to coarse-grained pilotaxitic basalt. Scarce plagioclase microphenocrysts (4%) are generally prismatic, and scarce olivine microphenocrysts (2%) are moderately altered to orange smectite, which also partly fills vesicles. Common equant magnetite (3%) and groundmass clinopyroxene and olivine are all unaltered. |

| | |
|--|--|
| <p>R31-705/710B Hand-picked fragments</p> | <p>This polished thin section represents six fragments of moderately to highly vesicular medium-grained pilotaxitic hypocrySTALLINE basalt, two fragments with opaque cryptocrystalline groundmass, and four fragments with orange vitric groundmass, slightly to moderately cryptocrystalline adjacent to crystal boundaries. Most vesicles are not coated, but a few are thickly coated with smectite, and both cryptocrystalline groundmass and glass have been lost near such vesicles. All fragments have similar primary mineralogy, with scarce to rare plagioclase microphenocrysts (1%), mostly prismatic but with two very strongly resorbed microphenocrysts, and with scarce olivine microphenocrysts (2%), generally unaltered but slightly altered to iddingsite within one vitric fragment. Common fine-grained equant magnetite (2%, median area <math><0.0001\text{ mm}^2</math>) is generally unaltered. A sandy sedimentary matrix (0.3%) that fills a few vesicles contains pale brown pumiceous glass, colorless massive glass, and 30% felsic phenocrysts, including quartz (60%), plagioclase (30%), and sanidine (10%). Most quartz has wavy extinction and thus represents a nonvolcanic source.</p> |
| <p>R31-705/710SS Hand-picked fragments</p> | <p>This polished thin section represents fragments of mafic sediment (sandstone to siltstone). Grains include quartz, amphibole, glass, and rare microcline and chert. Fragments of basaltic lithology are very abundant; fragments of plutonic lithology are rare. Dacitic constituents are very rare.</p> |
| <p>R31-725/730 Hand-picked fragments</p> | <p>This polished thin section represents 10 moderately rounded pyroclasts of vitric colorless pumice; one is also moderately pilotaxitic and another slightly pilotaxitic. Plagioclase phenocrysts, often prismatic or wormy, are scarce to common (6%), hornblende is abundant (4%), and orthopyroxene is scarce (0.2%). Hornblende, somewhat dissolved at rims and along cleavage, displays thin blackened rims within the moderately pilotaxitic pumice and is blackened to pseudomorphs within the slightly pilotaxitic pumice. Scarce to common magnetite (0.13%) and ilmenite (150 ppm of the sample by volume) are unaltered except within the two pilotaxitic pumices, where magnetite is slightly to moderately exsolved and ilmenite is strongly oxidized to pseudobrookite. Five grains of apatite were observed. These hornblende-phyric pumice clasts have a primary mineralogy indicating that they represent dacite of Sawyer Dome. Sandy argillite (2%), which partly fills some vesicles, contains 20% felsic phenocrysts, including plagioclase (50% of felsics) and quartz (50%).</p> |
| <p>R31-730/735 2- to 4-mm sieve fraction</p> | <p>This polished thin section consists of more than 50 fragments of lithics, pumice, silty argillite, and sandy argillite. The fragments of silty and sandy argillite represent lenses and layers within alluvial deposits, and the lithics and pumice clasts probably represent a concentrate of large clasts within this alluvium. Smaller grains within argillite include vitric colorless shards and scarce to common felsic crystals (7.1%) that are primarily plagioclase (91%) from volcanic sources and much lesser, small quartz (9%), probably derived from nonvolcanic sources. Mafics within the sedimentary matrix are dominantly hornblende (2.6%) in most fragments, with 28 grains observed, with much lesser orthopyroxene (0.3%), with a single grain observed. One grain of zircon and seven grains of biotite were also observed, with most of the biotite present within a single fragment of micaceous silty argillite. Colorless pumice is abundant (21%), almost entirely vitric, with only a single argillic pumice observed. By area, 89% of the pumice clasts are plagioclase- and hornblende-phyric. In contrast, 76% by area of the abundant lithics (44%) are plagioclase- and pyroxene-phyric, with pyroxene dominated by orthopyroxene. The pyroxene-phyric lithics may represent the upper dacite of Pajarito Mountain, and the hornblende-phyric lithics may represent dacite of Sawyer Dome. By area, 35% of all lithics are vitric and generally vesicular. Except for single, small lithics of highly argillic Miocene basalt and silty argillite, all pumice and lithics appear to represent the Tschicoma Formation. XRD analysis reveals traces of dolomite and clinoptilolite unrecognized in thin section.</p> |

March 2002

D-4

ER2001-0704

| | |
|--|--|
| R31-760/765 2- to 4-mm sieve fraction | This polished thin section consists of 44 fragments of lithics and 7 fragments of argillic sandstone. The fragments represent argillic sandstone within alluvial deposits, with the 44 lithics representing a concentrate of large clasts within this alluvium. Sand grains within argillic sandstone are pyroclasts, crystals, and lithics. Pyroclasts all remain vitric and include colorless shards, pale brown shards, and small colorless pumice. Scarce felsic crystals (5% within argillic sandstone) include plagioclase (50%) and quartz (20%) from volcanic sources and quartz from nonvolcanic sources (30%); four grains each were observed of clinopyroxene and altered hornblende. Psilomelane fills a single vug and the adjacent matrix in a single fragment of argillic sandstone. Lithics (87% of sample) are entirely volcanic and include dominant dacite, probably of the Tschicoma Formation (53% of sample), probable rhyodacite of Rendija Canyon (30%), and two different flows of Miocene basalt (3%). By area, 12% of all lithics are vitric, and glass constitutes 17% of the sample. Dacite clasts are dominated by the plagioclase- and pyroxene-phyric varieties (36% of sample), with only a single plagioclase- and hornblende-phyric fragment (4%). Others (12%) are phyric in both pyroxene and hydrous mafics. Dacite lithics generally contain scarce to common plagioclase phenocrysts, averaging 4.8%. Aphyric lithics, mafic-poor lithics with very strongly resorbed plagioclase phenocrysts, and lithics with quartz phenocrysts were generally assigned as rhyodacite of Rendija Canyon. These rhyodacite lithics contain scarce plagioclase phenocrysts (1.2%), a much lower content than typical rhyodacite of Rendija Canyon. |
| R31-830/835 2- to 4-mm sieve fraction | This polished thin section consists of 55 fragments, mostly angular lithics concentrated from sedimentary rock. No matrix is present, but XRD analysis of a split that includes matrix indicates the presence of glass that was not observed in thin section; kaolinite also revealed by XRD probably reflects the occurrence of hydrothermally altered lithics. Three fragments are large single felsic crystals from nonvolcanic sources representing 4% of the sample and consisting of quartz (51% of felsics), sericitic plagioclase (36%), and microcline (13%). The remaining fragments are diverse and include lithics from volcanic (52%) and nonvolcanic (42%) sources. Nonvolcanic lithics, mostly from Precambrian sources, include fine- to coarse-grained, micaceous to nonmicaceous quartzite (24%), both microcline- and orthoclase-bearing granite (16%), and a single silty argillite (2%). Volcanic lithics, all lava with a single exception, are all devitrified, and many have vapor-phase crystallization, and represent fairly equal proportions of several types. Lavas that are poor in felsic and mafic phenocrysts represent 22% of the split; a quarter of these, including a single moderately welded tuff, contain quartz and/or sanidine, and all represent rhyodacite of Rendija Canyon. The remaining lithics of lava are generally plagioclase-phyric; 16% are also phyric in the hydrous mafics biotite and/or hornblende, and 14% are also phyric in pyroxene. These lavas probably represent a variety of dacite units within the Tschicoma Formation. |
| R31-920/925 2- to 4-mm sieve fraction | This polished thin section consists of 69 fragments, mostly angular lithics from sedimentary rock. Fragments include two with sedimentary matrix and one zeolitic pumice, and lithics including one leucogranite and one vitric moderately welded tuff; remaining lithics are all lava, all devitrified and many with vapor-phase crystallization, except for a single vitric lava. Sedimentary matrix includes silty and sandy argillite. The silty argillite (0.3% of sample) is well sorted, with 15% moderately angular to moderately rounded felsic crystals, including plagioclase (60% of felsics; largest plagioclase 0.0013 mm ²), quartz (30%), and sanidine (10%). Small grains include three of biotite; two grains each of muscovite, orthopyroxene, and zircon; and one grain of hornblende. The sandy argillite (1.3% of sample) is mantled by argillic sandstone and, overall, contains 8% moderately angular to moderately rounded felsic crystals, including plagioclase (50% of felsics), quartz (35%), and sanidine (15%). Tiny grains observed include eight of strongly dissolved hornblende, four of biotite, and a single large sphen. Within the sandy matrix are vitric colorless shards and smectite that mantles the argillite lens. Zeolitic pumice (0.8%) contains 12% quartz as the sole felsic phenocryst and probably accounts for the clinoptilolite found by XRD. The leucogranite is mostly plagioclase (mostly altered to sericite) and quartz with wavy extinction, plus minor microcline. The vitric moderately welded tuff (2%) has scarce to rare felsic phenocrysts of plagioclase, sanidine, and quartz, and scarce to rare orthopyroxene. Lavas are dominantly poor in felsic and mafic phenocrysts, including 38 clasts, 12 containing quartz and/or sanidine; these lavas represent rhyodacite of Rendija Canyon. The remaining clasts of lava are generally plagioclase-phyric; 11 are also phyric in the hydrous mafics biotite and/or hornblende, 9 are also phyric in pyroxene, and 3 are phyric in both types of mafics. These lavas probably represent a variety of dacite units within the Tschicoma Formation. |

| | |
|--|---|
| <p>R31-1005/1010 2- to 4-mm sieve fraction</p> | <p>This polished thin section consists of 55 fragments, including 26 lithics, 27 pumice clasts, and 2 fragments of matrix concentrated from sedimentary rock. Matrix fragments (4%) are slightly silty argillite. This matrix contains shards and small pumice, both with colorless glass, but few lithics. Felsic phenocrysts (2%) are quartz (60% of felsics), plagioclase (25%), and sanidine (15%), and other minerals observed include five of biotite, four of hornblende, and single grains of sphene, clinopyroxene, and muscovite. Pumice clasts (49% of fragments), colorless except for a single pale brown clast, are generally vitric, although a few are entirely argillic, and some are partly vitric, partly argillic. About half of the pumices contain abundant phenocrysts of hornblende (3%), scarce to common plagioclase (5%), and rare orthopyroxene (200 ppm of these pumices by volume). Most of the remaining pumice clasts are crystal poor, but one contains mafics of biotite and lesser hornblende, and two completely argillic pumice clasts contain phenocrysts of quartz, sanidine, and pseudomorphic pyroxene. The trace of mordenite found by XRD analysis may be associated with the argillic pumice. A variety of lithics, mostly lava, represent 47% of the fragments. Lavas are dominantly poor in felsic and mafic phenocrysts (31%); 29% of the lavas contain sphene, quartz and/or sanidine and represent rhyodacite of Rendija Canyon. The remaining clasts of lava are generally plagioclase-phyric; 5% are also phyric in the hydrous mafics biotite and/or hornblende, and 4% are also phyric in pyroxene, half of these vitric with brown glass. These lavas probably represent a variety of dacite units within the Tschicoma Formation. The remaining 7% of lithics include equal abundances of granite and coarse-grained quartzite, both from Precambrian sources.</p> |
| <p>R31-1010/1015 2- to 4-mm sieve fraction</p> | <p>This polished thin section consists of 46 fragments, including 2 fragments of matrix, 4 crystal fragments, 17 pumice clasts, and 23 lithics, concentrated from sedimentary rock. One matrix fragment is slightly silty argillite (1% of sample) that contains tiny lithics to 0.0025 mm² and 1% felsic crystals, the largest a 0.0020 mm² quartz, and smaller colorless vitric shards. The silt-bearing portion mantles a larger lens of nearly silt-free argillite. The other matrix fragment (2%) is argillic sandstone with shards and small pumice clasts, both vitric and colorless, small lithics, and 25% felsic phenocrysts of plagioclase (65% of felsics), quartz (30%), and sanidine (5%), and six grains of hornblende, three of biotite, two of orthopyroxene, and a single zircon. Half of the quartz, including the largest crystal, was derived from volcanic sources, and the largest lithic represents rhyodacite of Rendija Canyon. Large single felsic crystals constitute 4% of the split, including nonvolcanic quartz (84%), volcanic quartz (12%), and nonvolcanic plagioclase (4%). Pumice clasts (37% of fragments) are all vitric and colorless; 59% of these clasts contain abundant phenocrysts of hornblende (3%) and scarce to common plagioclase (5%). Three of the remaining pumice clasts are crystal poor and contain quartz phenocrysts or sphene, and the other four all contain plagioclase phenocrysts, with two also containing pyroxene. A variety of lithics, mostly lava, represent half of the fragments. Lavas are dominantly poor in felsic and mafic phenocrysts (26% of split) and represent rhyodacite of Rendija Canyon. The remaining clasts of lava are generally plagioclase-phyric and include two with mineralogies similar to the prevalent pumice and single fragments that are either vitric or hydrothermally altered. These lavas probably represent a variety of dacite units within the Tschicoma Formation. Remaining lithics include 9% granite, half containing microcline and the other half lacking potassium feldspar, and 2% coarse-grained quartzite from Precambrian sources.</p> |
| <p>R31-1050/1055A Hand-picked lavas</p> | <p>Except for 6 fragments, all 49 fragments within the thin section labeled R31-1050/1055 represent orange-brown cryptocrystalline and pilotaxitic latite or dacite lava, slightly to moderately vesicular, with mostly round vesicles to 0.2 mm filled with pale orange brown fibrous silica, probably cristobalite. (The other six fragments, designated as sample R31-1050/1055B, represent colorless microgranophyric dacite or latite lava.) Prismatic and often wormy plagioclase phenocrysts are common to abundant (15%); unaltered, occasionally wormy clinopyroxene phenocrysts are abundant (3%); and small iddingsite pseudomorphs after olivine phenocrysts are rare (100 ppm of the lithology by volume). Common to abundant magnetite phenocrysts (0.7%) are unaltered, and 22 grains of apatite were observed.</p> |

March 2002

D-6

ER2001-0704

| | |
|--|--|
| <p>R31-1050/1055B Hand-picked lavas</p> | <p>Six fragments of the 49 fragments within the thin section labeled R31-1050/1055 represent colorless microgranophyric dacite or latite lava. (The other fragments, designated as sample R31-1050/1055A, represent orange brown cryptocrystalline and pilotaxitic latite or dacite lava.) Blocky, optically negative, and often very strongly resorbed microphenocrysts and occasional phenocrysts of plagioclase are common to abundant (15%). Strongly altered pyroxene phenocrysts are abundant (5%), with many relicts, all clinopyroxene. Abundant microphenocrysts of strongly blackened mafics include biotite (2%) and hornblende (0.5%). Very abundant magnetite phenocrysts (2%) are strongly oxidized to maghemite with some limonite, and 14 grains of apatite and 2 grains of zircon were observed.</p> |
| <p>R31-1095/1100 2- to 4-mm sieve fraction</p> | <p>This polished thin section consists of 50 fragments of angular lithics concentrated from sedimentary rock. These lithics are mostly volcanic rocks (82%) and include much lesser quartzite (15%) and granite (3%), both from Precambrian sources. Volcanic lithics are almost entirely lava, but 3% of the lithics are represented by two clasts of devitrified moderately welded tuff from different sources, one plagioclase-phyric, and the other aphyric. Most lava is devitrified, often accompanied by vapor-phase crystallization, but 25% of such lithics are vitric, including lavas with colorless glass as well as brown glass, with a total glass content of 11%. The lithics of lava represent many unrecognized stratigraphic units (clast groups), but lithics of rhyodacite of Rendija Canyon are recognizable from strongly resorbed plagioclase phenocrysts, abundant acicular groundmass pyroxene, quartz phenocrysts, and sphene. The rhyodacite of Rendija Canyon appears to constitute 31% of the lavas. These rhyodacite lithics contain scarce plagioclase phenocrysts (1.5%), a much lower content than typical rhyodacite of Rendija Canyon. Dacite clasts, all probably Tschicoma Formation, include plagioclase-phyric varieties, except for a single fragment that contains minor quartz phenocrysts. Anhydrous mafics dominate in 32% of the lavas, hydrous mafics dominate in 12%, and mafics of both types occur within the remaining 25%. Dacites generally contain common plagioclase phenocrysts, averaging 9.6%. Quartzite occurs in two varieties, one equant fine-grained, and often containing significant muscovite, and the other equant and coarse-grained with few minerals besides quartz. Both lithics of granite are microcline-bearing leucogranite.</p> |

ER2001-0704

D-7

March 2002

Appendix E

Moisture and Matric-Potential Results

| Sample ID | Upper Depth (ft) | Lower Depth (ft) | Lithology | Activity (H ₂ O) | Temperature (°C) | Matric Potential (cm) | Gravimetric Moisture (%) |
|-----------|------------------|------------------|----------------|-----------------------------|------------------|-----------------------|--------------------------|
| R31-4.5 | 4.4 | 4.5 | Alluvium | 0.993 | 27.38 | -9922 | 11.10 |
| R31-7.5 | 7.4 | 7.5 | Alluvium | 0.9995 | 27.15 | -706 | 17.13 |
| R31-12.5 | 12.4 | 12.5 | Alluvium | 0.9995 | 27.09 | -706 | 13.71 |
| R31-17.5 | 17.4 | 17.5 | Alluvium | 0.9985 | 27.18 | -2119 | 12.74 |
| R31-22.5 | 22.4 | 22.5 | Alluvium | 0.9985 | 27.00 | -2118 | 8.92 |
| R31-27.5 | 27.4 | 27.5 | Otowi ash flow | 0.997 | 27.12 | -4240 | 10.99 |
| R31-32.5 | 32.4 | 32.5 | Otowi ash flow | 0.997 | 27.09 | -4240 | 11.31 |
| R31-37.5 | 37.4 | 37.5 | Otowi ash flow | 0.9955 | 27.05 | -6363 | 10.67 |
| R31-42.5 | 42.4 | 42.5 | Otowi ash flow | 0.9965 | 27.03 | -4946 | 12.16 |
| R31-47.5 | 47.4 | 47.5 | Otowi ash flow | 0.996 | 27.01 | -5654 | 11.93 |
| R31-52.5 | 52.4 | 52.5 | Otowi ash flow | 0.9965 | 27.05 | -4947 | 12.27 |
| R31-57.5 | 57.4 | 57.5 | Otowi ash flow | 0.9975 | 27.14 | -3533 | 12.06 |
| R31-62.5 | 62.4 | 62.5 | Otowi ash flow | 0.9965 | 27.28 | -4951 | 12.17 |
| R31-67.5 | 67.4 | 67.5 | Otowi ash flow | 0.996 | 27.31 | -5660 | 12.70 |
| R31-72.5 | 72.4 | 72.5 | Otowi ash flow | 0.996 | 27.28 | -5659 | 13.13 |
| R31-77.5 | 77.4 | 77.5 | Otowi ash flow | 0.996 | 27.46 | -5663 | 12.46 |
| R31-82.5 | 82.4 | 82.5 | Otowi ash flow | 0.9945 | 27.40 | -7790 | 12.26 |
| R31-87.5 | 87.4 | 87.5 | Otowi ash flow | 0.996 | 27.38 | -5661 | 12.40 |
| R31-92.5 | 92.4 | 92.5 | Otowi ash flow | 0.9945 | 27.42 | -7791 | 12.33 |
| R31-97.5 | 97.4 | 97.5 | Otowi ash flow | 0.994 | 28.66 | -8536 | 11.56 |
| R31-102.5 | 102.4 | 102.5 | Otowi ash flow | 0.995 | 28.72 | -7111 | 12.57 |
| R31-107.5 | 107.4 | 107.5 | Otowi ash flow | 0.9965 | 28.52 | -4971 | 12.93 |
| R31-112.5 | 112.4 | 112.5 | Otowi ash flow | 0.994 | 29.20 | -8552 | 13.04 |
| R31-117.5 | 117.4 | 117.5 | Otowi ash flow | 0.9945 | 29.08 | -7834 | 13.52 |
| R31-122.5 | 122.4 | 122.5 | Otowi ash flow | 0.9955 | 28.92 | -6403 | 15.35 |
| R31-127.5 | 127.4 | 127.5 | Otowi ash flow | 0.995 | 28.78 | -7113 | 13.66 |
| R31-132.5 | 132.4 | 132.5 | Otowi ash flow | 0.9955 | 28.68 | -6398 | 13.91 |
| R31-137.5 | 137.4 | 137.5 | Otowi ash flow | 0.9965 | 28.48 | -4970 | 13.50 |
| R31-142.5 | 142.4 | 142.5 | Otowi ash flow | 0.9975 | 25.82 | -3517 | 14.46 |
| R31-147.5 | 147.4 | 147.5 | Otowi ash flow | 0.995 | 26.09 | -7050 | 15.04 |
| R31-152.5 | 152.4 | 152.5 | Otowi ash flow | 0.997 | 26.25 | -4228 | 14.91 |
| R31-157.5 | 157.4 | 157.5 | Otowi ash flow | 0.997 | 26.21 | -4227 | 14.41 |
| R31-162.5 | 162.4 | 162.5 | Otowi ash flow | 0.997 | 26.27 | -4228 | 14.71 |
| R31-167.5 | 167.4 | 167.5 | Otowi ash flow | 0.9985 | 26.34 | -2113 | 15.27 |
| R31-172.5 | 172.4 | 172.5 | Otowi ash flow | 0.997 | 24.92 | -4209 | 15.50 |
| R31-177.5 | 177.4 | 177.5 | Otowi ash flow | 0.9975 | 25.19 | -3510 | 15.29 |
| R31-182.5 | 182.4 | 182.5 | Otowi ash flow | 0.9975 | 25.67 | -3515 | 15.51 |
| R31-187.5 | 187.4 | 187.5 | Otowi ash flow | 0.996 | 25.97 | -5634 | 14.36 |
| R31-192.5 | 192.4 | 192.5 | Otowi ash flow | 0.996 | 26.14 | -5638 | 14.94 |

| Sample ID | Upper Depth (ft) | Lower Depth (ft) | Lithology | Activity (H ₂ O) | Temperature (°C) | Matric Potential (cm) | Gravimetric Moisture (%) |
|-----------|------------------|------------------|---------------------|-----------------------------|------------------|-----------------------|--------------------------|
| R31-197.5 | 197.4 | 197.5 | Otowi ash flow | 0.996 | 26.27 | -5640 | 15.07 |
| R31-202.5 | 202.4 | 202.5 | Otowi ash flow | 0.9955 | 26.49 | -6351 | 14.71 |
| R31-207.5 | 207.4 | 207.5 | Otowi ash flow | 0.997 | 26.64 | -4233 | 15.40 |
| R31-212.5 | 212.4 | 212.5 | Otowi ash flow | 0.996 | 26.71 | -5648 | 14.73 |
| R31-217.5 | 217.4 | 217.5 | Otowi ash flow | 0.996 | 27.36 | -5661 | 15.59 |
| R31-222.5 | 222.4 | 222.5 | Otowi ash flow | 0.9965 | 27.21 | -4949 | 18.22 |
| R31-227.5 | 227.4 | 227.5 | Otowi ash flow | 0.996 | 27.07 | -5655 | 14.62 |
| R31-232.5 | 232.4 | 232.5 | Otowi ash flow | 0.9965 | 26.95 | -4945 | 14.36 |
| R31-237.5 | 237.4 | 237.5 | Otowi ash flow | 0.9945 | 26.84 | -7776 | 16.43 |
| R31-242.5 | 242.4 | 242.5 | Otowi ash flow | 0.9955 | 26.82 | -6358 | 14.68 |
| R31-247.5 | 247.4 | 247.5 | Otowi ash flow | 0.9965 | 26.75 | -4942 | 14.40 |
| R31-255 | 254.5 | 255.0 | Otowi ash flow | 0.9945 | 26.22 | -7760 | 10.41 |
| R31-260 | 259.5 | 260.0 | Otowi ash flow | 0.9965 | 26.42 | -4936 | 8.62 |
| R31-265 | 264.5 | 265.0 | Guaje Pumice Bed | 1.001 | 26.30 | 1407 | 15.48 |
| R31-270 | 269.5 | 270.0 | Guaje Pumice Bed | 0.997 | 26.76 | -4235 | 13.58 |
| R31-275 | 274.5 | 275.0 | Guaje Pumice Bed | 0.997 | 26.92 | -4237 | 16.63 |
| R31-280 | 279.5 | 280.0 | Guaje Pumice Bed | 0.9985 | 27.08 | -2118 | 16.07 |
| R31-285 | 284.5 | 285.0 | sediment/paleosol | 0.986 | 27.23 | -19904 | 7.05 |
| R31-295 | 294.0 | 295.0 | Cerros del Rio lava | 0.627 | 27.51 | -659617 | 0.64 |
| R31-300 | 299.5 | 300.0 | Cerros del Rio lava | 0.984 | 27.12 | -22762 | 1.19 |
| R31-305 | 304.5 | 305.0 | Cerros del Rio lava | 0.987 | 27.15 | -18468 | 2.63 |
| R31-310 | 309.5 | 310.0 | Cerros del Rio lava | 0.89533 | 27.50 | -156222 | 2.63 |
| R31-315 | 314.0 | 315.0 | Cerros del Rio lava | 0.977 | 27.39 | -32866 | 2.10 |
| R31-320 | 319.5 | 320.0 | Cerros del Rio lava | 0.51675 | 27.70 | -933493 | 1.76 |
| R31-325 | 324.5 | 325.0 | Cerros del Rio lava | 0.967 | 25.77 | -47143 | 2.45 |
| R31-330 | 329.5 | 330.0 | Cerros del Rio lava | 0.8875 | 26.35 | -167993 | 1.45 |
| R31-335 | 334.0 | 335.0 | Cerros del Rio lava | 0.79875 | 26.47 | -316423 | 1.84 |
| R31-340 | 339.5 | 340.0 | Cerros del Rio lava | 0.9965 | 26.19 | -4933 | 8.19 |
| R31-345 | 344.5 | 345.0 | Cerros del Rio lava | 0.993 | 26.24 | -9884 | 3.09 |
| R31-350 | 349.0 | 350.0 | Cerros del Rio lava | 0.9965 | 26.30 | -4934 | 9.79 |
| R31-355 | 354.5 | 355.0 | Cerros del Rio lava | 0.996 | 26.36 | -5642 | 12.74 |

Appendix F

Westbay'sTM MP55 Well Components Installed in R-31

Summary MP Casing Log

Company: LANL
Well: R31
Site:
Project: Hydrogeology Characterization

Job No: WB777
Author: DL

Well Information

Reference Datum: ground level
Elevation of Datum: 0.00 ft.
MP Casing Top: 0.00 ft.
MP Casing Length: 1060.65 ft.
Well Description:
Plastic MP55 System
Other References:
5.0 in ID SS casing+screens: LANL2/17/00
Backfill after LANL 2/17/00
MagneticCollars 2.5 ft below port top

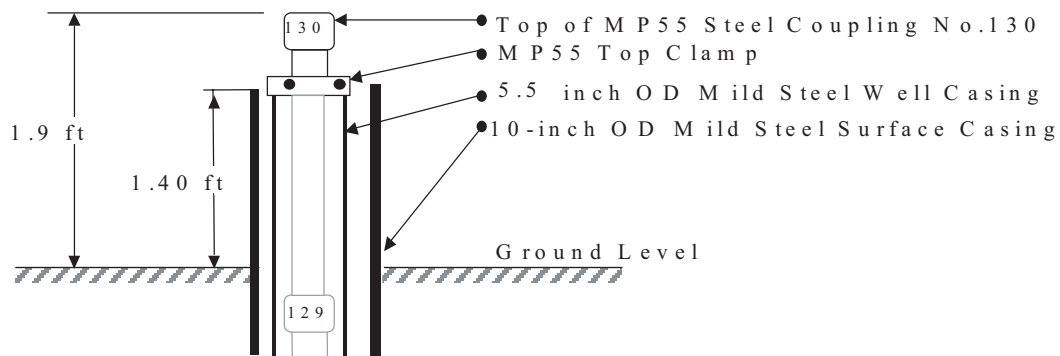
Borehole Depth: 1103.00 ft.
Borehole Inclination: vertical
Borehole Diameter: 10.00 in.

File Information

File Name: 777_R31.WWD
Report Date: Tue Aug 08 12:24:41 2000
File Date: Apr 07 21:47:21 2000

Sketch of Wellhead Completion

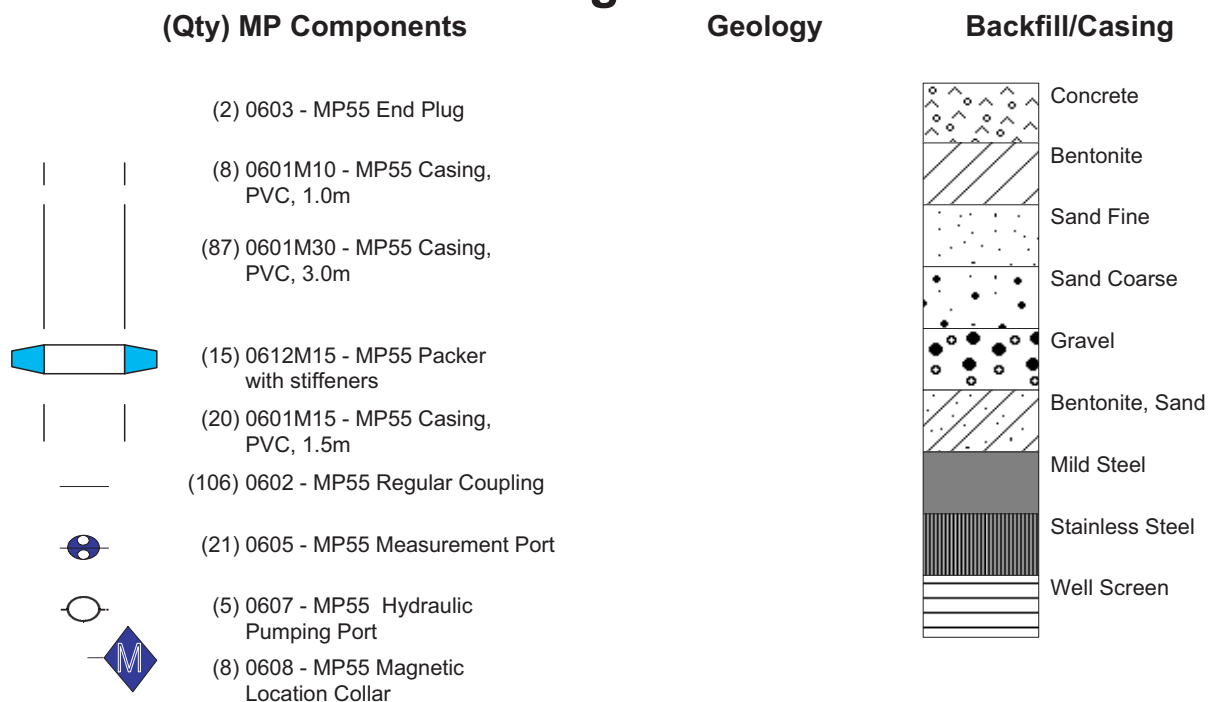
R 3 1 S u r f a c e C o m p l e t i o n



Summary MP Casing Log
LANL

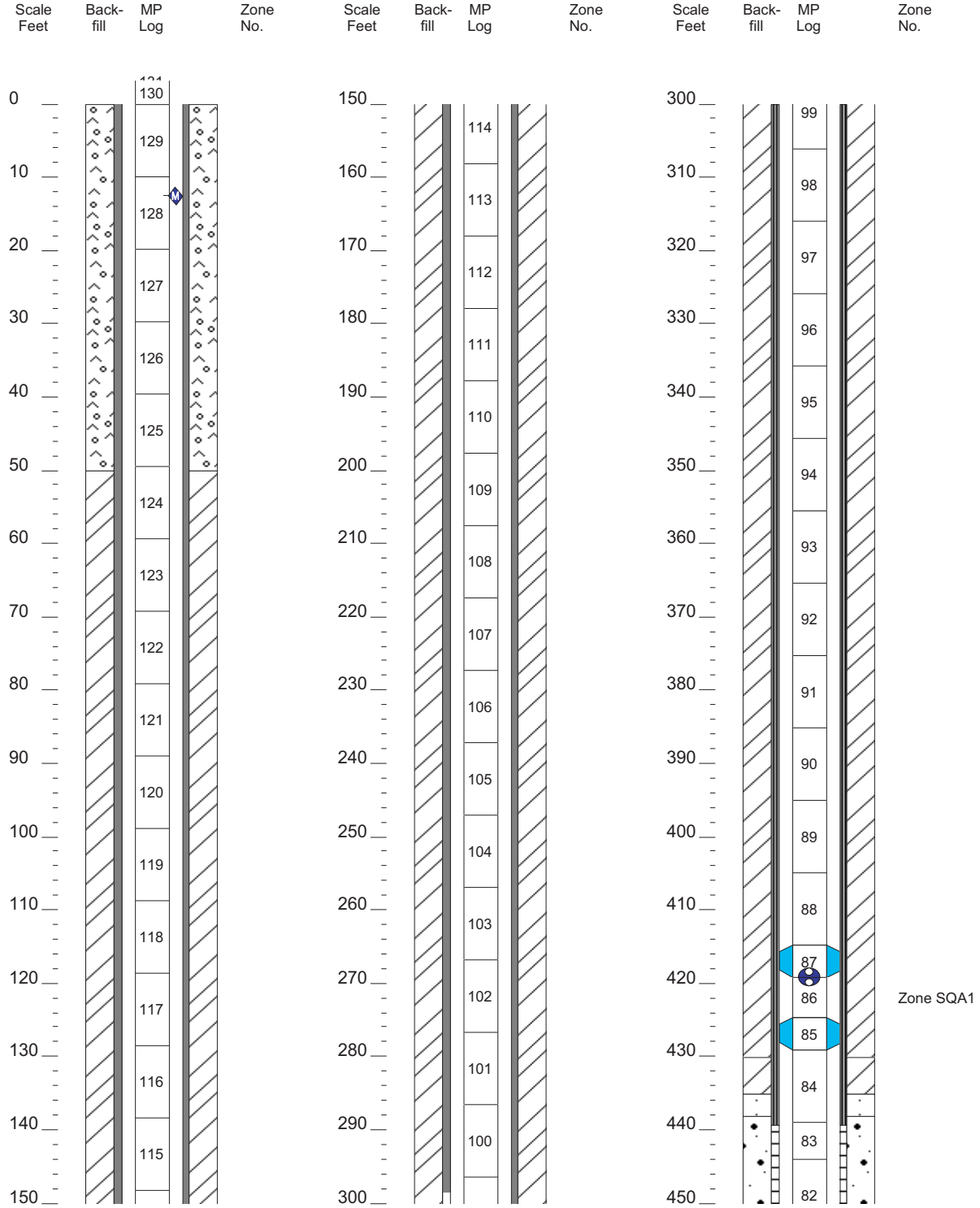
Job No: WB777
Well: R31

Legend



Summary MP Casing Log
LANL

Job No: WB777
Well: R31



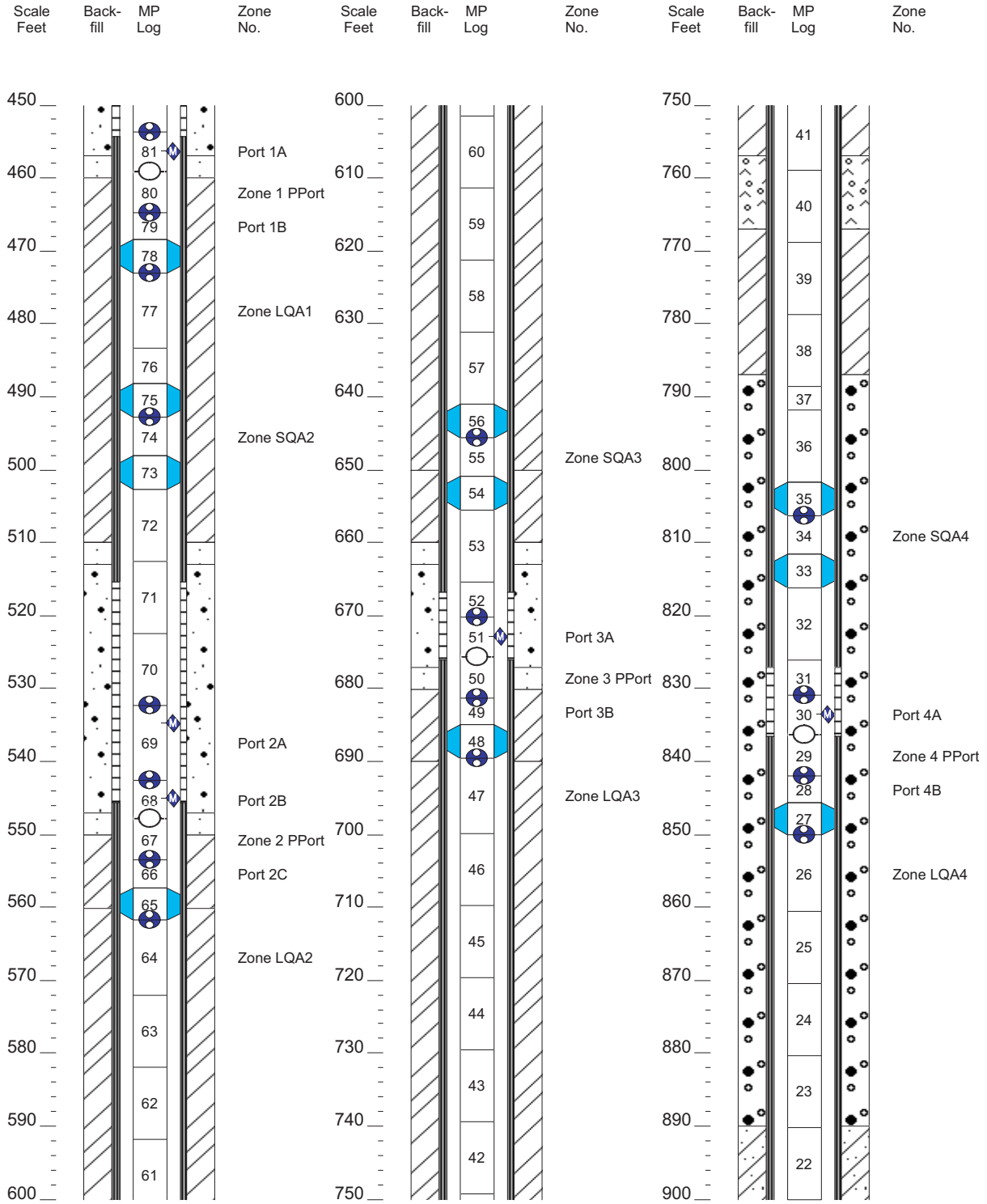
(c) Westbay Instruments Inc. 1998

Tue Aug 08 12:24:42 2000

Page: 3

Summary MP Casing Log
LANL

Job No: WB777
Well: R31



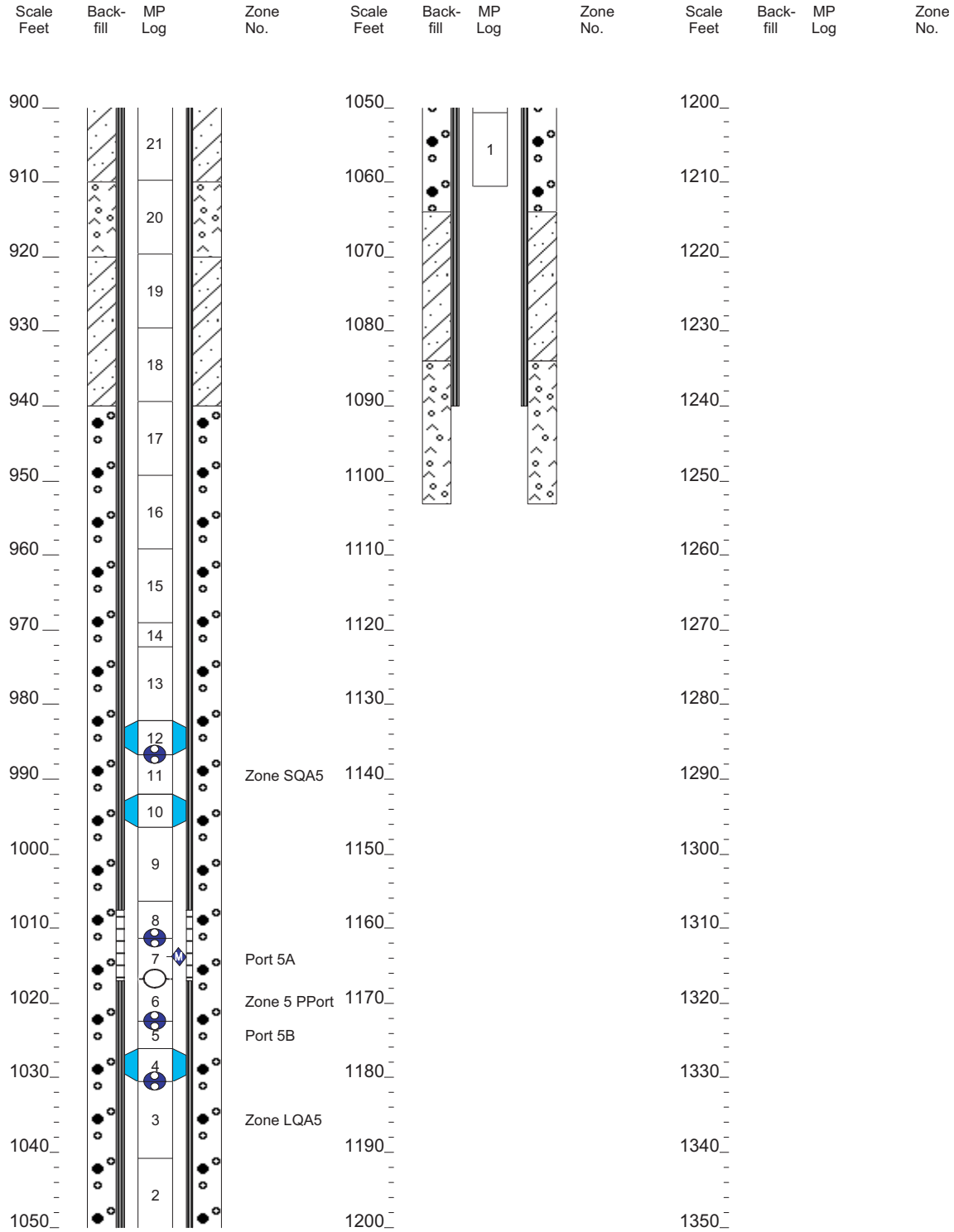
(c) Westbay Instruments Inc. 1998

Tue Aug 08 12:24:48 2000

Page: 4

Summary MP Casing Log
LANL

Job No: WB777
Well: R31



This report has been reproduced directly from the best available copy. It is available electronically on the Web (<http://www.doe.gov/bridge>).

Copies are available for sale to U.S. Department of Energy employees and contractors from—

Office of Scientific and Technical Information
P.O. Box 62
Oak Ridge, TN 37831
(865) 576-8401

Copies are available for sale to the public from—

National Technical Information Service
U.S. Department of Commerce
5285 Port Royal Road
Springfield, VA 22616
(800) 553-6847



Los Alamos NM 87545